



Calhoun: The NPS Institutional Archive
DSpace Repository

Theses and Dissertations

1. Thesis and Dissertation Collection, all items

1989

Evaluation of system identification algorithms
for aspect-independent radar target classification.

Larison, Peter David.

Monterey, California. Naval Postgraduate School

<https://hdl.handle.net/10945/25910>

Downloaded from NPS Archive: Calhoun



Calhoun is the Naval Postgraduate School's public access digital repository for research materials and institutional publications created by the NPS community. Calhoun is named for Professor of Mathematics Guy K. Calhoun, NPS's first appointed -- and published -- scholarly author.

Dudley Knox Library / Naval Postgraduate School
411 Dyer Road / 1 University Circle
Monterey, California USA 93943

<http://www.nps.edu/library>



1950
1951
1952

1953

1954

NAVAL POSTGRADUATE SCHOOL Monterey, California



THESIS

L2676

EVALUATION OF SYSTEM IDENTIFICATION
ALGORITHMS FOR ASPECT-INDEPENDENT
RADAR TARGET CLASSIFICATION

by

Peter David Larison
D O O

December 1989

Thesis Advisor:

Michael Morgan

Approved for public release; distribution is unlimited

REPORT DOCUMENTATION PAGE

Form Approved
OMB No 0704-0188

1a REPORT SECURITY CLASSIFICATION UNCLASSIFIED			1b RESTRICTIVE MARKINGS			
2a SECURITY CLASSIFICATION AUTHORITY			3 DISTRIBUTION / AVAILABILITY OF REPORT Approved for public release; distribution is unlimited			
2b DECLASSIFICATION / DOWNGRADING SCHEDULE			4. PERFORMING ORGANIZATION REPORT NUMBER(S)			
4. PERFORMING ORGANIZATION REPORT NUMBER(S)			5 MONITORING ORGANIZATION REPORT NUMBER(S)			
6a NAME OF PERFORMING ORGANIZATION Naval Postgraduate School		6b OFFICE SYMBOL (If applicable) 62		7a NAME OF MONITORING ORGANIZATION Naval Postgraduate School		
6c. ADDRESS (City, State, and ZIP Code) Monterey, California 93943-5000			7b ADDRESS (City, State, and ZIP Code) Monterey, California 93943-5000			
8a. NAME OF FUNDING / SPONSORING ORGANIZATION		8b OFFICE SYMBOL (If applicable)		9 PROCUREMENT INSTRUMENT IDENTIFICATION NUMBER		
8c. ADDRESS (City, State, and ZIP Code)			10 SOURCE OF FUNDING NUMBERS			
			PROGRAM ELEMENT NO	PROJECT NO	TASK NO	WORK UNIT ACCESSION NO
11 TITLE (Include Security Classification) EVALUATION OF SYSTEM IDENTIFICATION ALGORITHMS FOR ASPECT-INDEPENDENT RADAR TARGET CLASSIFICATION						
12 PERSONAL AUTHOR(S) LARISON, Peter David						
13a TYPE OF REPORT Master's Thesis		13b TIME COVERED FROM _____ TO _____		14 DATE OF REPORT (Year, Month, Day) 1989 December		15 PAGE COUNT 159
16 SUPPLEMENTARY NOTATION The views expressed in this thesis are those of the author and do not reflect the official policy or position of the Department of Defense or the US Government.						
17 COSATI CODES			18 SUBJECT TERMS (Continue on reverse if necessary and identify by block number)			
FIELD	GROUP	SUB-GROUP	Prony's Method; Kumaresan-Tufts Algorithm; Cadzow-Solomon Algorithm			
19 ABSTRACT (Continue on reverse if necessary and identify by block number)						
A radar target, acting as a scatterer of an incident electromagnetic wave, can be considered as a linear time-invariant system. Previous work has shown that the target's pole locations are independent of the incident electromagnetic excitation, including incident wave shape, aspect and polarization. This thesis develops the Kumaresan-Tufts and Cadzow-Solomon signal processing algorithms into computer routines and evaluates their pole extraction performance. Data used to evaluate the extraction algorithms includes synthetic and integral equation generated signals with additive noise, in addition to measurements of scattering by scale models made in an anechoic chamber.						
20 DISTRIBUTION / AVAILABILITY OF ABSTRACT <input checked="" type="checkbox"/> UNCLASSIFIED/UNLIMITED <input type="checkbox"/> SAME AS RPT <input type="checkbox"/> DTIC USERS				21 ABSTRACT SECURITY CLASSIFICATION UNCLASSIFIED		
22a NAME OF RESPONSIBLE INDIVIDUAL MORGAN, Michael			22b TELEPHONE (Include Area Code) 408-646-2677		22c OFFICE SYMBOL 62Mw	

Approved for public release; distribution is unlimited

EVALUATION OF SYSTEM IDENTIFICATION ALGORITHMS FOR ASPECT-
INDEPENDENT RADAR TARGET CLASSIFICATION

by

Peter David Larison
Captain, United States Marine Corps
B.S., Xavier University, 1981

Submitted in partial fulfillment of requirements
for the degree of

MASTER OF SCIENCE IN ELECTRICAL ENGINEERING

from the

NAVAL POSTGRADUATE SCHOOL
December 1989

ABSTRACT

A radar target, acting as a scatterer of an incident electromagnetic wave, can be considered as a linear time-invariant system. Previous work has shown that the target's pole locations are independent of the incident electromagnetic excitation, including incident wave shape, aspect and polarization. This thesis develops the Kumaresan-Tufts and Cadzow-Solomon signal processing algorithms into computer routines and evaluates their pole extraction performance. Data used to evaluate the extraction algorithms includes synthetic and integral equation generated signals with additive noise, in addition to measurements of scattering by scale models made in an anechoic chamber.

TABLE OF CONTENTS

I.	INTRODUCTION	1
	A. THE PROBLEM	2
	B. BACKGROUND	3
	C. HISTORY	8
II.	POLE EXTRACTION ALGORITHMS	9
	A. PREVIOUS WORK	9
	1. Direct Minimization	9
	2. Prony's Method	11
	B. KUMARESAN-TUFTS ALGORITHM	12
	1. Equations	13
	2. Singular Value Decomposition	14
	3. Bias Compensation	16
	4. Kumaresan and Tufts Compensation	16
	5. Compensation Based on Eigenvalue Shifting Theorem	17
	6. Performance	19
	a. Synthetically Generated Data	19
	1. Noise Performance	19
	b. Thin Wire Integral Equation Generated	29
	c. Scale Model Measurements	38
	1. Wire Targets	50
	2. Aircraft Models	50
	C. CADZOW-SOLOMON ALGORITHM	63
	1. Applicability	68
	2. Equations	68
	3. Excess Poles and Noise Removal	69
	4. Singular Value Decomposition	70
	5. Bias Compensation in the Cadzow-Solomon Formulation	70
	6. Performance	72
	a. Synthetically Generated Data	72
	1. Noise Performance	72
	b. Thin Wire Integral Equation Generated Data	80
	c. Scale Models	80
	1. Wire Targets	92
	2. Model Aircraft	92

III. SUMMARIES AND CONCLUSIONS	108
A. KUMARESAN-TUFTS	108
B. CADZOW-SOLOMON	111
C. CONCLUSIONS	112
APPENDIX A. THE KUMARESAN-TUFTS POLE EXTRACTION ALGORITHM	113
APPENDIX B. THE CADZOW-SOLOMON POLE EXTRACTION ALGORITHM	125
APPENDIX C. MATRIX MULTIPLICATION	140
APPENDIX D. GRAPHICS ROUTINE	141
LIST OF REFERENCES	145
INITIAL DISTRIBUTION LIST	147

LIST OF FIGURES

Figure 1.	Signal Containing two S-Plane Poles, 90.0 dB SNR	21
Figure 2.	Kumaresan-Tufts Poles, Synthetic Data, 90.0 dB SNR	22
Figure 3.	Kumaresan-Tufts Poles, Synthetic Data, 30.0 dB SNR	23
Figure 4.	Kumaresan-Tufts Poles, Synthetic Data, 20.0 dB SNR	24
Figure 5.	Kumaresan-Tufts Poles, Synthetic Data, 10.0 dB SNR	25
Figure 6.	Kumaresan-Tufts Poles, Synthetic Data, 7.0 dB SNR	26
Figure 7.	Signal Containing Two S-Plane Poles, 7.0 dB SNR	27
Figure 8.	Kumaresan-Tufts Pole Extraction, 7.0 dB SNR	28
Figure 9.	Double Gaussian Pulse	30
Figure 10.	Integral Equation Thin Wire Scattering, 30 Degree Aspect	32
Figure 11.	Integral Equation Thin Wire Scattering, 45 Degree Aspect	33
Figure 12.	Integral Equation Thin Wire Scattering, 60 Degree Aspect	34
Figure 13.	Integral Equation Thin Wire Scattering, 90 Degree Aspect	35
Figure 14.	Kumaresan-Tufts Poles, Noiseless Thin Wire Data	36
Figure 15.	Integral Equation Thin Wire Scattering, 20.0 dB SNR, 45 Degree Aspect	37
Figure 16.	Kumaresan-Tufts Poles, 20.0 dB SNR	39

Figure 17.	Integral Equation Thin Wire Comparison, Noiseless vs. 20.0 dB SNR, 30 Degree Aspect	40
Figure 18.	Integral Equation Thin Wire Comparison, Noiseless vs. 20.0 dB SNR, 45 Degree Aspect	41
Figure 19.	Integral Equation Thin Wire Comparison, Noiseless vs. 20.0 dB SNR, 60 Degree Aspect	42
Figure 20.	Integral Equation Thin Wire Comparison, Noiseless vs. 20.0 dB SNR, 90 Degree Aspect	43
Figure 21.	Integral Equation Thin Wire Scattering, 7.0 dB SNR, 45 Degree Aspect	44
Figure 22.	Kumaresan-Tufts Poles, 7.0 dB SNR	45
Figure 23.	Integral Equation Thin Wire Comparison, Noiseless vs. 7.0 dB SNR, 30 Degree Aspect	46
Figure 24.	Integral Equation Thin Wire Comparison, Noiseless vs. 7.0 dB SNR, 45 Degree Aspect	47
Figure 25.	Integral Equation Thin Wire Comparison, Noiseless vs. 7.0 dB SNR, 60 Degree Aspect	48
Figure 26.	Integral Equation Thin Wire Comparison, Noiseless vs. 7.0 dB SNR, 90 Degree Aspect	49
Figure 27.	Measured Thin Wire Scattering, 30 Degree Aspect	51
Figure 28.	Measured Thin Wire Scattering, 45 Degree Aspect	52
Figure 29.	Measured Thin Wire Scattering, 60 Degree Aspect	53
Figure 30.	Measured Thin Wire Scattering, 90 Degree Aspect	54
Figure 31.	Kumaresan-Tufts Poles, Measured Thin Wire	55

Figure 32.	Thin Wire Comparison, Measured vs. Integral Equation	56
Figure 33.	Target 1 Scattering, 30 Degrees from Nose on	57
Figure 34.	Target 1 Scattering, Nose on	58
Figure 35.	Target 2 Scattering, 30 Degrees from Nose on	59
Figure 36.	Target 2 Scattering, Nose on	60
Figure 37.	Kumaresan-Tufts Poles, Target 1	61
Figure 38.	Kumaresan-Tufts Poles, Target 1	63
Figure 39.	Kumaresan-Tufts Poles, Target 1	64
Figure 40.	Kumaresan-Tufts Poles, Target 2	65
Figure 41.	Kumaresan-Tufts Poles, Target 2	66
Figure 42.	Kumaresan-Tufts Poles, Target 2	67
Figure 43.	Signal Containing Two S-Plane Poles, 90.0 dB SNR	73
Figure 44.	Cadzow-Solomon Poles, Synthetic Data, 90.0 dB SNR	74
Figure 45.	Cadzow-Solomon Poles, Synthetic Data, 30.0 dB SNR	75
Figure 46.	Cadzow-Solomon Poles, Synthetic Data, 20.0 dB SNR	76
Figure 47.	Cadzow-Solomon Poles, Synthetic Data, 10.0 dB SNR	77
Figure 48.	Cadzow-Solomon Poles, Synthetic Data, 7.0 dB SNR	78
Figure 49.	Cadzow-Solomon Poles, Noiseless Thin Wire Data	81
Figure 50.	Cadzow-Solomon Poles, 20.0 dB SNR	82
Figure 51.	Integral Equation Thin Wire Comparison, Noiseless vs. 20.0 dB SNR, 30 Degree Aspect	83

Figure 52.	Integral Equation Thin Wire Comparison, Noiseless vs. 20.0 dB SNR, 45 Degree Aspect	84
Figure 53.	Integral Equation Thin Wire Comparison, Noiseless vs. 20.0 dB SNR, 60 Degree Aspect	85
Figure 54.	Integral Equation Thin Wire Comparison, Noiseless vs. 20.0 dB SNR, 90 Degree Aspect	86
Figure 55.	Cadzow-Solomon Poles, 7.0 dB SNR . . .	87
Figure 56.	Integral Equation Thin Wire Comparison, Noiseless vs. 7.0 dB SNR, 30 Degree Aspect	88
Figure 57.	Integral Equation Thin Wire Comparison, Noiseless vs. 7.0 dB SNR, 45 Degree Aspect	89
Figure 58.	Integral Equation Thin Wire Comparison, Noiseless vs. 7.0 dB SNR, 60 Degree Aspect	90
Figure 59.	Integral Equation Thin Wire Comparison, Noiseless vs. 7.0 dB SNR, 90 Degree Aspect	91
Figure 60.	Cadzow-Solomon Poles, Measured Thin Wire	93
Figure 61.	Thin Wire Comparison, Measured vs. Integral Equation	94
Figure 62.	Cadzow-Solomon Poles Target 1, Three Aspects	95
Figure 63.	Cadzow-Solomon Poles Target 1, Three Aspects	96
Figure 64.	Cadzow-Solomon Poles Target 1, All Six Aspects	97
Figure 65.	Cadzow-Solomon Poles Target 2, Three Aspects	98
Figure 66.	Cadzow-Solomon Poles Target 2, Three Aspects	99

Figure 67.	Cadzow-Solomon Poles Target 2, All Six Aspects	100
Figure 68.	Pole Comparisons, Target 1, All Six Aspects	101
Figure 69.	Pole Comparisons, Target 2, All Six Aspects	102
Figure 70.	Target 3 Scattering, Nose-on	104
Figure 71.	Target 4 Scattering, Nose-on	105
Figure 72.	Cadzow-Solomon Pole Comparisons, 4 Targets, Nose on	106

I. INTRODUCTION

A radar target, acting as a scatterer of a specified incident electromagnetic wave, can be considered as a single input, single output, linear time-invariant (LTI) system for a fixed field observation point. The target can thus be considered as a transfer function with poles and zeros. Baum demonstrated at the Air Force Weapons Laboratory that a target's induced current response to an incident electromagnetic wave has identifiable poles determined by the composition and structural geometry of the target [1]. In 1974, Moffatt and Mains proposed that the target's scattered field pole locations are independent of the incident electromagnetic excitation, including aspect and polarization [2]. Morgan has proven theoretically that, for the case of a conducting target, the scattering response contains complex natural resonances which are independent of the incident electromagnetic excitation [3]. By determining the poles of a target's response, aspect independent target identification can be accomplished through the use of electromagnetic natural resonances.

Although the concept of radar target identification through the use of natural resonances was first proposed in 1974 by Mains and Moffatt [2], only recently have signal

processing techniques been applied to locate the poles in a radar target's response in the presence of noise. Kumaresan-Tufts [4] and Cadzow-Solomon [5] have each developed algorithms which have proven successful in the presence of noise. This thesis develops computer routines based upon these two algorithms and examines their respective performance and appropriateness using a variety of scattering data.

A. THE PROBLEM

Since the performance of signal processing methods varies under different conditions, a system employed to identify targets would possibly reach a decision based on the combined output of several signal processing methods. For example, the Kumaresan-Tufts and Cadzow-Solomon methods could be used to extract poles from the response of scale model targets. The information so gathered could be used to build a data base for comparison with data similarly obtained in actual field use. The results of this system would serve as one input to a larger system. Other methods would provide input to the system, such as the K-pulse method of Kennaugh [6] and the annihilation filter used by Dunavin [7], Morgan and Dunavin [8] and Chen [9]. As the name suggests, an annihilation filter annihilates the target's poles. A system using the annihilation filter concept would contain many such filters, each previously designed to cancel the poles of a specific

known target. In actual field use, a radar target's response would be input into each of the filters, and the target selected would be that matching the filter whose output exhibits the lowest signal energy.

A system used to identify radar targets would require the following concept of employment. First, information required by each of the sub-systems would be obtained for every target class of concern. In actual field use, this information would be compared against actual radar target responses. The system would then determine the identity of the target based on the input from each of its sub-systems.

B. BACKGROUND

Consider a perfectly conducting target illuminated by an electromagnetic field. The current induced on the surface of this target at a given point must satisfy the magnetic field integral equation (MFIE), [10]

$$\bar{J}(\mathbf{r}, t) = 2\hat{n} \times \bar{H}^i(\bar{\mathbf{r}}, t) + \iint_{S_{pv}} \tilde{K}(\bar{\mathbf{r}}, \bar{\mathbf{r}}', t) \bar{J}(\mathbf{r}, \frac{t - |\bar{\mathbf{r}} - \bar{\mathbf{r}}'|}{c}) dS \quad (1)$$

where \hat{n} is an outward unit vector normal to the surface of the object, \bar{J} is the surface current density, \bar{H}^i is the incident magnetic field, and \tilde{K} is a Green's function dyadic. The entire equation is most easily understood as the sum of driven currents and "feedback" currents corresponding to the

cross-product term and surface integral term respectively. The term driven by the magnetic field, $2\hat{n}\times\bar{H}^i$, forms the physical optics portion of the total current. Physical optics describes the cross-product term as the induced current without interaction with the rest of the body. The Green's function kernel describes the current at a point on the object due to the feedback of currents from every other point on the object, as previously illuminated by the incident field. The current at each point is then summed over the surface of the object. Note that the surface integral term is of principal-value type; the integral excludes the point $\bar{r}=\bar{r}'$.

Once the incident magnetic field is no longer present, the solutions of (1) are considered the natural modes of the object. These natural modes are of the form, $J_n \exp(s_n)$. The natural resonance frequencies s_n are of the form,

$$s_n = \sigma_n + j\omega_n \quad (2)$$

where σ_n is the damping rate in Nepers/sec and ω_n is the frequency in radians/sec. The natural resonances of (2) are functions of the structural geometry of the object and are independent of the incident magnetic field. To understand how these natural resonances are unique to the geometry and composition of the object, consider a set of points on the object previously illuminated by the incident field, so that $\bar{H}^i=0$. The current at a given point in the set is due to the

infinite number of feedback currents from every other point in the set. Recall that these feedbacks are described by the Green's function kernel in the integral term of (1). Since the set of points previously illuminated is physically located on the same object, the infinite number of paths that connect a point with all other points in the set is the same for all points in the set. The infinite number of paths are unique to the structural geometry of the object and correspond exactly to the infinite number of paths taken by currents which feedback to a given point via the Green's function kernel. Finally, the composition of the target determines the surface current density on the object. Although an infinite number of resonances exists in any object, only a limited number of these will be measurably excited by an incident field of finite bandwidth. These resonances described in (2) appear as complex conjugate pairs in the left-half portion of the s-plane.

In the far-field, the back-scattered response of a target to an incident plane wave is of the form

$$\vec{H}^S(-r\hat{p}, t) = \frac{1}{4\pi cr} \frac{\partial}{\partial t} \iint_S \hat{p} \times \vec{J}(\vec{r}', t - |\vec{r} - \vec{r}'|/c) dS' \quad (3)$$

where c is the speed of light and \hat{p} is the unit vector whose direction matches that of the plane wave's propagation.

Equation (3) is the result of integrating the current at each point on the target surface for a fixed point in the far-field. Recall that the current at each point on the target is defined by (1). Thus, the back-scattered far-field can be obtained by substituting (1) into (3):

$$\bar{H}^S(-r\hat{p}, t) = u(t-r/c) \left\{ H_{p_0}(-r\hat{p}, t) + \sum_{\substack{n=-\infty \\ n \neq 0}}^{\infty} H_n(-r\hat{p}, t) \exp(s_n t) \right\} \quad (4)$$

The currents in (1) produce the field in (4). In fact, each term in (4) corresponds to the term in (1) which produced it. Specifically, the first term in (4) describes the physical optics scattered field generated by the $2\hat{n} \times \bar{H}^1$ current which, of course, is the first term in (1). Similarly, the second term in (4) is produced by the source-free currents defined by the second term in (1). Like the current described in (1), the field in (4) is the sum of two terms, a driven term and a term containing feedbacks.

The results of (4) can also be seen as two forms of the Singularity Expansion Method (SEM) developed by Baum [1]. As shown by Morgan [10], during the early-time portion of the target's response, the scattered field is composed of the physical optics scattered field and a "Class 2" form of the SEM expansion. The class 2 SEM expansion corresponds to the second term of (4), wherein the coefficients H_n are time-varying as the wave passes over the target, since the currents

producing this portion of the field are integrated over a time-varying surface area. At the instant the wave passes the last point of the target, the physical optics field vanishes and the remaining term in (4) is produced by constant coefficients H_n . The coefficients H_n are constant at this instant since the surface area in the integral in (3) is now constant. This instant also marks the transition of (4) from a "class 2" SEM expansion of time-varying coefficients to a "class 1" SEM expansion of constant coefficients. The scattered field due to a plane wave is therefore composed of a physical optics term and a class 2 SEM expansion in the early-time, and a simple class 1 expansion in the late-time.

Actual measurement of the scattered far-zone field would be greatly aided by knowledge of the transition time of the field from early time to late time. From [10], this transition for a monostatic radar would occur at $\Delta t = T + 2(D+d)/c$ seconds after radar turn-on. Here, T is the pulse duration, D is the target's dimension along the direction of wave propagation, d is the distance between the target and the measurement point and c is the speed of light.

The discussion presented in this section was extracted from work done by Morgan in [10]. The reader is referred to this work for a more detailed treatment of the material in this section.

C. HISTORY

The results of the previous section form the basis for the hypothesis that the natural resonances found in the scattering response of a target to an incident electromagnetic wave are unique to that target. Additionally, only a finite set of these natural resonances are measurably excited by a wave of finite bandwidth. In 1974, Moffatt and Mains proposed that the extraction of resonances from a target's response to electromagnetic excitation could be used for target identification. This work related to earlier work in 1965, when Kennaugh and Moffatt first developed the concept of a radar target as a linear time invariant system. Poles in the z-plane are directly related to the natural resonances of a target

$$z_n = e^{s_n \Delta t} \quad (5)$$

where s_n is given by (2) and Δt is the sampling interval in seconds. Hence, pole extraction involves resonance identification. The use of pole extraction algorithms is discussed in the next chapter.

II. POLE EXTRACTION ALGORITHMS

The use of pole extraction algorithms to identify radar targets is discussed in this chapter. A brief discussion of two methods precedes the in-depth evaluation of the Kumaresan-Tufts and Cadzow-Solomon algorithms. The evaluation of the latter two algorithms occurs in two stages. First, each algorithm will be evaluated in its ability to extract poles from data with known poles. Some of the data processed was generated at various signal to noise ratios by a computer program written by Morgan [11]. Additional data was produced by Morgan's time-domain thin wire integral equation computer program [12]. In the second stage, a side by side comparison is made of poles extracted by each method using transient scattering measurements for a thin wire and for various model aircraft. Comparisons between the two methods are made as the aspect of the aircraft is varied.

A. PREVIOUS WORK

1. Direct Minimization

The most direct way to determine the natural resonances in a target's response is to minimize the mean-square error between the modeled signal and the received signal. In [10], Morgan determined that the late-time target

response to a radar could be represented as a sum of damped sinusoids given by

$$\hat{y}(t) = \sum_{i=1}^{\infty} A_i e^{\sigma_i t} \cos(\omega_i t + \theta_i) \quad (6)$$

The frequency, ω_i , and damping rate, σ_i , are the same parameters found in the natural resonance defined in (2). Phase, θ_i , and amplitude, A_i , are the remaining parameters. The representation in (6) is the sum of an infinite number of resonances. The sampled response to an incident wave of finite bandwidth can be modeled as

$$\hat{y}(n\Delta t) = \hat{y}_n = \sum_{i=1}^N A_i e^{\sigma_i n\Delta t} \cos(\omega_i n\Delta t + \theta_i) \quad (7)$$

where Δt is the sampling interval in seconds. The four parameters of (7) must be adjusted to minimize the sampled mean-square error signal

$$e_n^2 = (y_n - \hat{y}_n)^2 \quad (8)$$

between the actual discrete sampled received signal y_n and the modeled signal \hat{y}_n . The processing required in this minimization problem is both inefficient and highly non-linear. Nevertheless, Chong used this method to process mathematically-generated data down to 15.0 dB signal-to-noise (SNR) ratio [13].

2. Prony's Method

As in direct minimization, Prony's approach to resonance classification focuses on the late-time portion of a radar target's response. However, linear processing and root solving are used. The late-time response is modeled as the output of an LTI system of order K_D . Each signal received at some discrete sample, n , is considered to be the weighted sum of K_D previous signals. Thus, the finite term approximation of the received late-time signal, \hat{y}_n , is defined by

$$Y_n = \sum_{i=1}^{K_D} b_i Y_{n-i} \quad (9)$$

The z-transform of (9) is

$$z^{K_D} - b_1 z^{K_D-1} - b_2 z^{K_D-2} \dots - b_{K_D} = 0 \quad (10)$$

The roots of this polynomial in z are the poles of the system model. Therefore, the key to extracting the poles in the system's response lies in solving for the coefficients b_i of (9).

A set of K_D+M received signals in M equations (9) can be arranged in matrix form as

$$\begin{bmatrix} Y_0 & \dots & Y_{K_D-1} \\ \vdots & & \vdots \\ Y_{M-1} & \dots & Y_{K_D+M-2} \end{bmatrix} \begin{bmatrix} b_{K_D} \\ \vdots \\ b_1 \end{bmatrix} = \begin{bmatrix} Y_{K_D} \\ \vdots \\ Y_{K_D+M-1} \end{bmatrix} \quad (11)$$

In Prony's original method, the data matrix D_y is exactly determined, and the coefficient vector, b , is solved using linear computations. In the presence of noise, Prony overdetermines the data matrix by setting $M > K_p$ and solves for the coefficient vector by obtaining the least-squares solution to the system of equations.

The Prony method has two major problems. First, the poles obtained by the least squares solution to the overdetermined matrix may be strongly perturbed by noise [14], since noise does not satisfy the causal model of the system. Second, the order of the system is generally not known *a priori*. When the estimated order is greater than the actual order, poles due to noise are generated. Prony's method offers no technique for distinguishing between the signal poles and the extra poles caused by overestimation of the system's order. If the estimated system order is less than the actual order, actual poles are lost and the remaining poles are perturbed from their true positions.

B. KUMARESAN-TUFTS ALGORITHM

The Kumaresan and Tufts pole extraction algorithm was developed by adapting Prony's method to reduce the problems addressed in the preceding section. The Kumaresan-Tufts algorithm modifies the least-squares Prony method in three ways:

1. Processed signals are arranged in a data matrix based on a non-casual model of the system.
2. The model of the system is deliberately overestimated.
3. The system of equations determined by the above two criteria is solved by using singular value decomposition (SVD).

Kumaresan demonstrates in [15] that the use of singular value decomposition tends to force the extra poles of the excess-order system inside the unit circle, while the non-causal arrangement of the signals tends to force the signal poles outside the unit circle. The excess order of the system model reduces the effects of noise on the actual poles. Since the noise is stationary and stable, it looks the same in forward and backward time.

1. Equations

Recall that in (9), Prony's technique defines the received late-time signal as the weighted sum of K_D previous signals, where K_D is presumed to be the order of the system. Kumaresan models the same late-time signal as the weighted sum of K_D future signals, where K_D is greater than the estimated order of the system. This non-casual model is given by

$$y_M = \sum_{l=1}^{K_D} b'_l y_{M+K_D+1-l} \quad (12)$$

A system of M such prediction equations can be written in matrix form as

$$\begin{bmatrix} Y_1 & \cdots & Y_{K_D} \\ \vdots & & \vdots \\ Y_M & \cdots & Y_{K_D+M-1} \end{bmatrix} \begin{bmatrix} b'_{K_D} \\ \vdots \\ b'_1 \end{bmatrix} = \begin{bmatrix} Y_0 \\ \vdots \\ Y_{M-1} \end{bmatrix} \quad (13)$$

Or, in matrix notation,

$$D_y \cdot b = y \quad (14)$$

As in Prony's method, the coefficients b'_i are coefficients of a polynomial in z that models the system's late-time response. Two simple manipulations of either data matrix leads to the relationship between the coefficients of the Prony model and the prediction coefficients of the Kumaresan-Tufts model. With $b_0 = -1$, a prediction coefficient is related to an autoregressive coefficient by

$$b'_i = - \frac{b_{i-1}}{b_{K_D}} \quad (15)$$

From the above relationship, it can be shown that the complex pole pairs of the causal model are merely conjugate reflections across the unit circle of the pole pairs in the non-causal model.

2. Singular Value Decomposition

The non-causal arrangement of late-time signals in a set of system equations, and subsequent processing through singular value decomposition, combine to separate the signal

and noise into orthogonal spaces. As discussed in the preceding paragraph, poles of the non-causal model are reflected outside the unit circle. Kumaresan demonstrates in [15] that the extra poles of the excess-order system can be forced inside the unit circle through the use of SVD.

Singular value decomposition factors the (MXK_D) data matrix D_y into the product of the matrices:

$$D_y = U \Sigma V^T \quad (16)$$

The columns of U (MXM) are eigenvectors of $D_y D_y^T$ and the columns of V ($K_D X K_D$) are eigenvectors of $D_y^T D_y$. If r is the rank of the data matrix, D_y , the diagonal matrix Σ (MXK_D) contains r singular values which are the square roots of the nonzero eigenvalues of both $D_y^T D_y$ and $D_y D_y^T$. By rearranging the three matrices in the product, the pseudoinverse of D_y can be obtained as

$$D_y^+ = V \Sigma^+ U^T \quad (17)$$

where Σ^+ is a $(K_D X M)$ matrix whose singular values on the diagonal are the reciprocals of those in the Σ matrix. Finally, the coefficient vector b^+ , of minimum Euclidian norm, is given by

$$b^+ = D_y^+ y \quad (18)$$

The coefficient vector b^* so obtained is the minimum length least-squares solution to (14). In other words, b^* is the best possible solution to (14). In the case of noiseless data, the extraneous poles generated by the excess-order model will always be inside the unit circle when b^* is used. This result is generally true for noisy data.

3. Bias Compensation

Kumaresan and Tufts [4] observed that the addition of noise perturbed the singular values of the Σ matrix of (16). If the perturbation of these singular values is not compensated, both the signal poles and extraneous poles are biased towards the unit circle. Kumaresan and Tufts used a compensation method which reduced the bias in their work, but did not derive an analytical justification. In [16], Norton derived a more valid bias compensation method based on the eigenvalue shifting theorem.

4. Kumaresan and Tufts Compensation

If the actual order of the system is K'_D , then the first K'_D singular values of the Σ matrix in (16) are non-zero. The remaining $K_D - K'_D$ singular values are considered noise singular values and are zero in the case of noiseless data. The addition of noise perturbs the first K_D signal singular values and increases the noise to some non-zero value. Kumaresan and Tufts compensated for this increase in the singular values due to the noise by subtracting the

Similarly, the expected value of $D_y^T D_y$, the other source of singular values, is

$$E[D_y^T D_y] = S^T S + \sigma_v^2 I \quad (22)$$

The assumption in the results of (21) and (22) is that the diagonals of $E[N^T N] = E[NN^T]$ equals the noise variance σ_v^2 . Equations (21) and (22) show that in the mean, the squares of the singular values of D_y are increased by the noise variance.

The results lead to the method of eigenvalue compensation recommended by Norton in [16]. Recall from (16) that the eigenvalues of D_y are on the diagonal of the Σ matrix returned by the singular value decomposition of D_y . If K_D' is the actual order of the system, and K_D is the estimated order of the system then the remaining $K_D - K_D'$ singular values of the Σ matrix can be squared and averaged to obtain an estimate of the noise variance, σ_v^2 . These noise singular values can then be set to zero. The first K_D singular values of the Σ matrix are then squared and reduced by subtracting the estimate of the noise variance. The square root of the difference becomes the new first K_D singular values of the compensated Σ matrix. Calculations according to (17) and (18) can then be carried out in a normal manner to obtain poles in the presence of the noise. Eigenvalue compensation requires an estimate of the actual order of the system. Methods to obtain this estimate are discussed in Chapter III.

6. Performance

The Kumaresan-Tufts algorithm was programmed in Fortran and tested on various types of data. The program appears in Appendix A.

a. Synthetically Generated Data

The starting point for evaluating the performance of the Kumaresan-Tufts algorithm was with synthetically generated data of the form given by (8) and shown here again for convenience

$$\hat{y}_n = \sum_{i=1}^N A_i e^{\sigma_i n \Delta t} \cos(\omega_i n \Delta t + \theta_i) \quad (8)$$

Again, $A_i, \sigma_i, \omega_i, \theta_i$, are the amplitude, damping rate, frequency and phase of a set of N damped sinusoids. Noisy data was created by adding stationary white noise.

1. Noise Performance

The algorithm was evaluated at various SNR's, ranging from 90.0 dB to 7.0 dB. These SNR's are ratios of signal energy to noise energy rather than the ratio of signal-to-noise power. Synthetic data so generated more closely resembles the exponential decay of signal power typical in actual radar measurements.

Figure 1 shows the signal produced by two s-plane poles at 90.0 dB. Figures 2 through 6 depict the poles extracted from this signal at SNR's ranging from 90.0 dB to 7.0 dB. Obtained poles are shown at their positions within the upper right hand quadrant of the unit circle in the z-plane. Not shown are conjugates of each pole which are located below the real axis outside the figure boundaries.

Figures 2 through 6 demonstrate outstanding performance on noisy data, even at SNR's of 7.0 dB. The scaling needed to show a discernible difference between results obtained at 30.0 dB and 7.0 dB would necessarily exclude one of the poles from the enlarged figure. The average distance of the trial poles obtained in the 7.0 dB SNR signal from the true poles is on the order of 10^{-3} . This magnitude corresponds to that of the average estimate of the noise variance obtained in successive trials with this signal. The correlation between the distance of trial poles from true poles and the noise variance estimate was consistently observed with each of the different signal-to-noise ratios used. Figure 7 depicts the signal of Figure 1 severely corrupted by noise having 7.0 dB SNR.

As discussed previously, the signal-to-noise ratio used in the synthetically generated data is the ratio of energy. Figure 8 depicts the results of pole extraction from the signal shown in Figure 7, but with a late-time

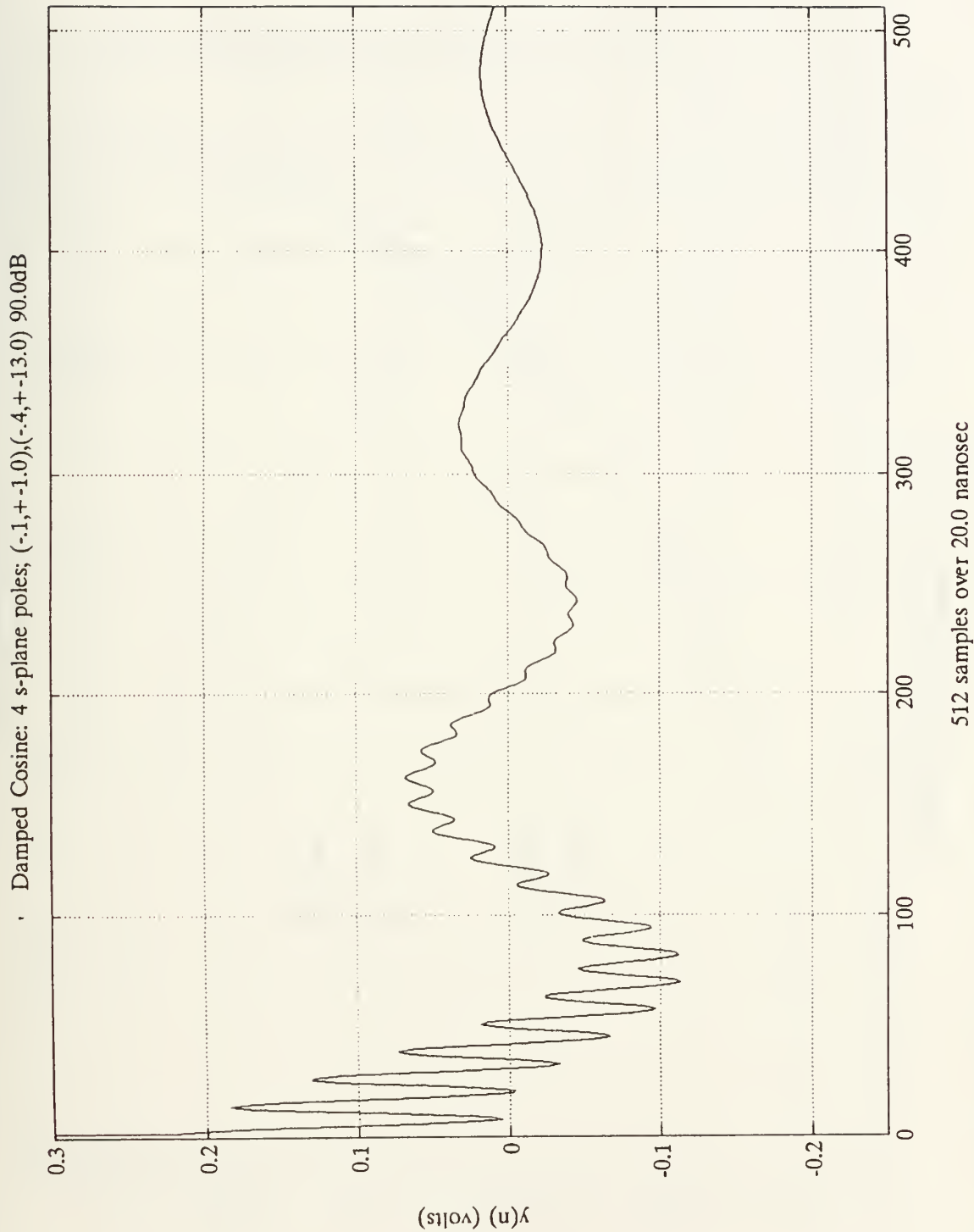


Figure 1. Signal Containing two S-Plane Poles, 90.0 dB SNR

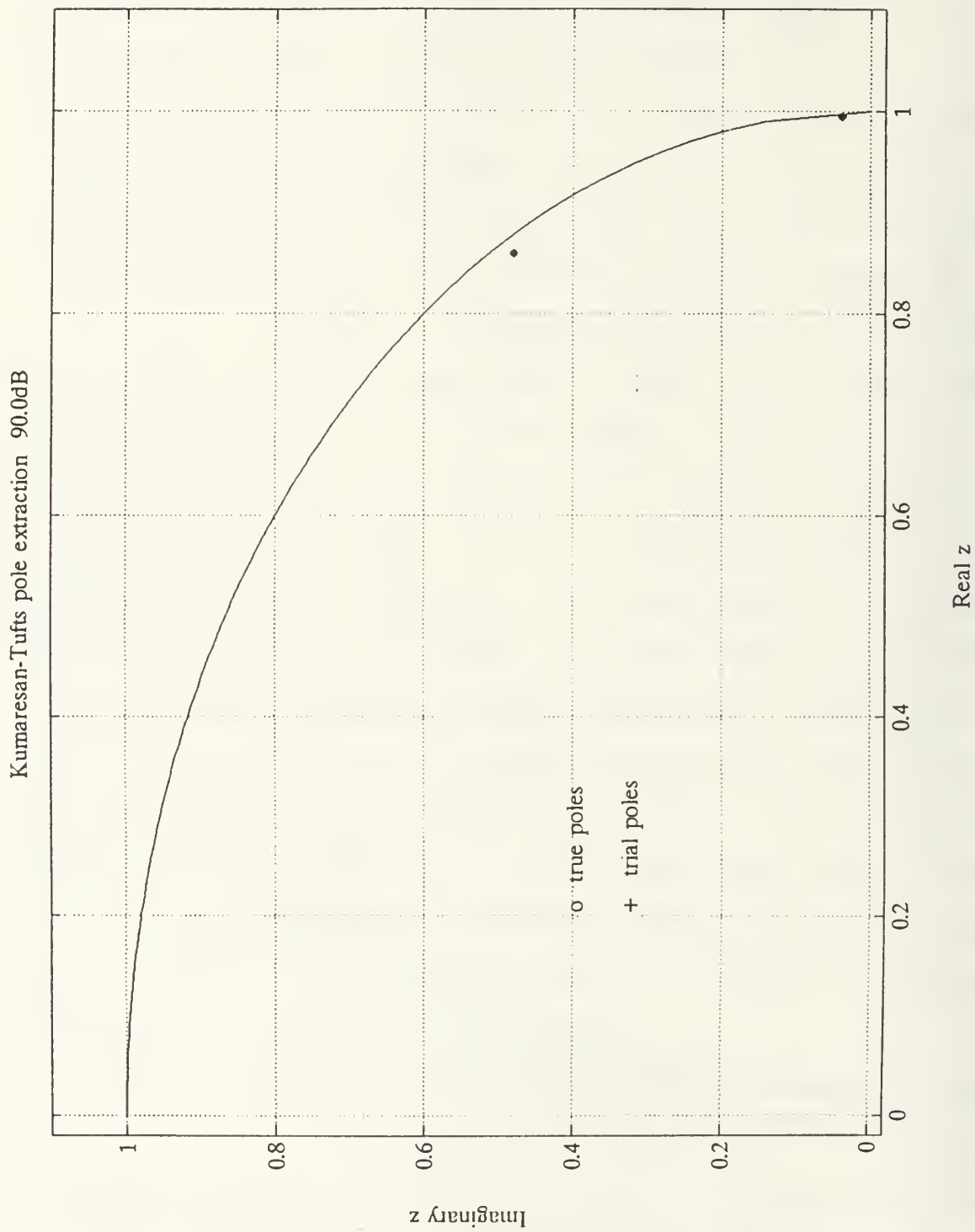


Figure 2. Kumaresan-Tufts Poles, Synthetic Data, 90.0 dB SNR

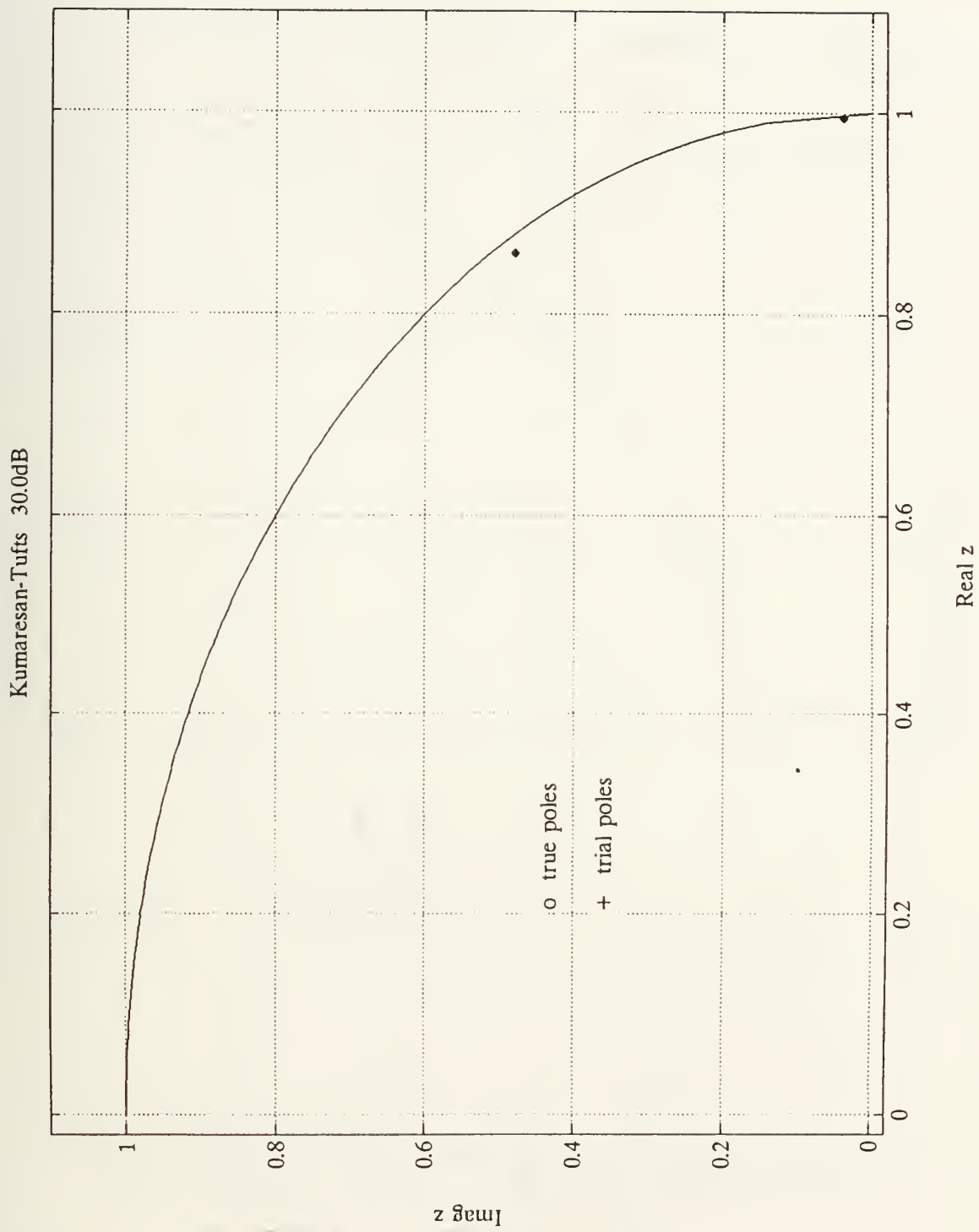


Figure 3. Kumaresan-Tufts Poles, Synthetic Data, 30.0 dB SNR

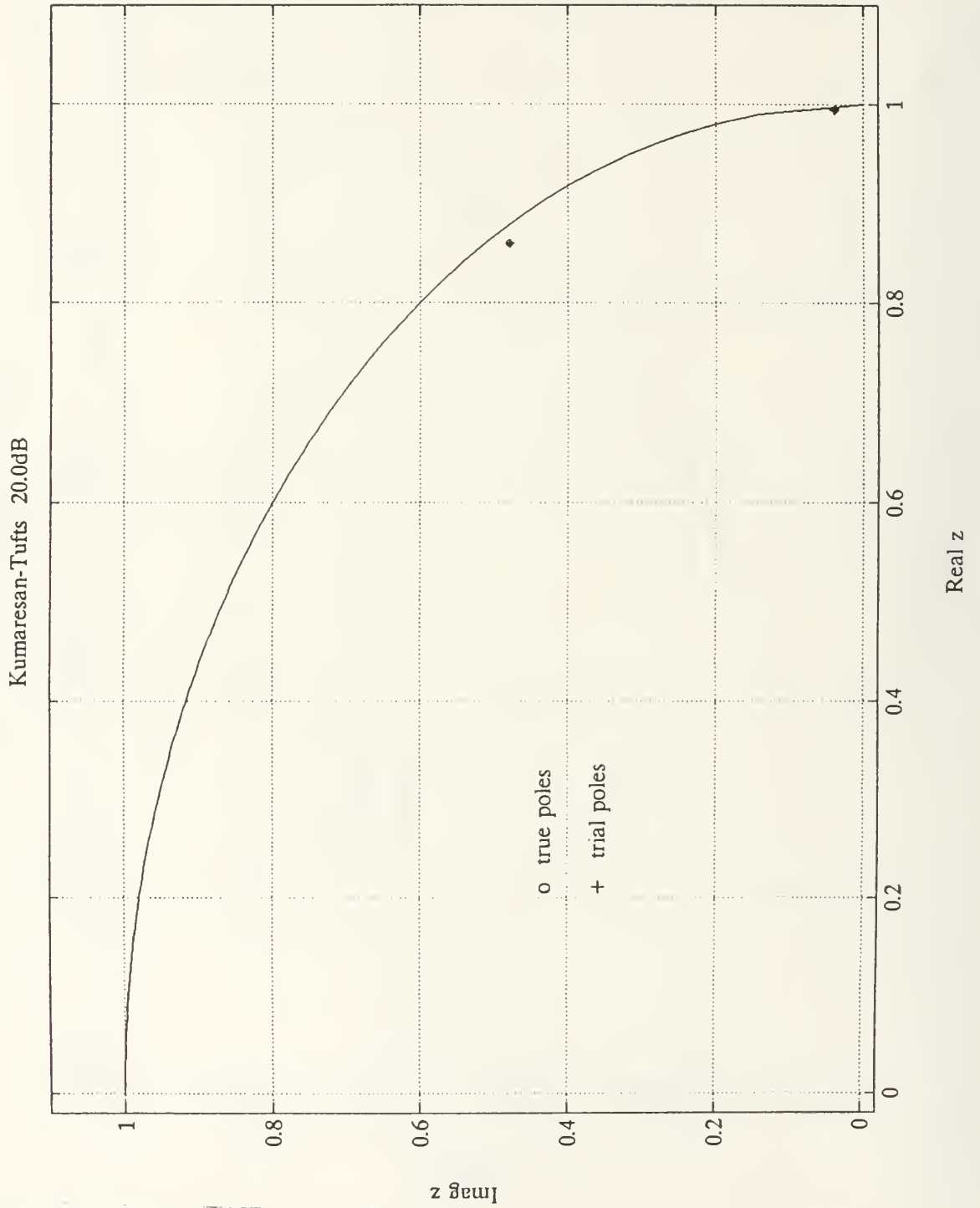


Figure 4. Kumaresan-Tufts Poles, Synthetic Data, 20.0 dB SNR

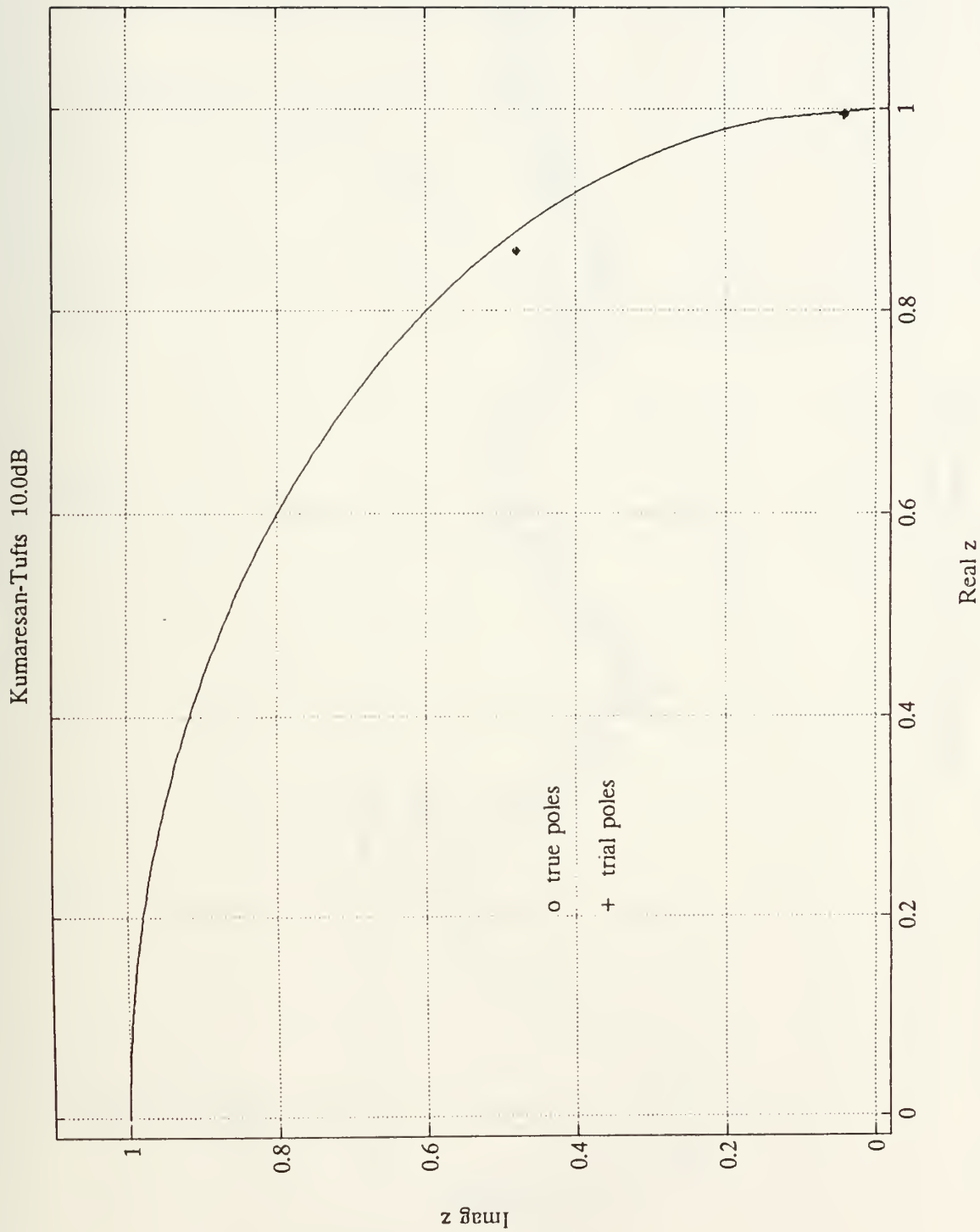


Figure 5. Kumaresan-Tufts Poles, Synthetic Data, 10.0 dB SNR

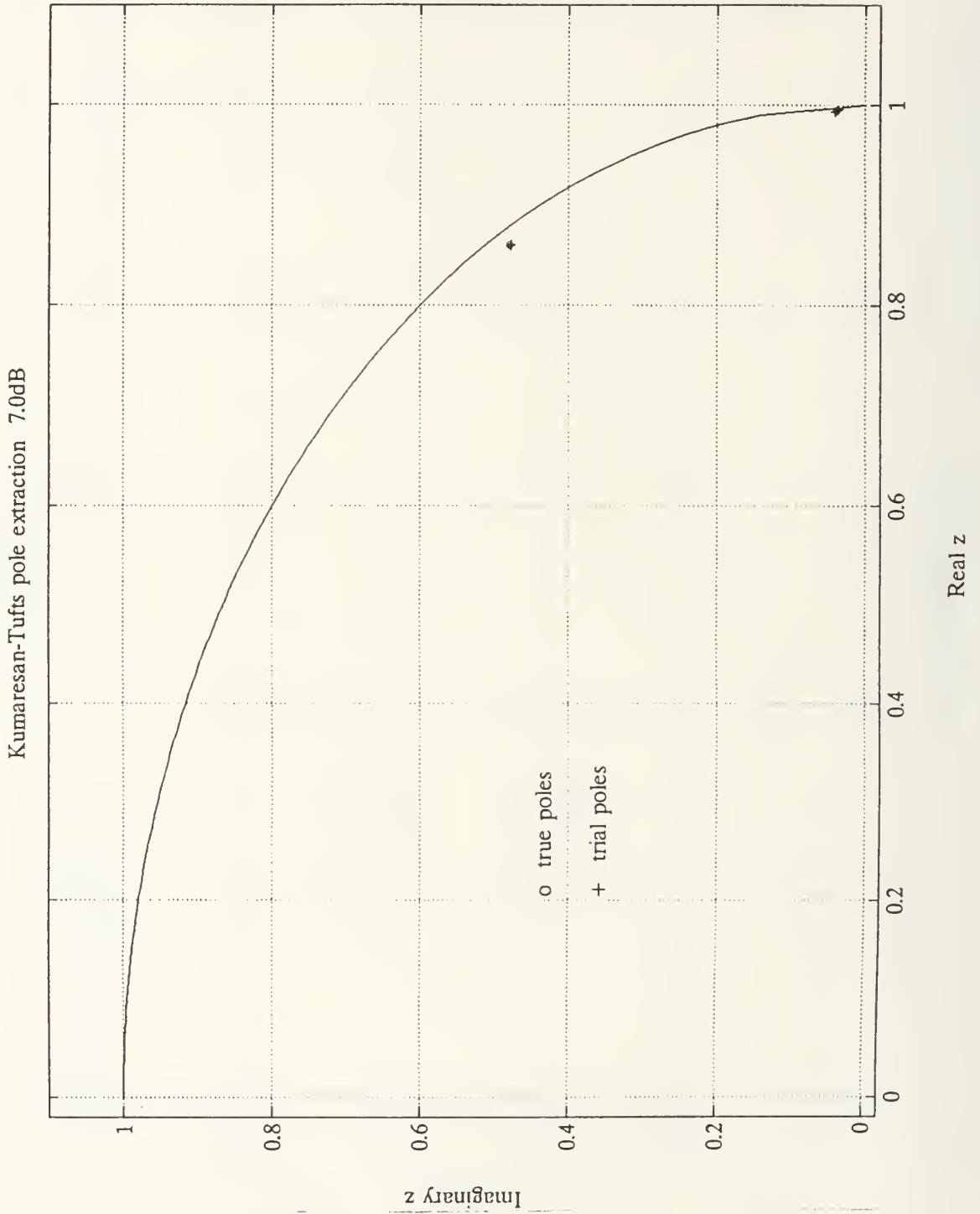
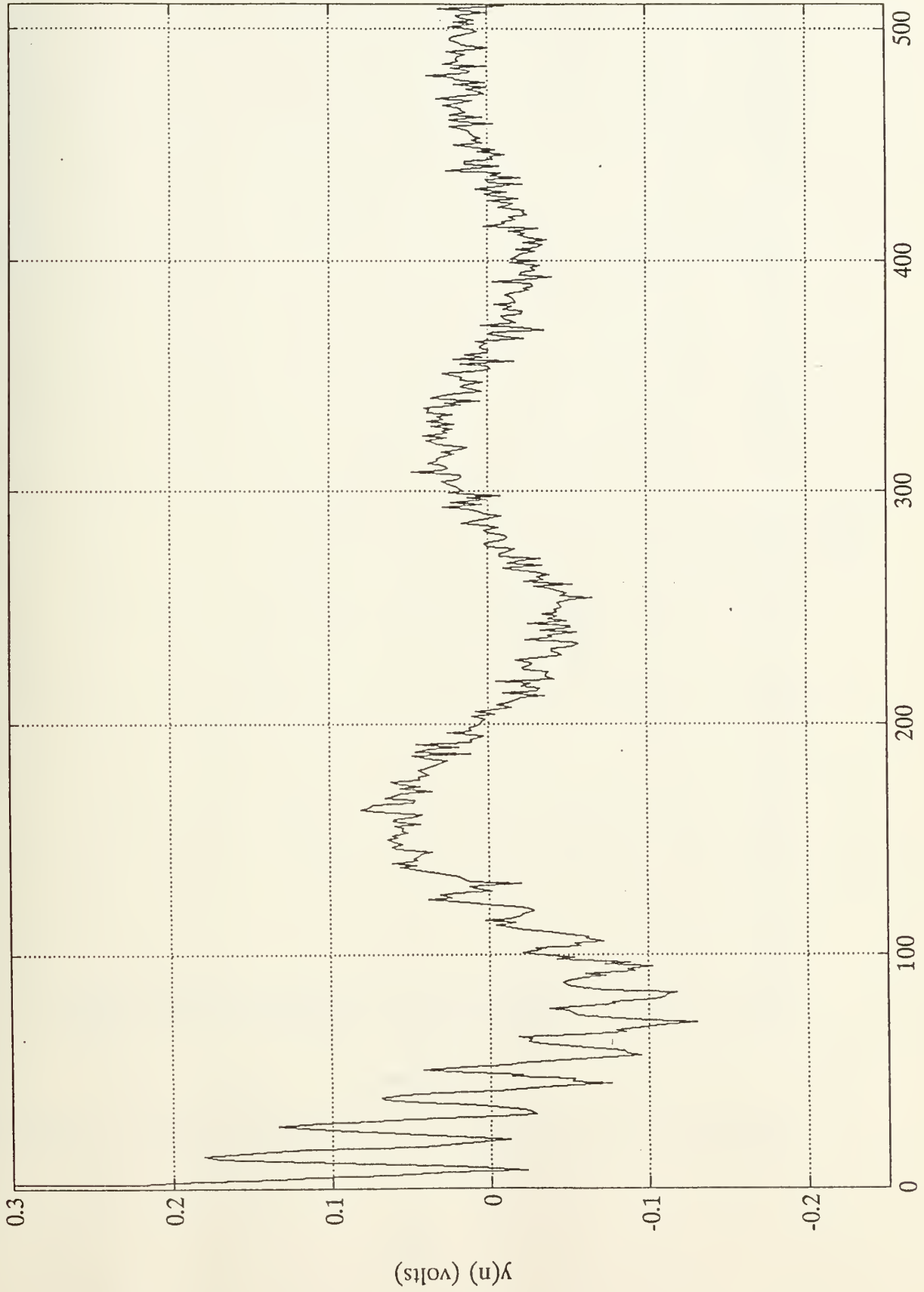


Figure 6. Kumaresan-Tufts Poles, Synthetic Data, 7.0 dB SNR

Damped Cosine: 4 s-plane poles; (-.1,+1.0),(-.4,+13.0) 7.0dB



512 samples over 20.0 nanosec

FIGURE 7 SIGNAL CONTAINING TWO S-PLANE POLES, 7.0dB

Kumaresan-Tufts pole extraction, 7.0dB, early time 10.0 nanosecs

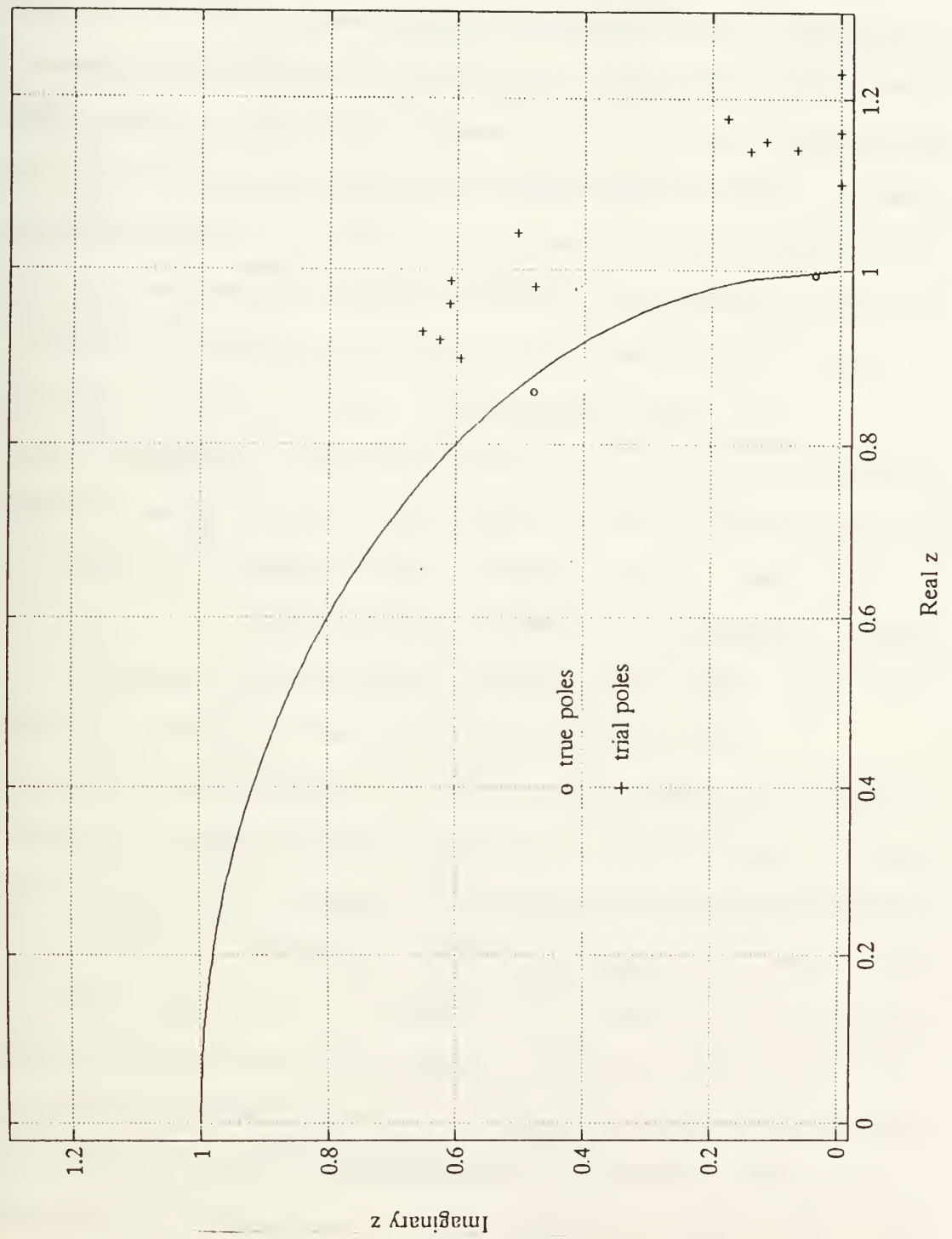


Figure 8. Kumaresan-Tufts Pole Extraction, 7.0 dB SNR

beginning ten nanoseconds later. Since the SNR is calculated over twenty nanoseconds for both signals, the signal power at some later time will clearly be less than the power ten nanoseconds earlier. The results in Figure 8 show complete breakdown of the algorithm's ability to extract poles. The trial poles shown are the poles closest to the true poles, and yet they are located at positions whose reflections are inside the unit circle where noise poles are typically located.

The preceding results show outstanding accuracy for full-length noisy data but a complete breakdown of the algorithm for the same signal with a later transition to late-time. These initial observations are supported by similar findings presented in this thesis.

b. Thin Wire Integral Equation Generated Data

For simple objects such as a thin wire, the radar response of that object can be computed by establishing boundary conditions on the object and numerically solving the integral equations that describe the surface current. Recall the magnetic field integral equation given by (1). Simulations produced by Morgan's time-domain thin wire integral equation computer program [12] were used to evaluate the pole extraction algorithm. The excitation waveform used is the double Gaussian pulse depicted in Figure 9. This pulse is a wide Gaussian pulse with a ten percent width of 0.3 nanoseconds subtracted from a narrow Gaussian pulse with a ten

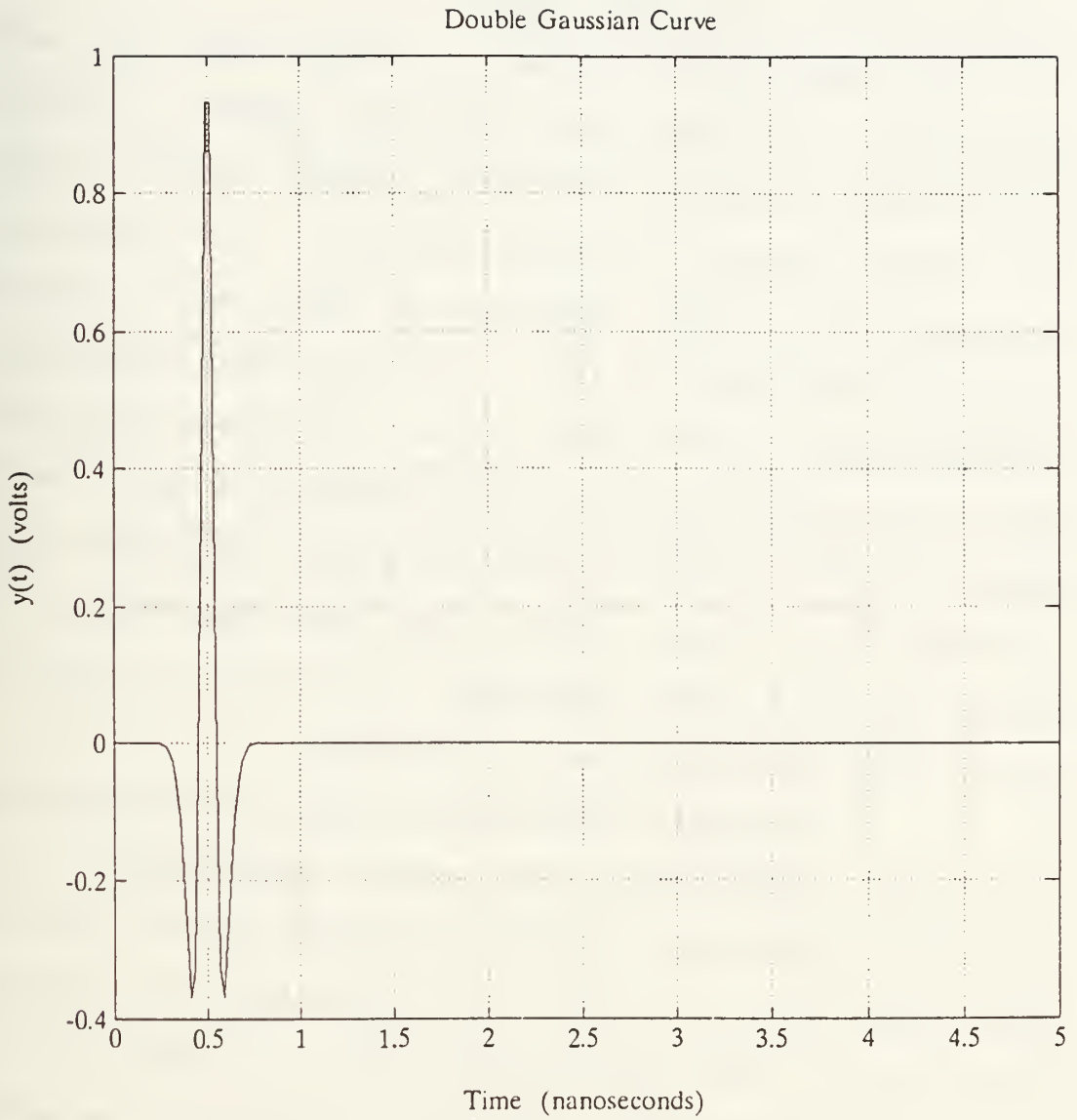


Figure 9. Double Gaussian Pulse

nanoseconds subtracted from a narrow Gaussian pulse with a ten percent width of 0.15 nanoseconds.

Figures 10 through 13 depict back scattering response of a 0.1 meter length thin-wire, having a radius of 0.00118 meter, computed at various incident aspects, ranging from thirty degrees to ninety degrees. The laboratory arrangement for actual measurements simulated by Morgan's program is described in [17]. Ninety degrees represents a broadside aspect, while thirty degrees represents the incident plane wave having nearly grazing incidence on the wire. The poles extracted at each of the four aspect angles are plotted in Figure 14. In this figure, and those that follow which depict extracted poles, the signal poles lie in or on the unit circle, and the noise poles lie outside.

The results obtained with this rigorous numerical computation demonstrate the aspect independence of the extracted poles using the Kumaresan-Tufts method. Note that only half of the poles were obtained for broadside illumination; two even-numbered poles can easily be seen outside the unit circle. This results because of the physical symmetry of both the wire and the incident field, thus precluding excitation of odd-symmetric modal currents and their associated natural resonances.

Figure 15 exemplifies the computed back-scattering response of the 0.1 meter thin wire corrupted artificially

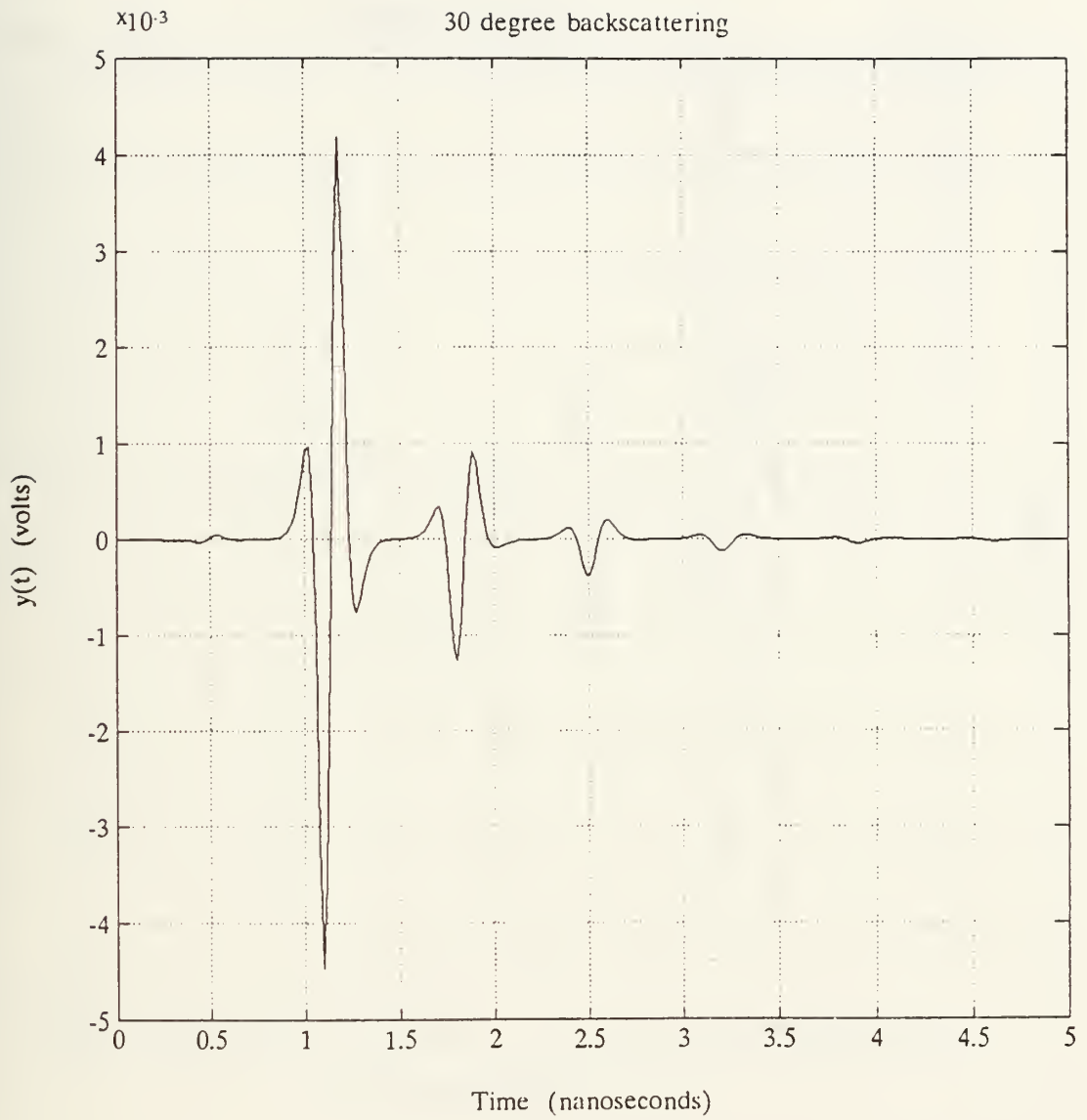


Figure 10. Integral Equation Thin Wire Scattering, 30 Degree Aspect

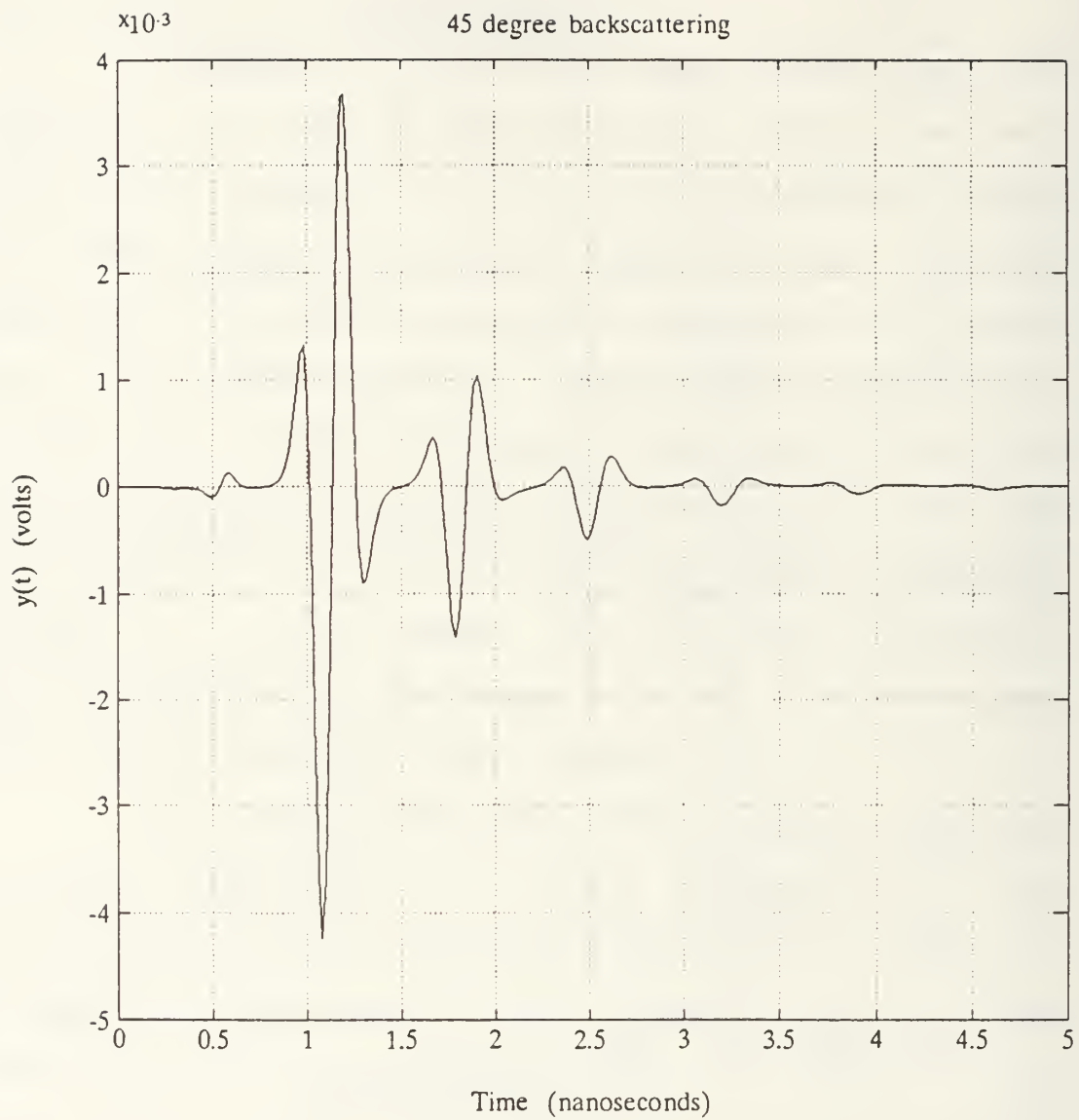


Figure 11. Integral Equation Thin Wire Scattering, 45 Degree Aspect

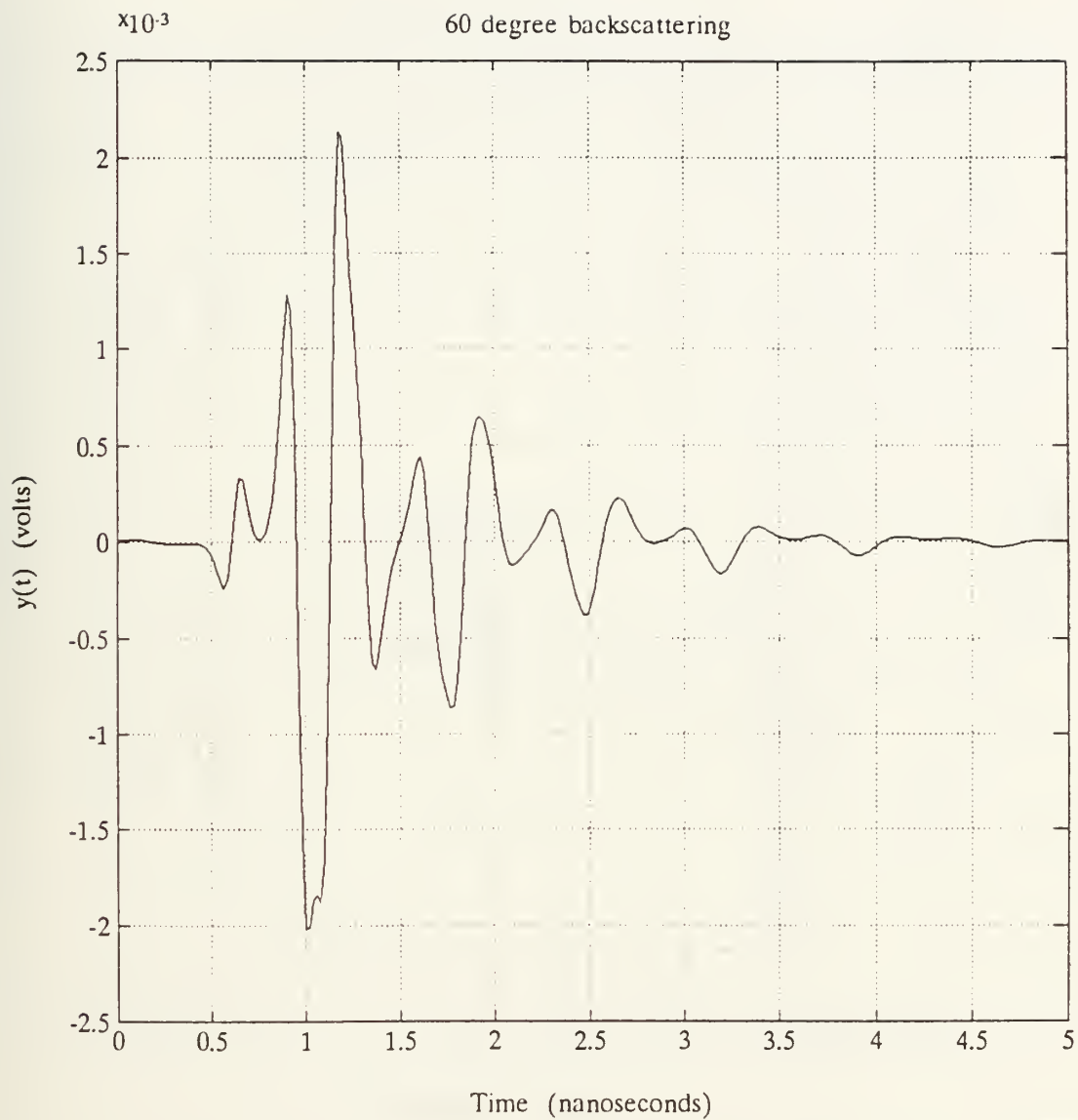


Figure 12. Integral Equation Thin Wire Scattering, 60 Degree Aspect

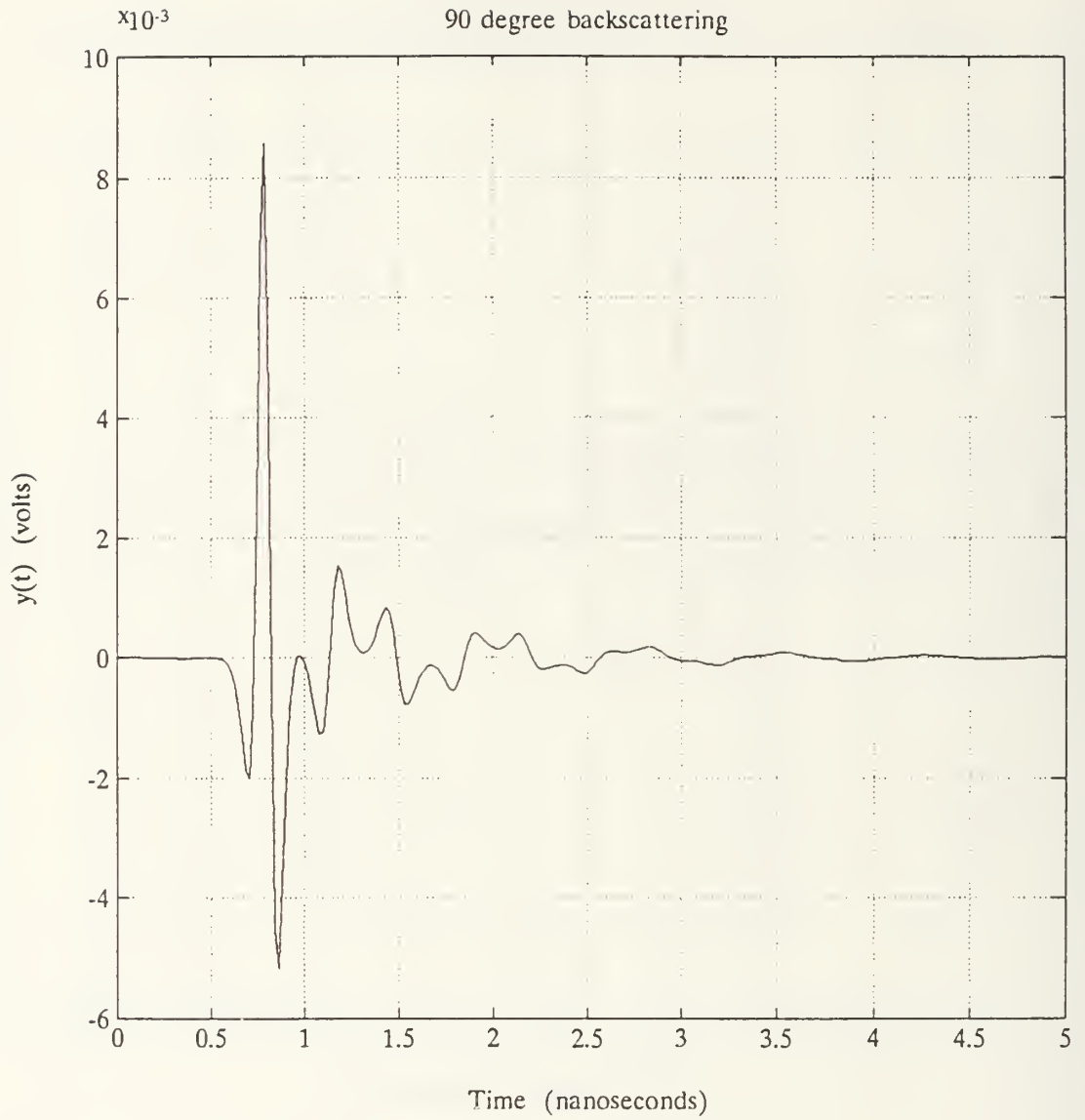


Figure 13. Integral Equation Thin Wire Scattering, 90 Degree Aspect

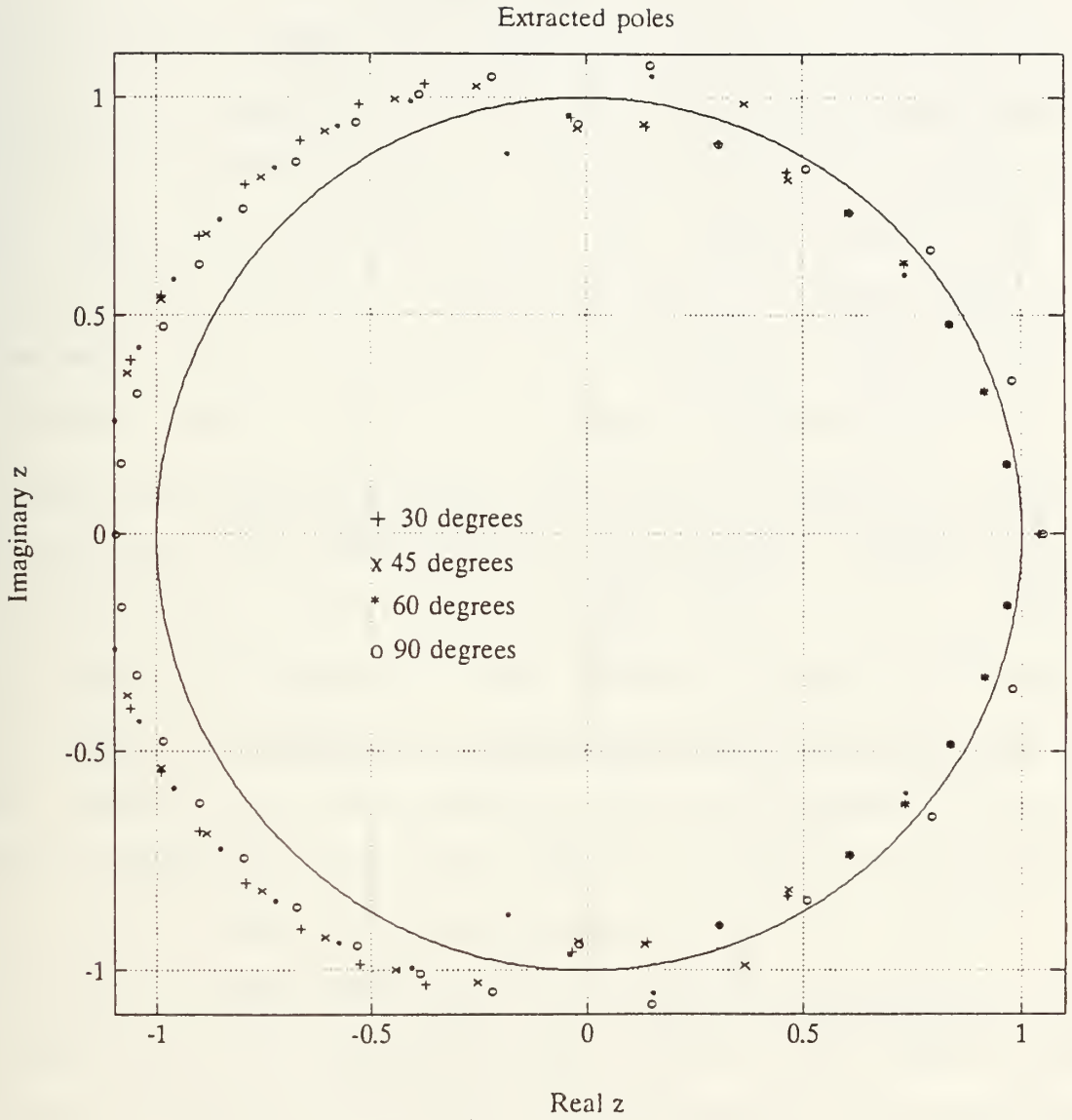


Figure 14. Kumaresan-Tufts Poles, Noiseless Thin Wire Data

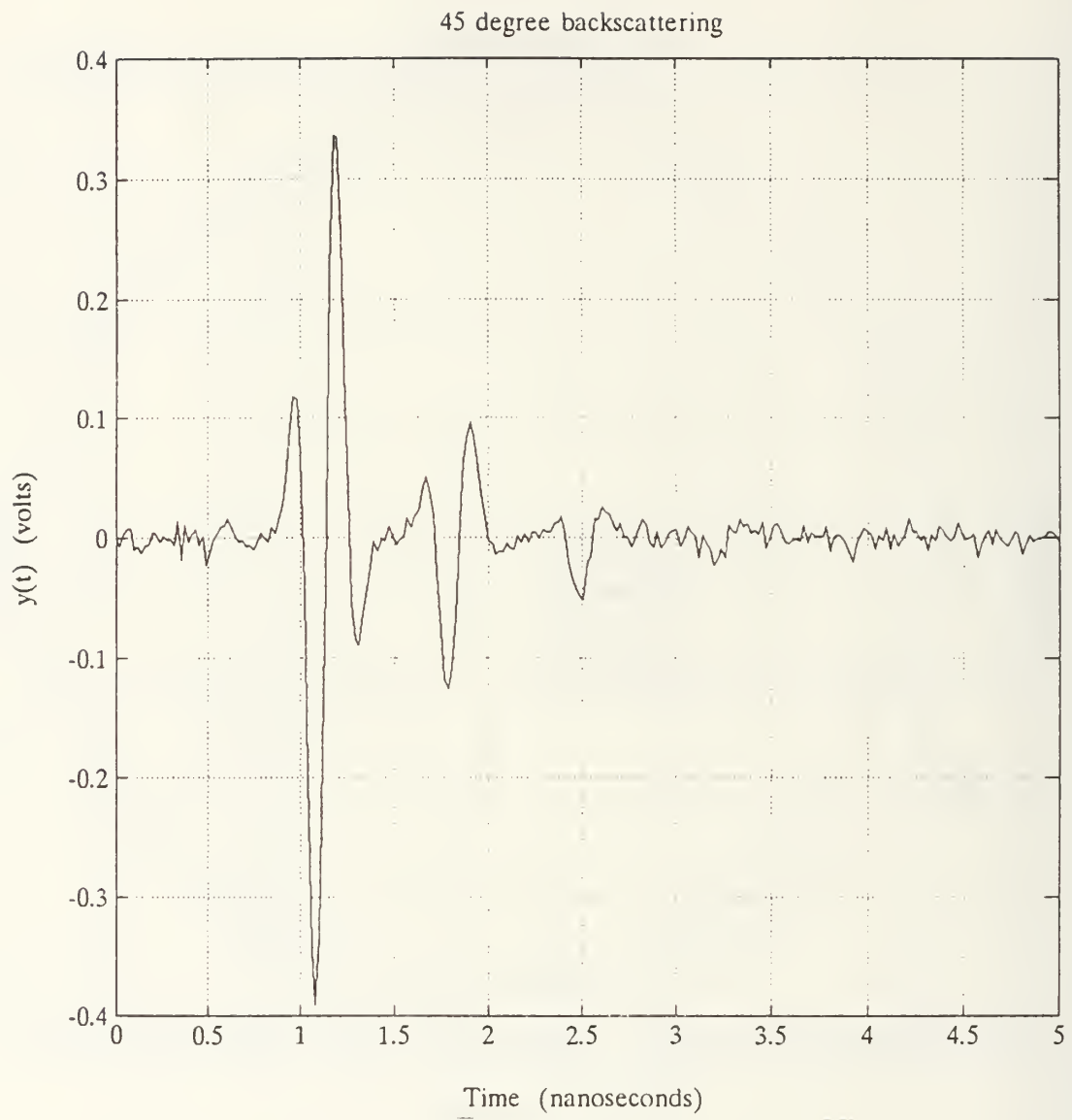


Figure 15. Integral Equation Thin Wire Scattering, 20.0 dB SNR, 45 Degree Aspect

with noise at a 20.0 dB SNR. Figure 16 shows the poles extracted at each of the four angles of incidence used previously in Figure 14. Poles of Figure 14 at 90° are now missing in Figure 16, and only the first three low frequency poles are tightly grouped. The loss of high frequency poles is expected because these have the highest damping and thus lose their energy at the fastest rate. Further comparison between results computed at 20.0 dB SNR and infinite SNR are offered, angle by angle, in Figures 17 through 20.

One additional test of the computed thin wire scattering was conducted at a 7.0 dB SNR. The corrupted waveforms are exemplified by Figure 21; the extracted poles are shown in Figure 22. The number of poles obtained has decreased with respect to the number obtained at 20.0 dB SNR. The grouping of the clusters has also expanded. Angle by angle comparisons are again offered in Figures 23 through 26.

c. Scale Model Measurements

The transient scattering measurements of scale models used for evaluation in this section were made by Walsh using the anechoic chamber of the Transient Electromagnetic Scattering Laboratory at the Naval Postgraduate School. The entire measurement process and laboratory setup are described in detail in [17].

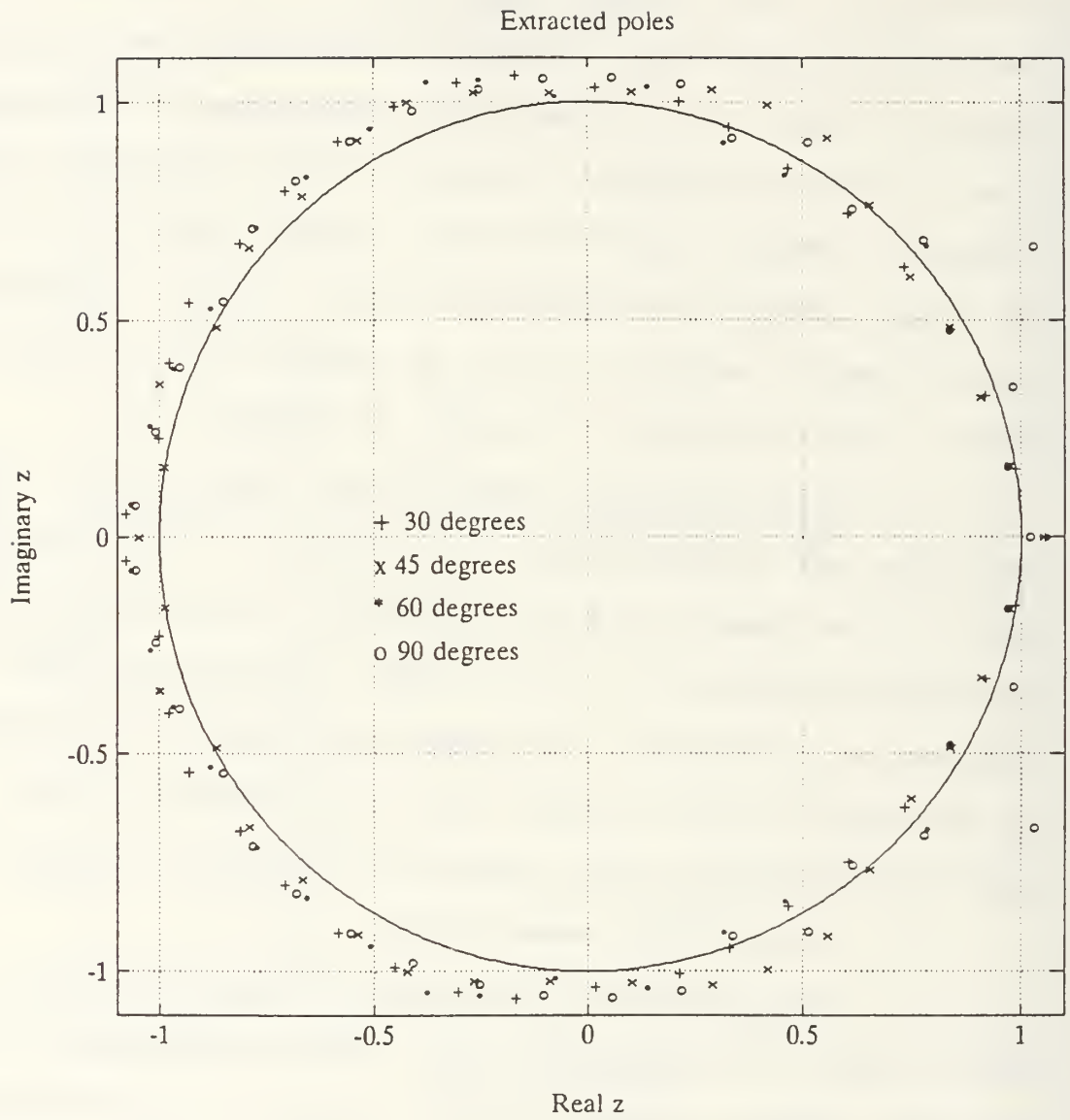


Figure 16. Kumaresan-Tufts Poles, 20.0 dB SNR

Extracted poles

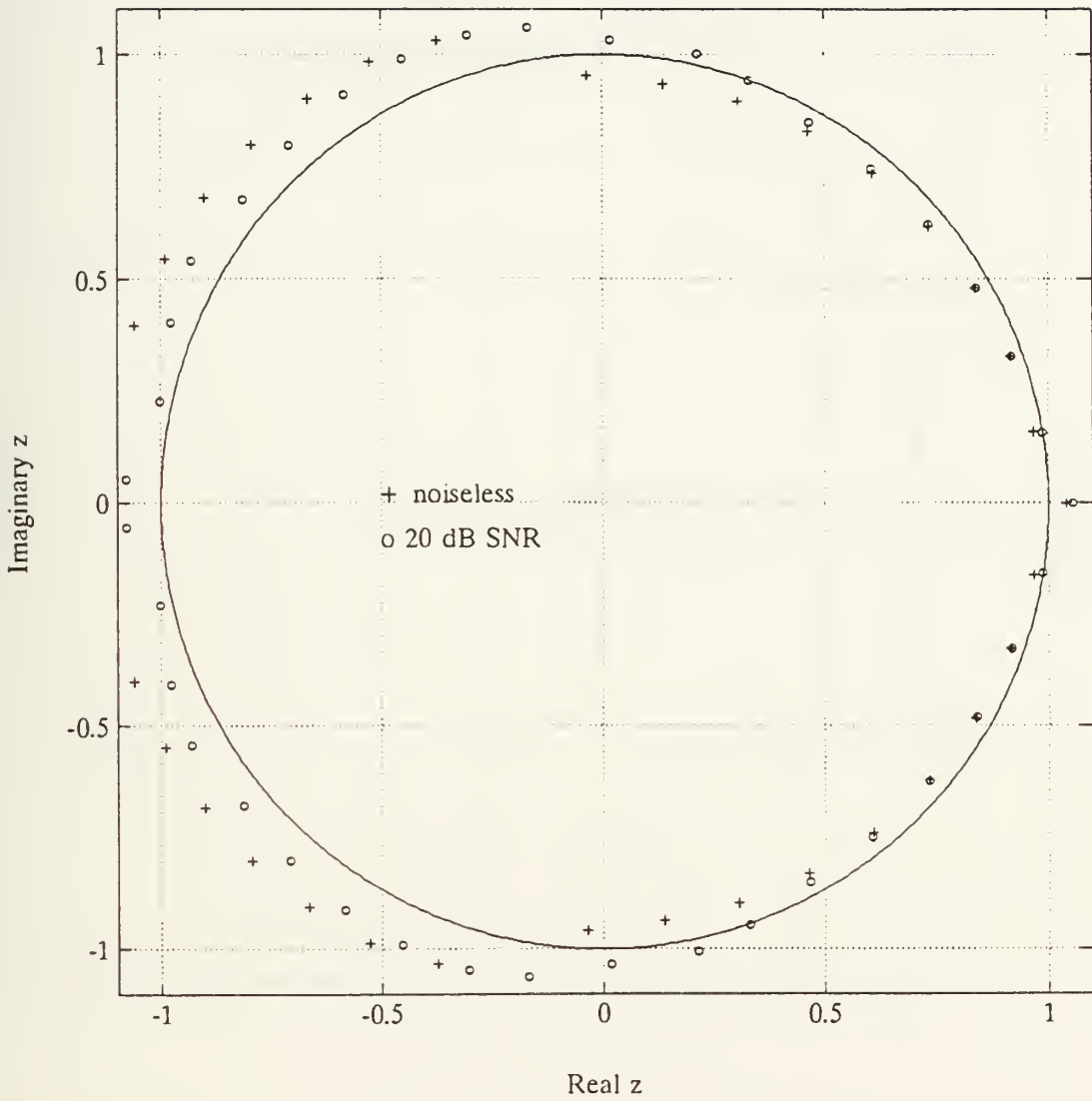


Figure 17. Integral Equation Thin Wire Comparison, Noiseless vs. 20.0 dB SNR, 30 Degree Aspect

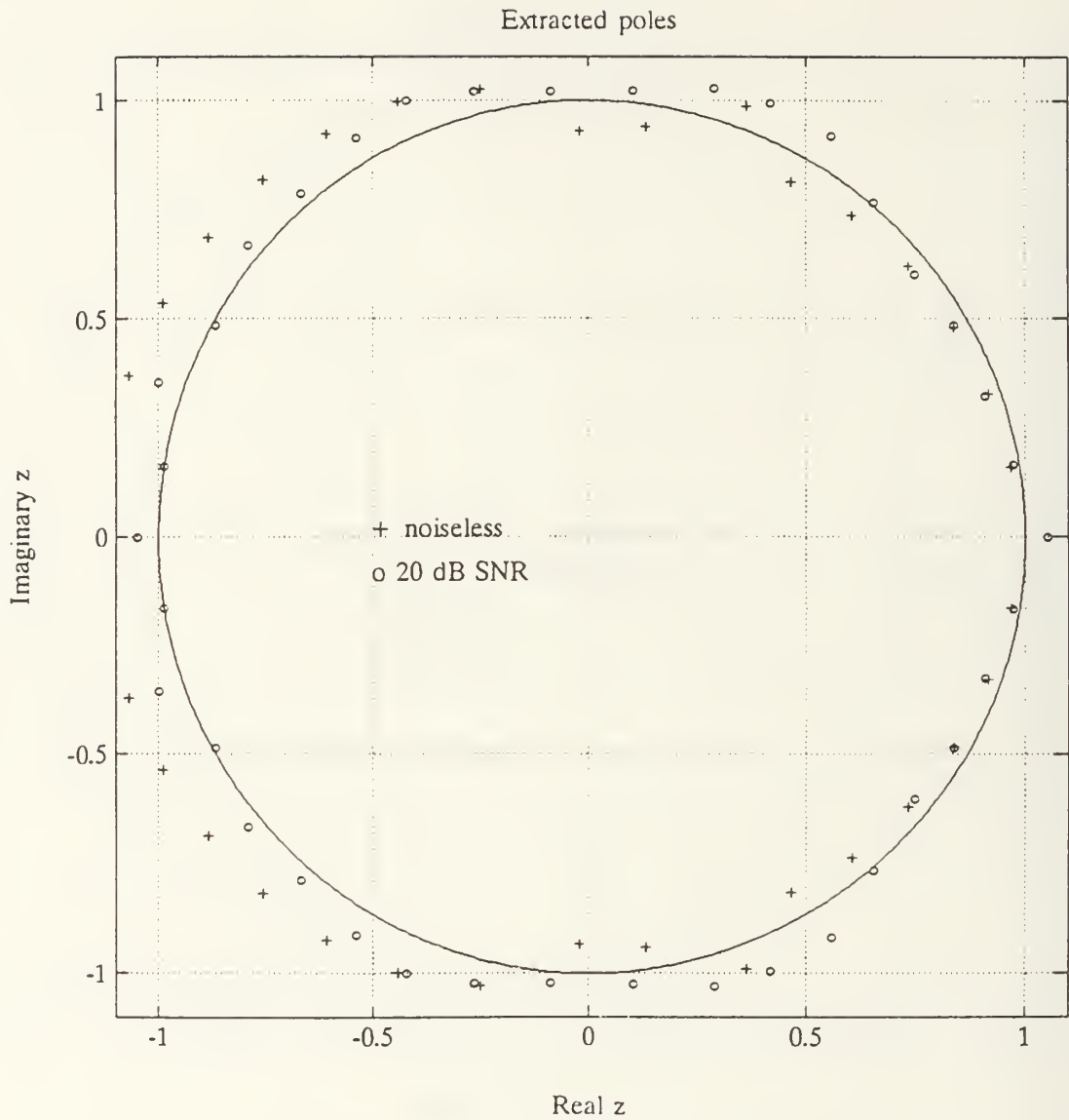


Figure 18. Integral Equation Thin Wire Comparison, Noiseless vs. 20.0 dB SNR, 45 Degree Aspect

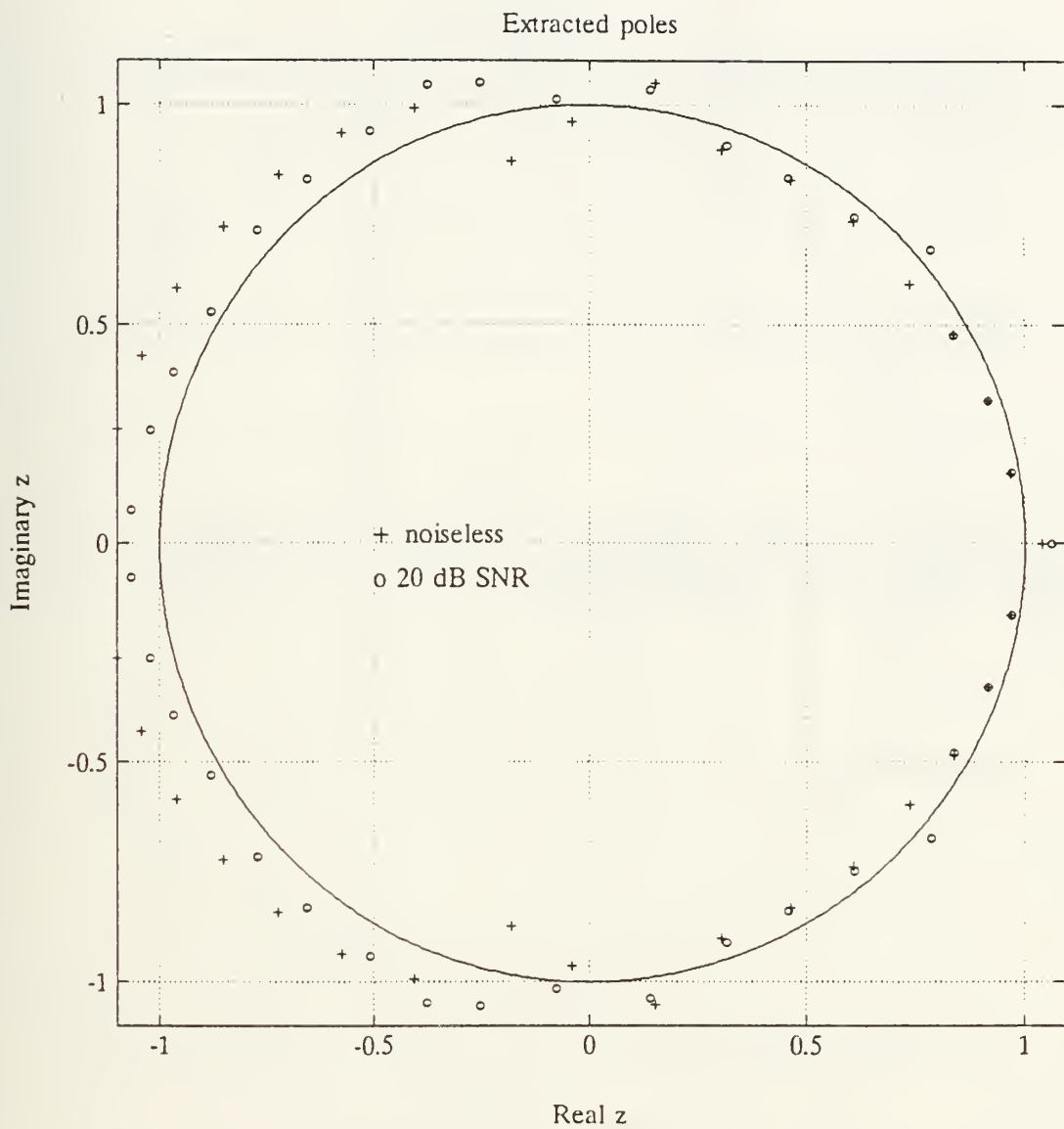


Figure 19. Integral Equation Thin Wire Comparison, Noiseless vs. 20.0 dB SNR, 60 Degree Aspect

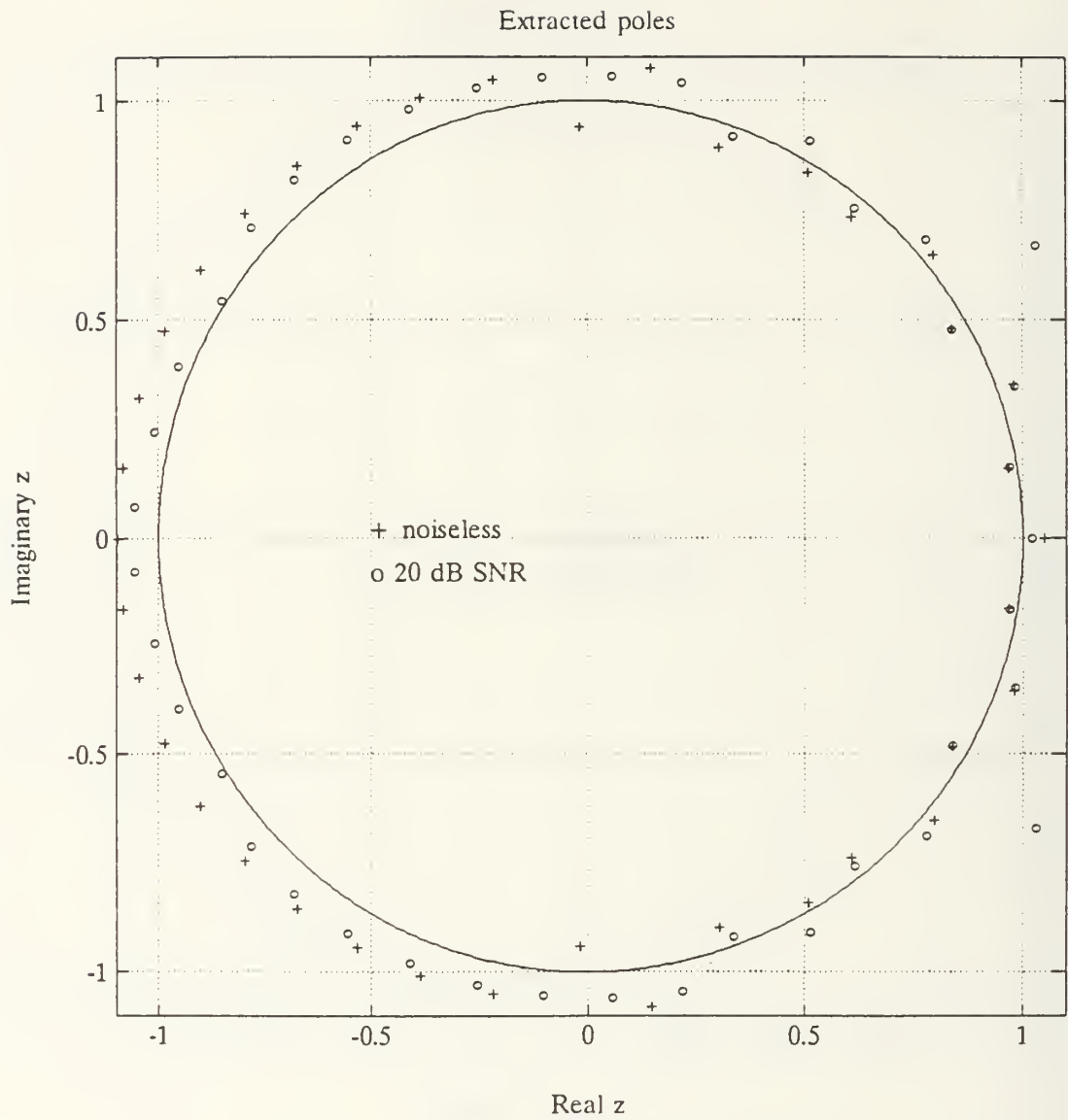


Figure 20. Integral Equation Thin Wire Comparison, Noiseless vs. 20.0 dB SNR, 90 Degree Aspect

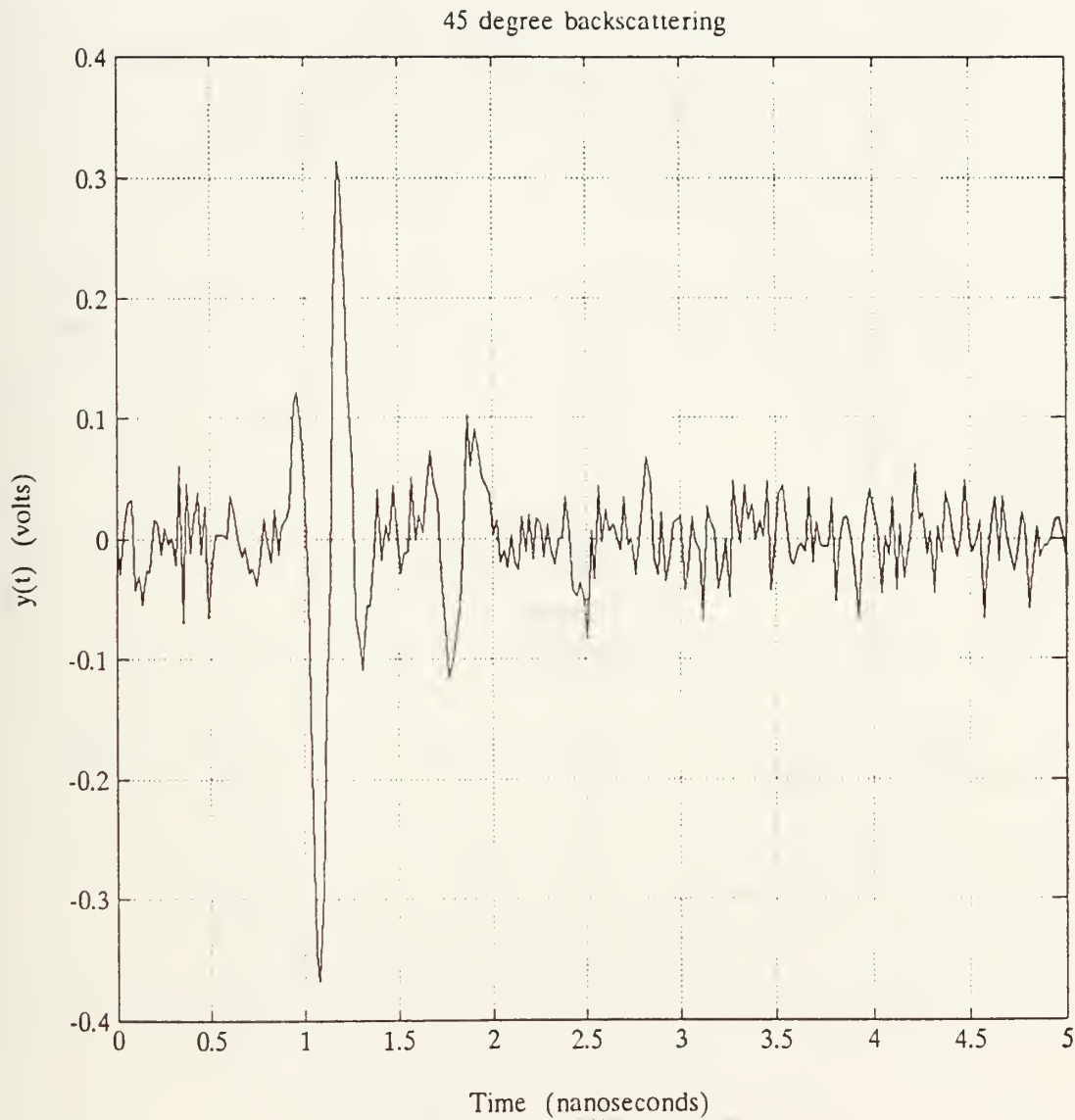


Figure 21. Integral Equation Thin Wire Scattering, 7.0 dB SNR, 45 Degree Aspect

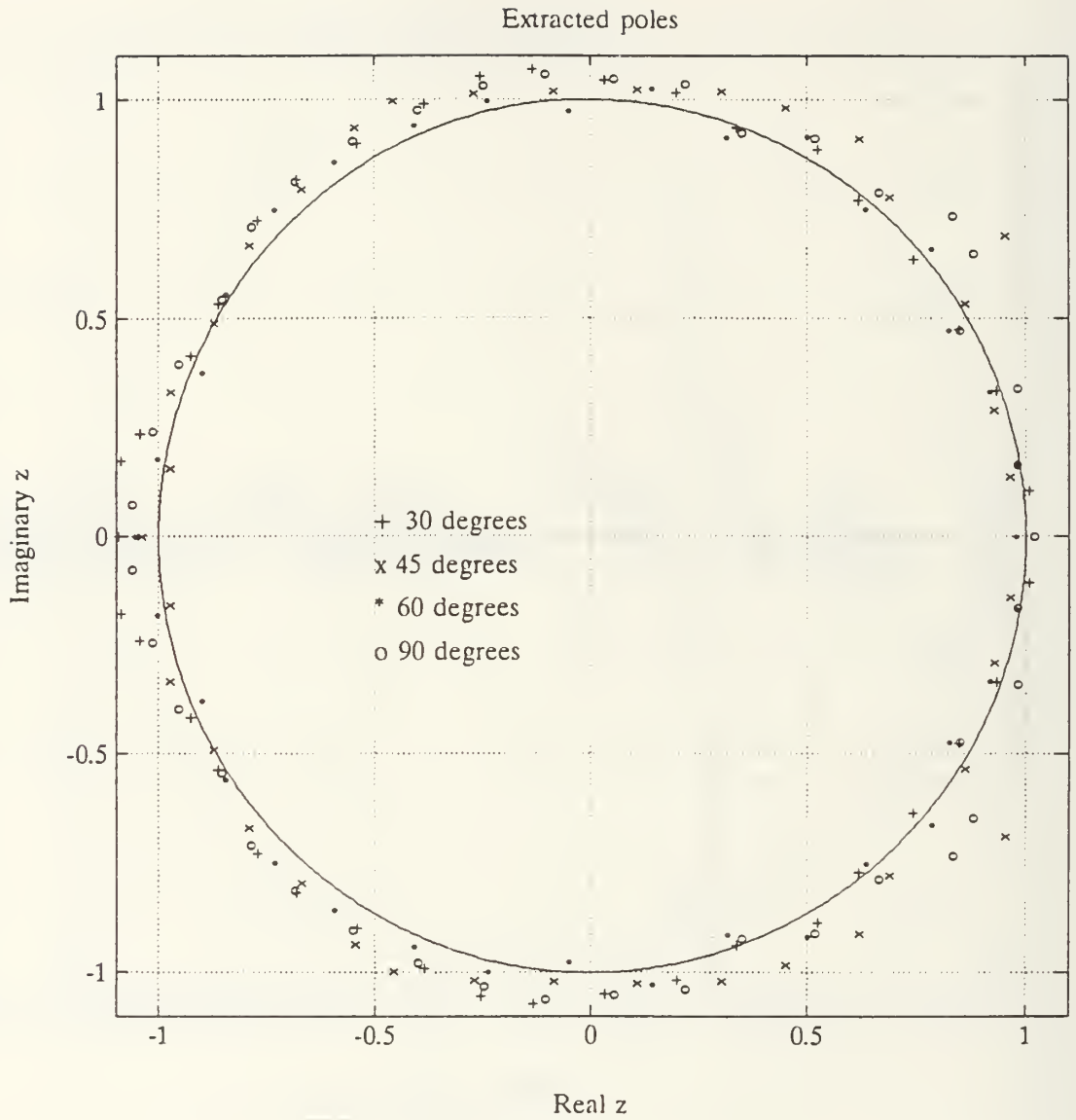


Figure 22. Kumaresan-Tufts Poles, 7.0 dB SNR

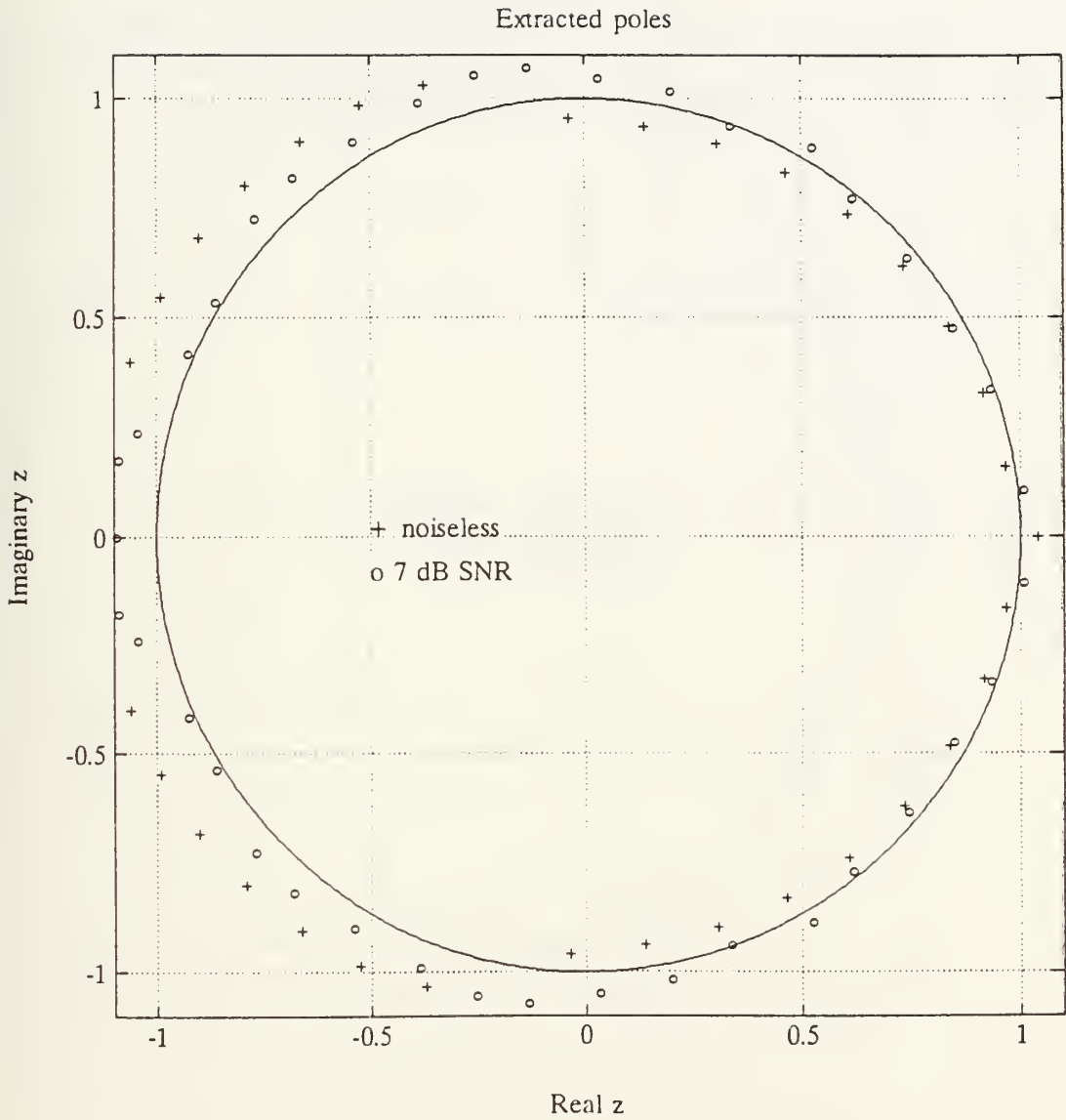


Figure 23. Integral Equation Thin Wire Comparison, Noiseless vs. 7.0 dB SNR, 30 Degree Aspect

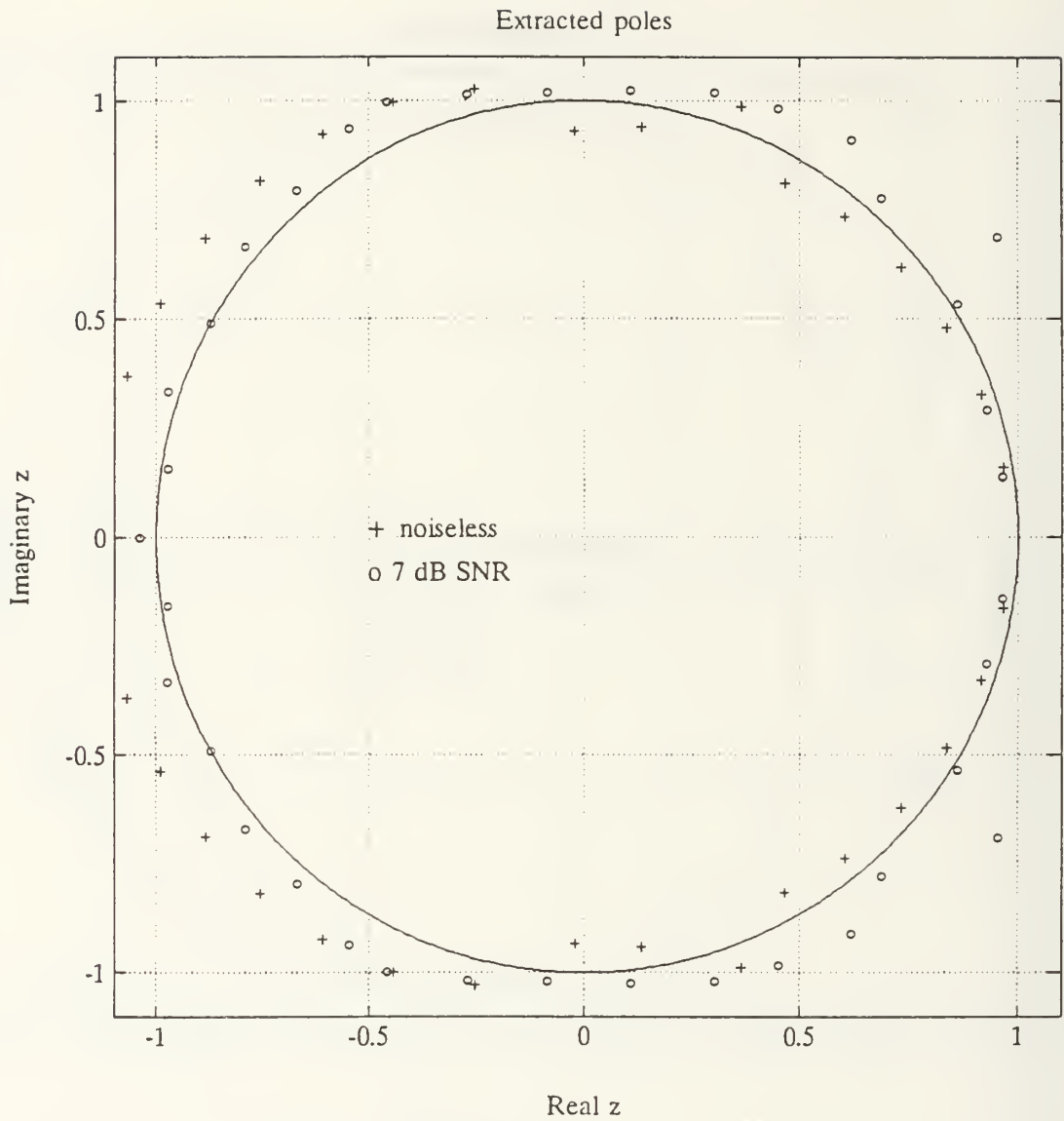


Figure 24. Integral Equation Thin Wire Comparison, Noiseless vs. 7.0 dB SNR, 45 Degree Aspect

Extracted poles

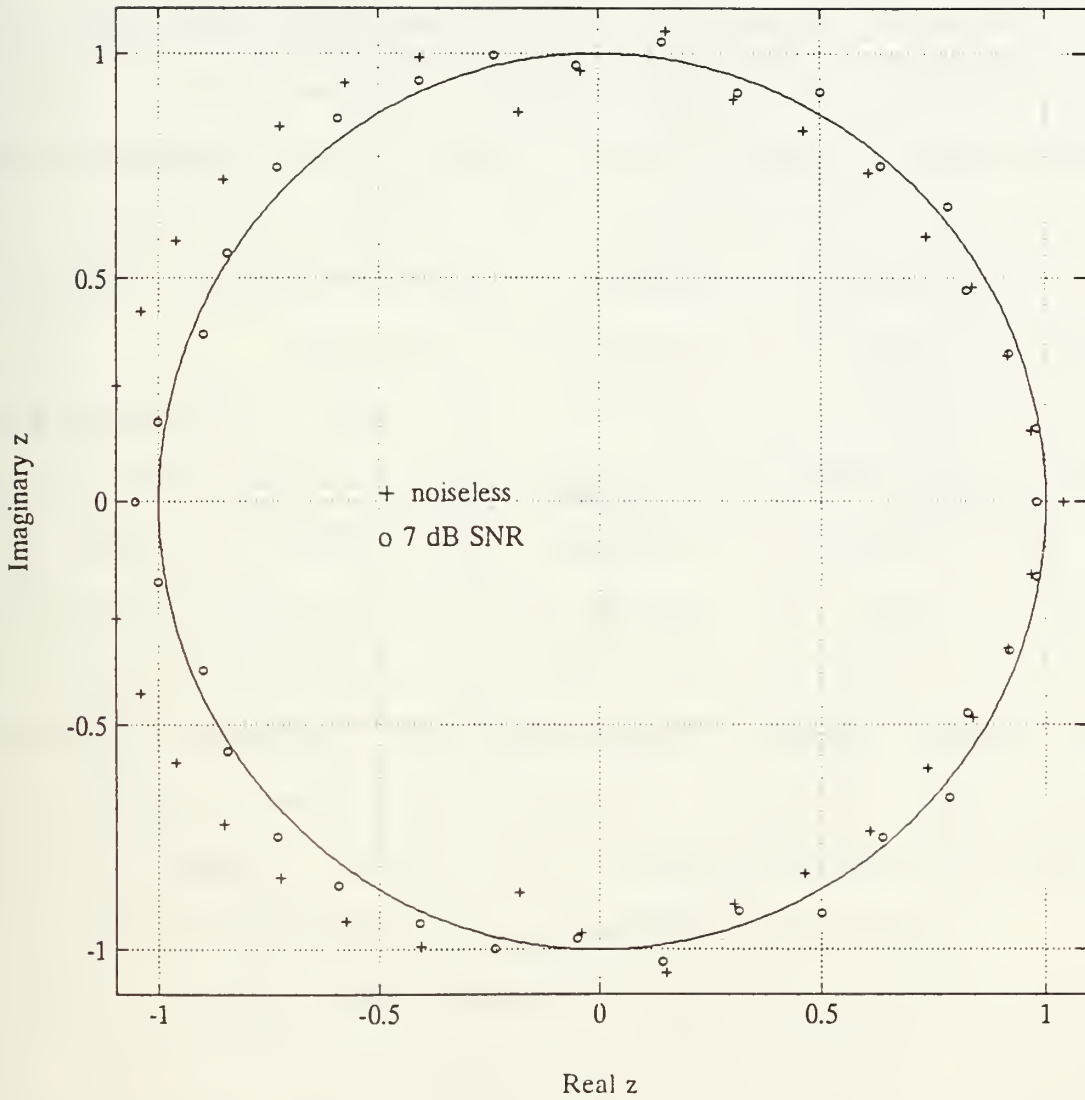


Figure 25. Integral Equation Thin Wire Comparison, Noiseless vs. 7.0 dB SNR, 60 Degree Aspect

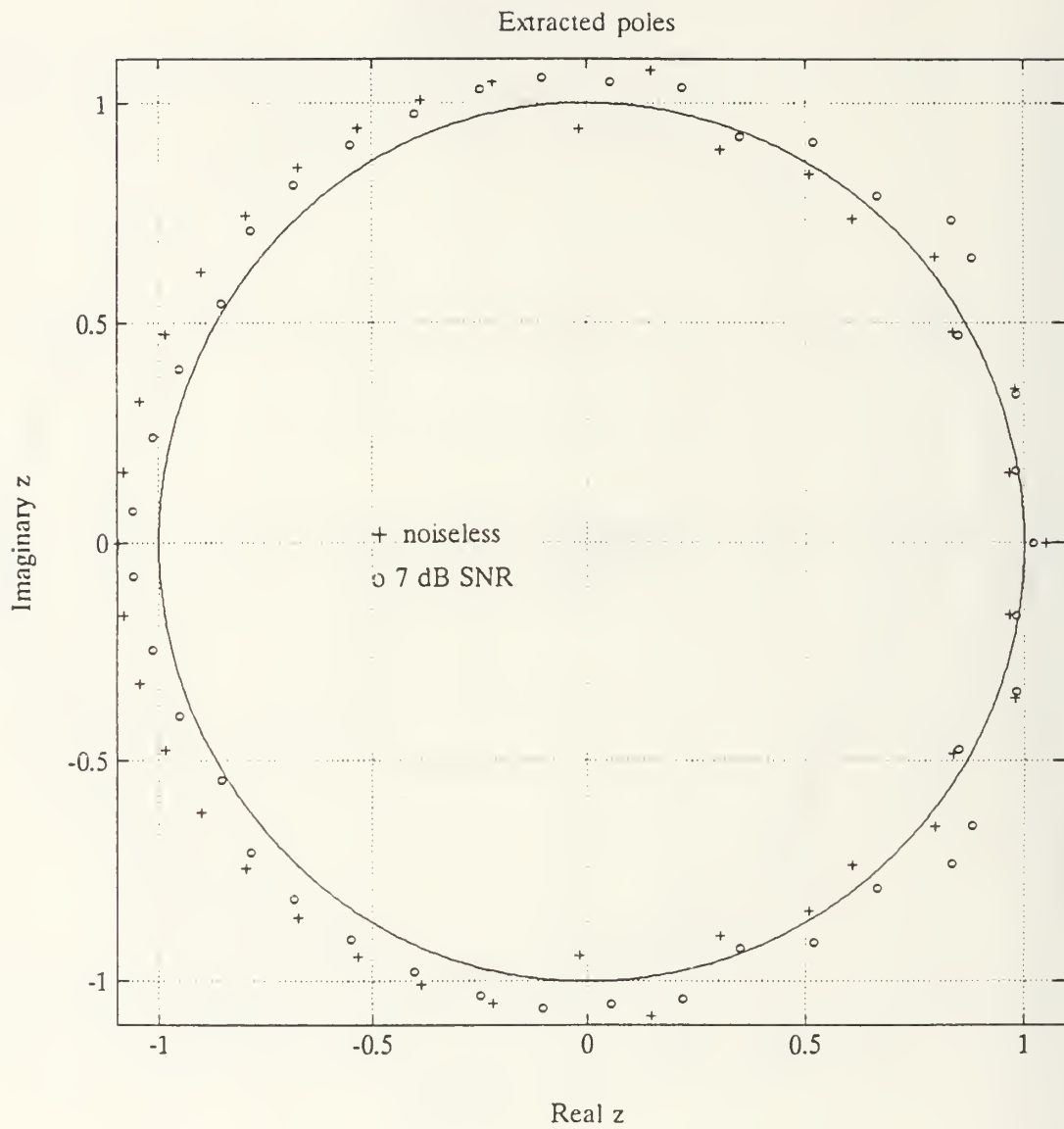


Figure 26. Integral Equation Thin Wire Comparison, Noiseless vs. 7.0 dB SNR, 90 Degree Aspect

1. Wire Targets

The thin wire measurements were obtained from the scattering response of a 0.1 meter length thin wire having radius 0.00118 meter. Recall that these are the same dimensions as the wire whose computed response was processed in the previous section. The measurements at each of four incident aspects are shown in Figures 27 through 30.

The poles extracted from the four measurements are depicted in Figure 31. As before in the computed noisy data, tight clusters occur only at the lowest frequencies. The poles in these tight clusters are those which are measurably present at various aspects. The poles extracted at higher frequencies are those which possessed sufficient measurable energy at the given aspect. Figure 32 depicts the comparison between poles extracted from the measured and computed signals. Again, the closest agreement between the two sets of poles occurs at the lowest frequencies.

2. Aircraft Models

Plastic 1/72 scale aircraft models, coated with silver, were used for transient scattering measurements. Representative scattering signatures of two aircraft targets, measured at six different aspects, are shown in Figures 33 through 36.

The results of pole extraction in target 1 are shown for a total of six different aspects in Figures 37 and

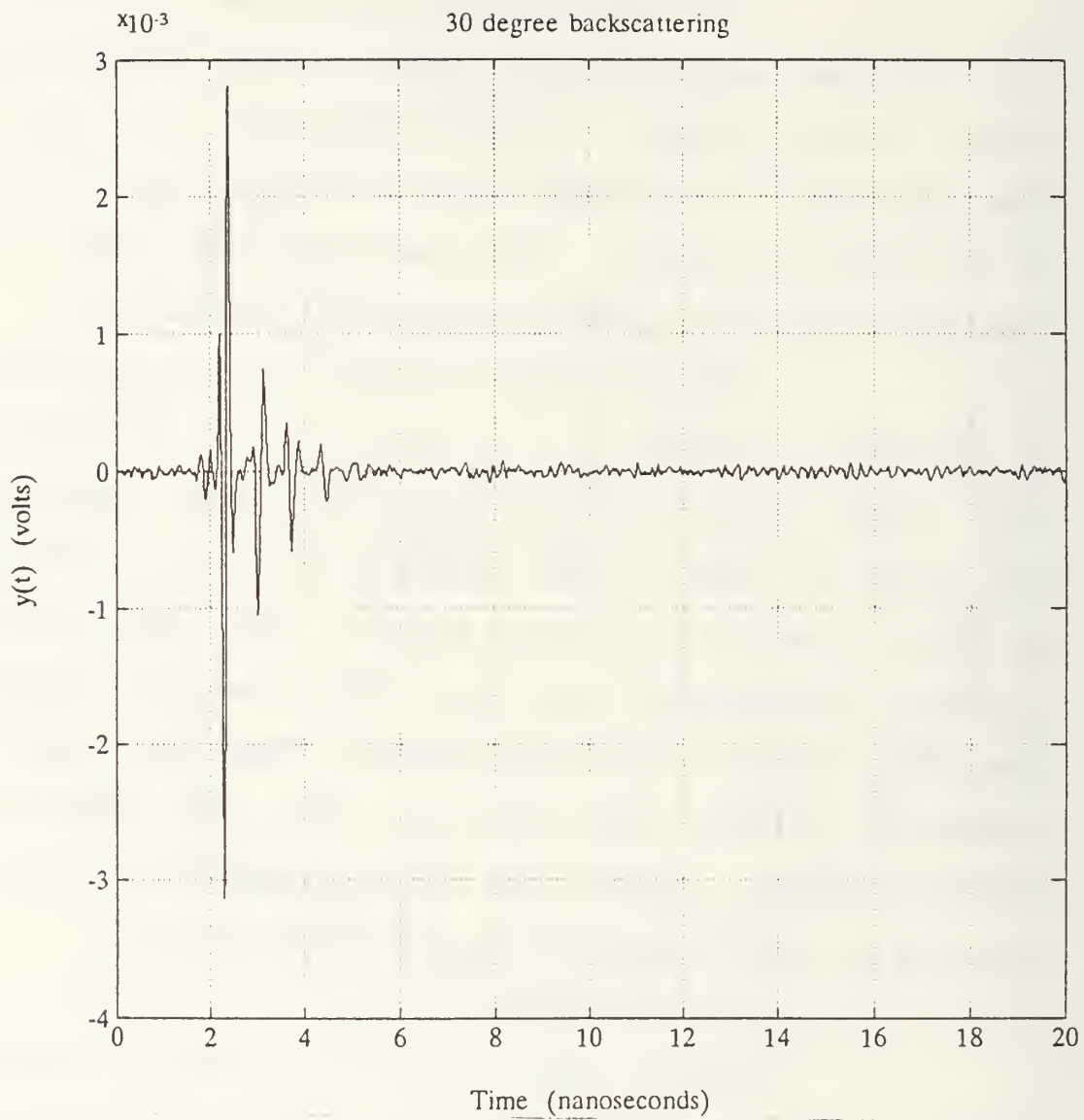


Figure 27. Measured Thin Wire Scattering, 30 Degree Aspect

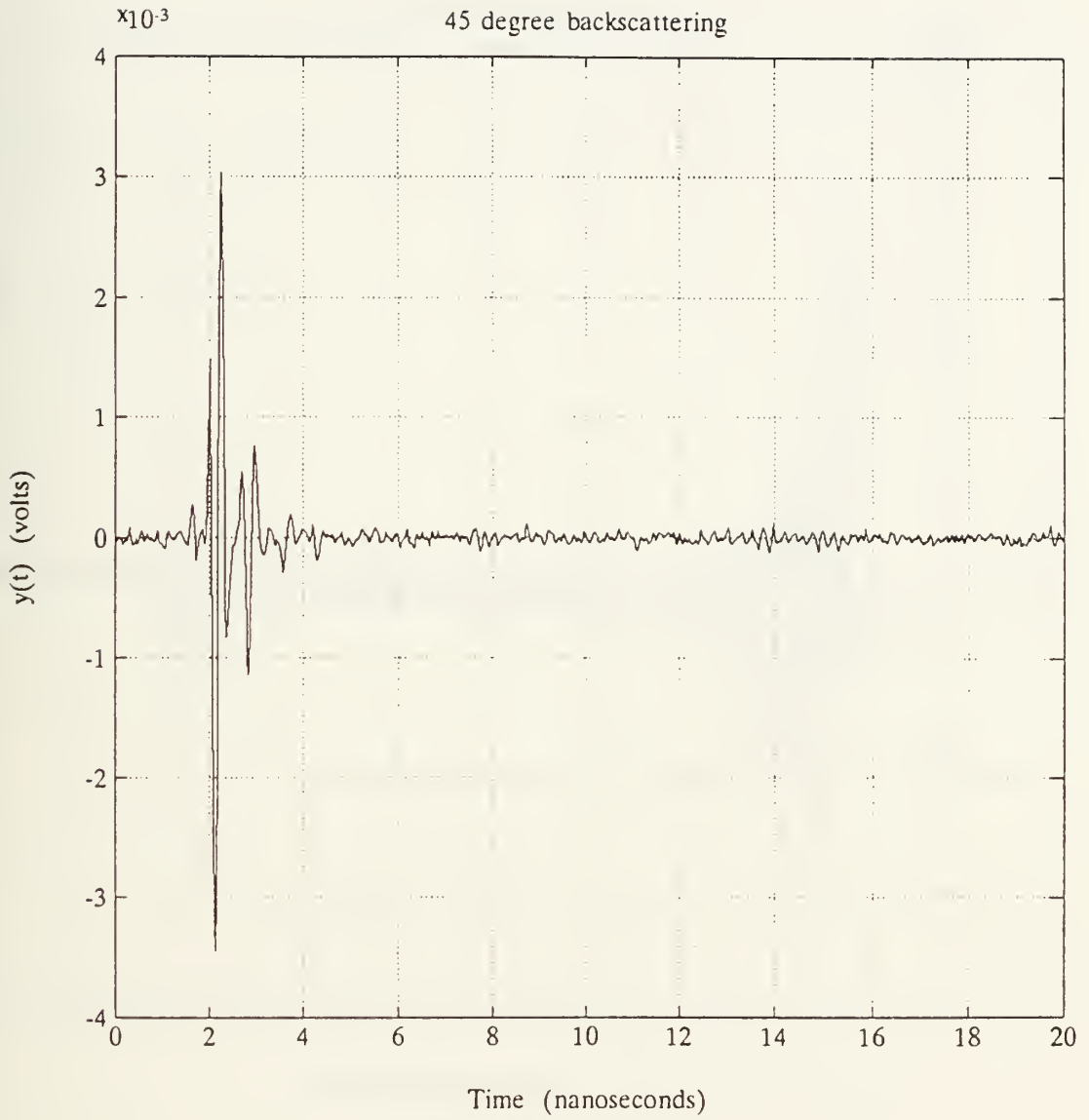


Figure 28. Measured Thin Wire Scattering, 45 Degree Aspect

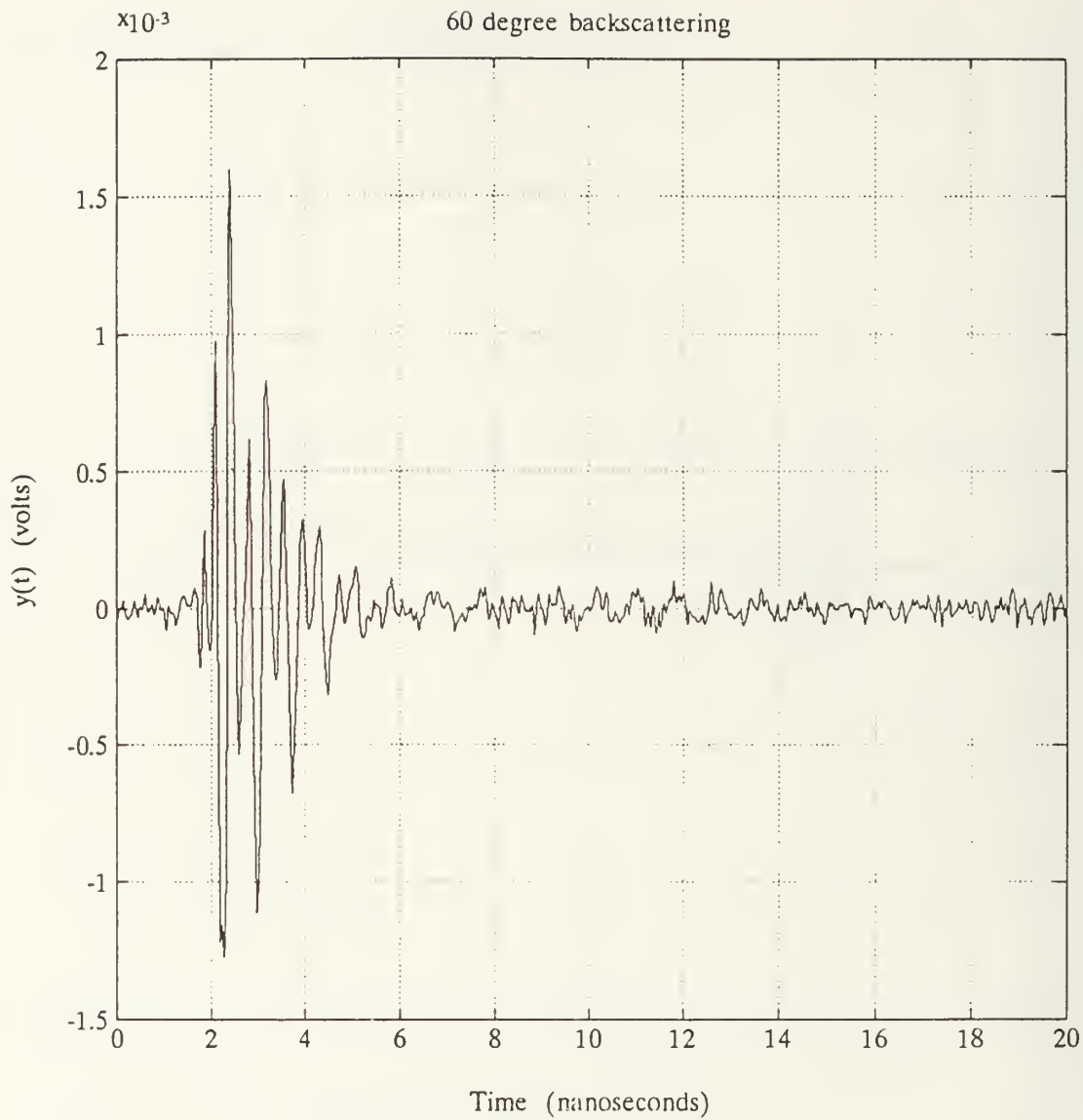


Figure 29. Measured Thin Wire Scattering, 60 Degree Aspect

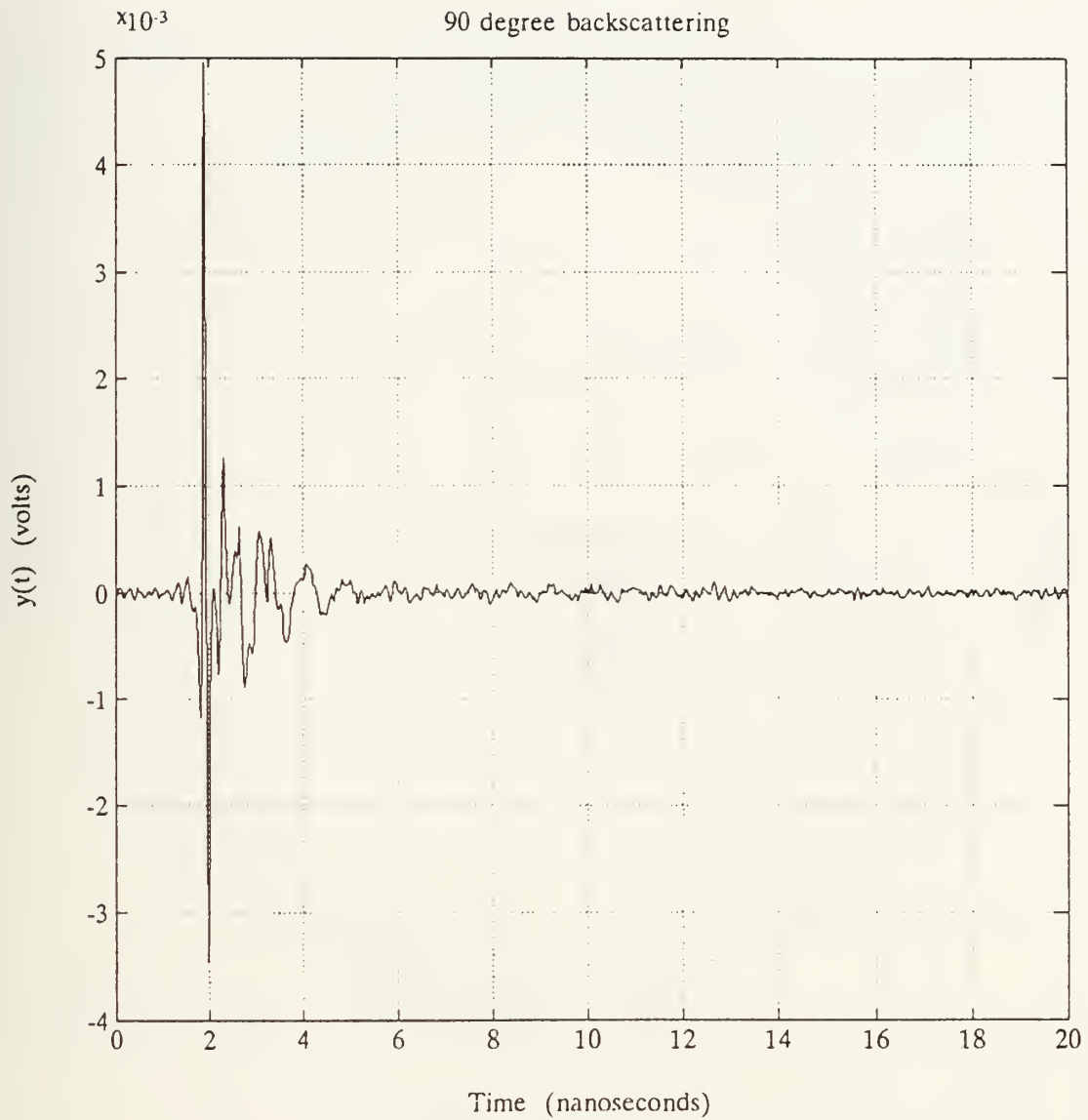


Figure 30. Measured Thin Wire Scattering, 90 Degree Aspect

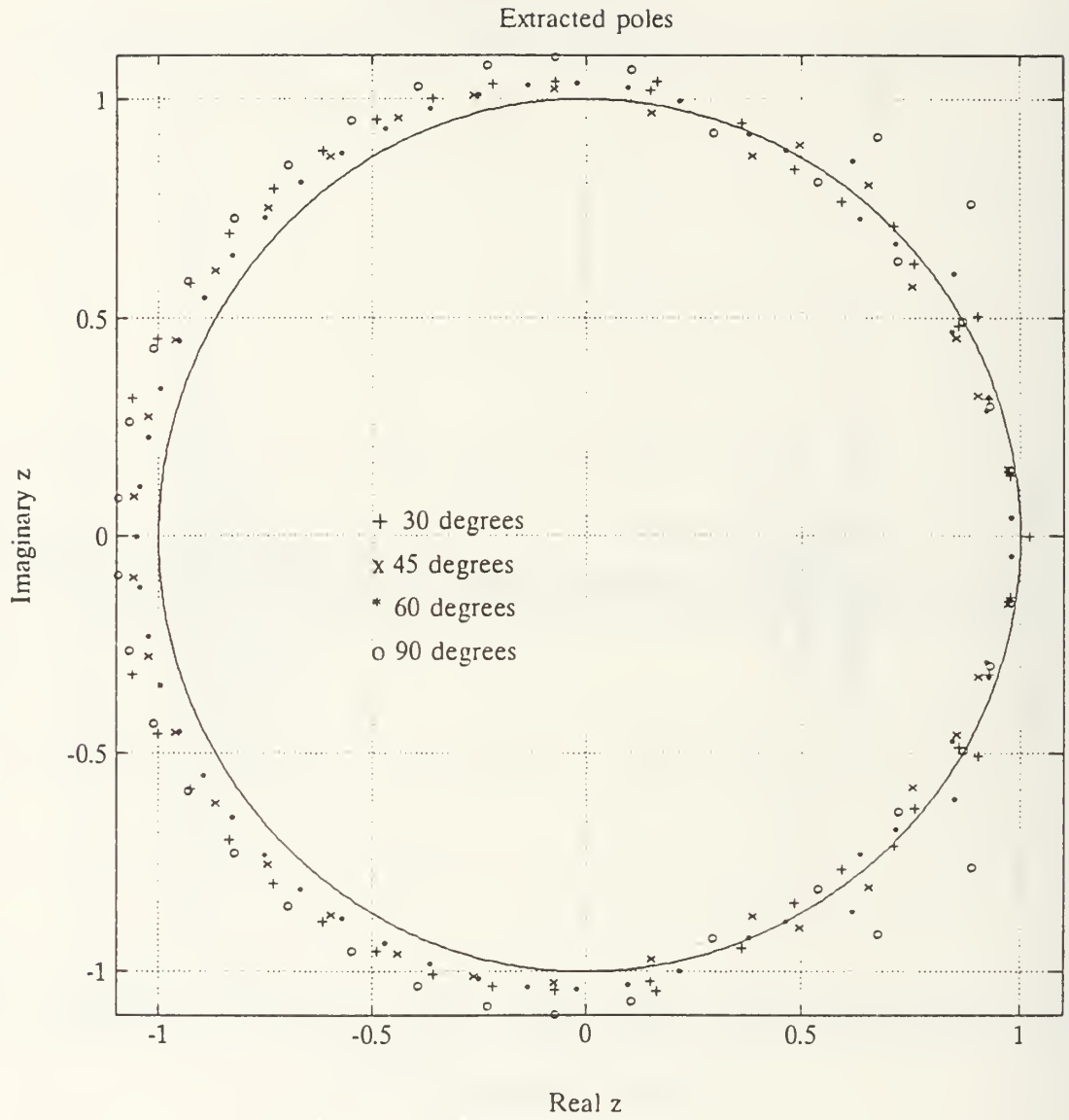


Figure 31. Kumaresan-Tufts Poles, Measured Thin Wire

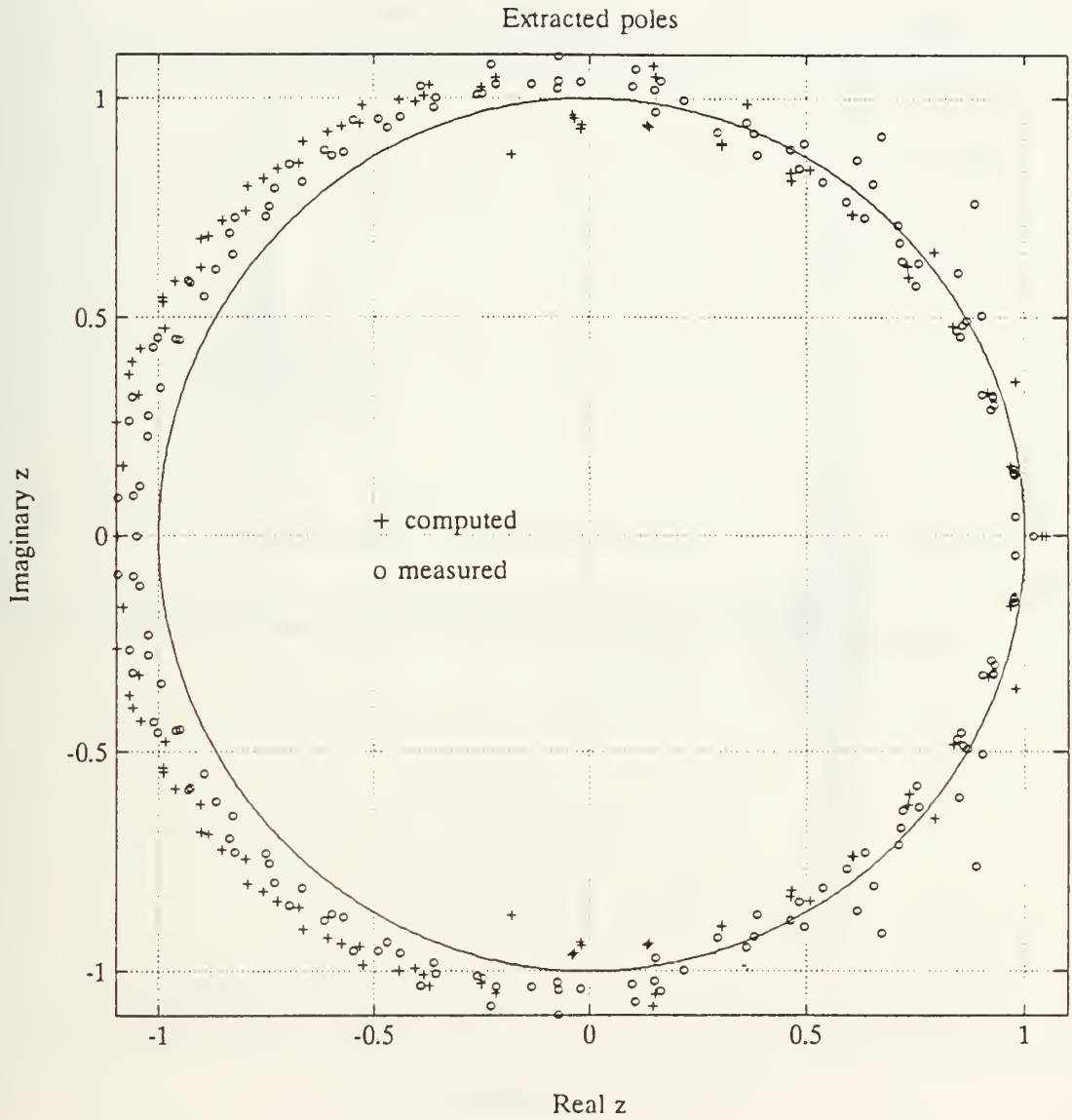


Figure 32. Thin Wire Comparison, Measured vs. Integral Equation

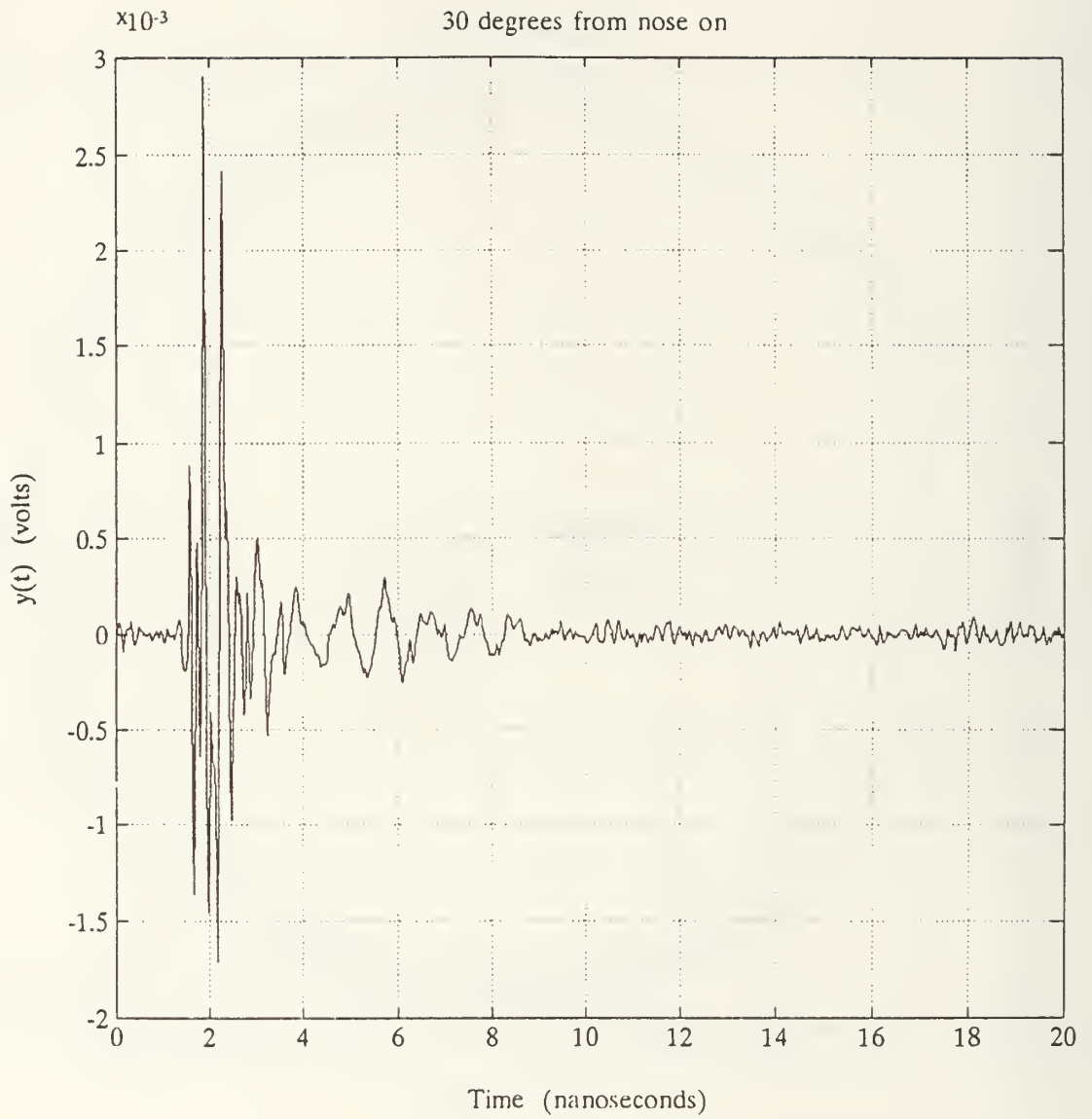


Figure 33. Target 1 Scattering, 30 Degrees from Nose on

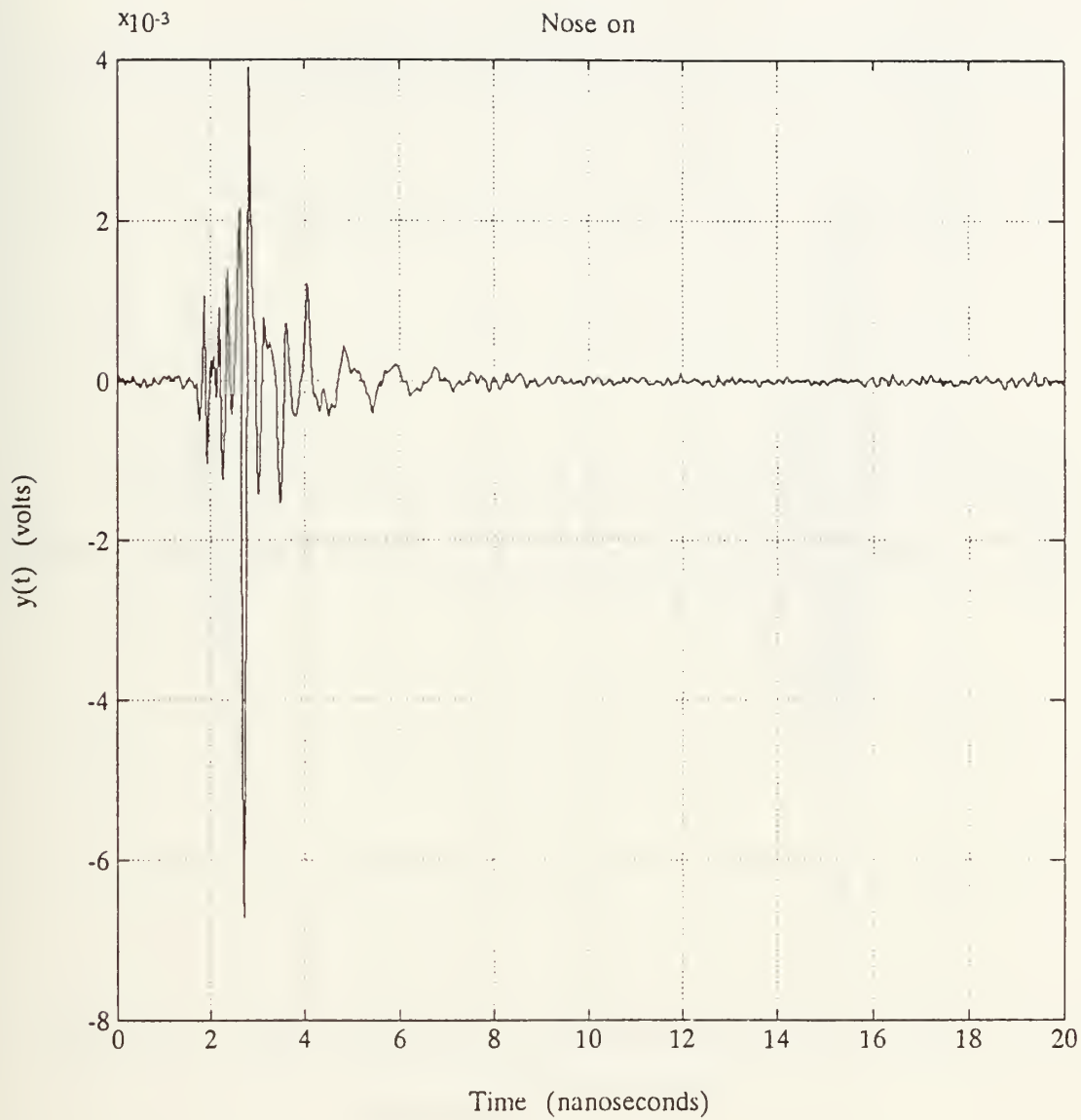


Figure 34. Target 1 Scattering, Nose on

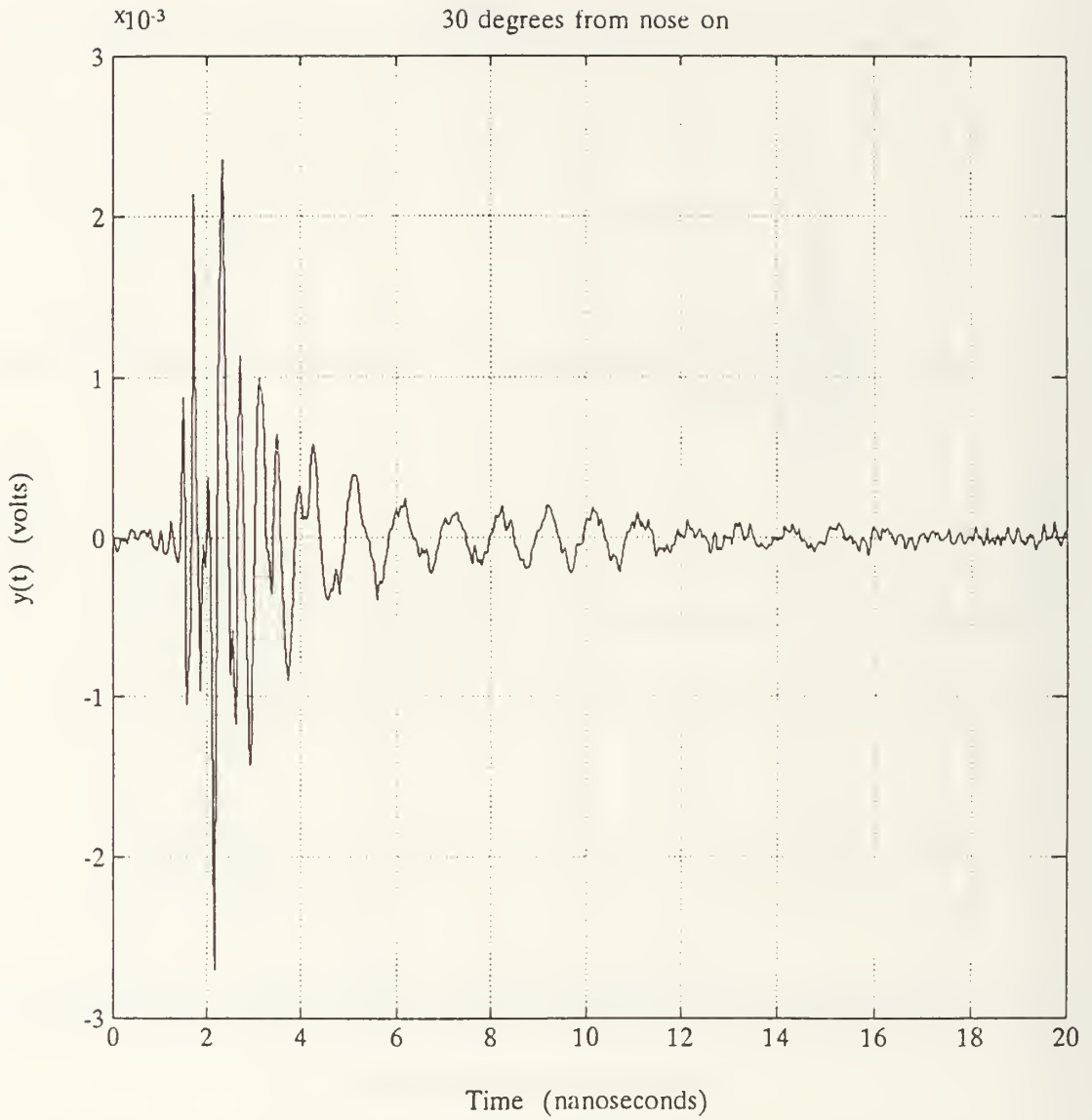


Figure 35. Target 2 Scattering, 30 Degrees from Nose on

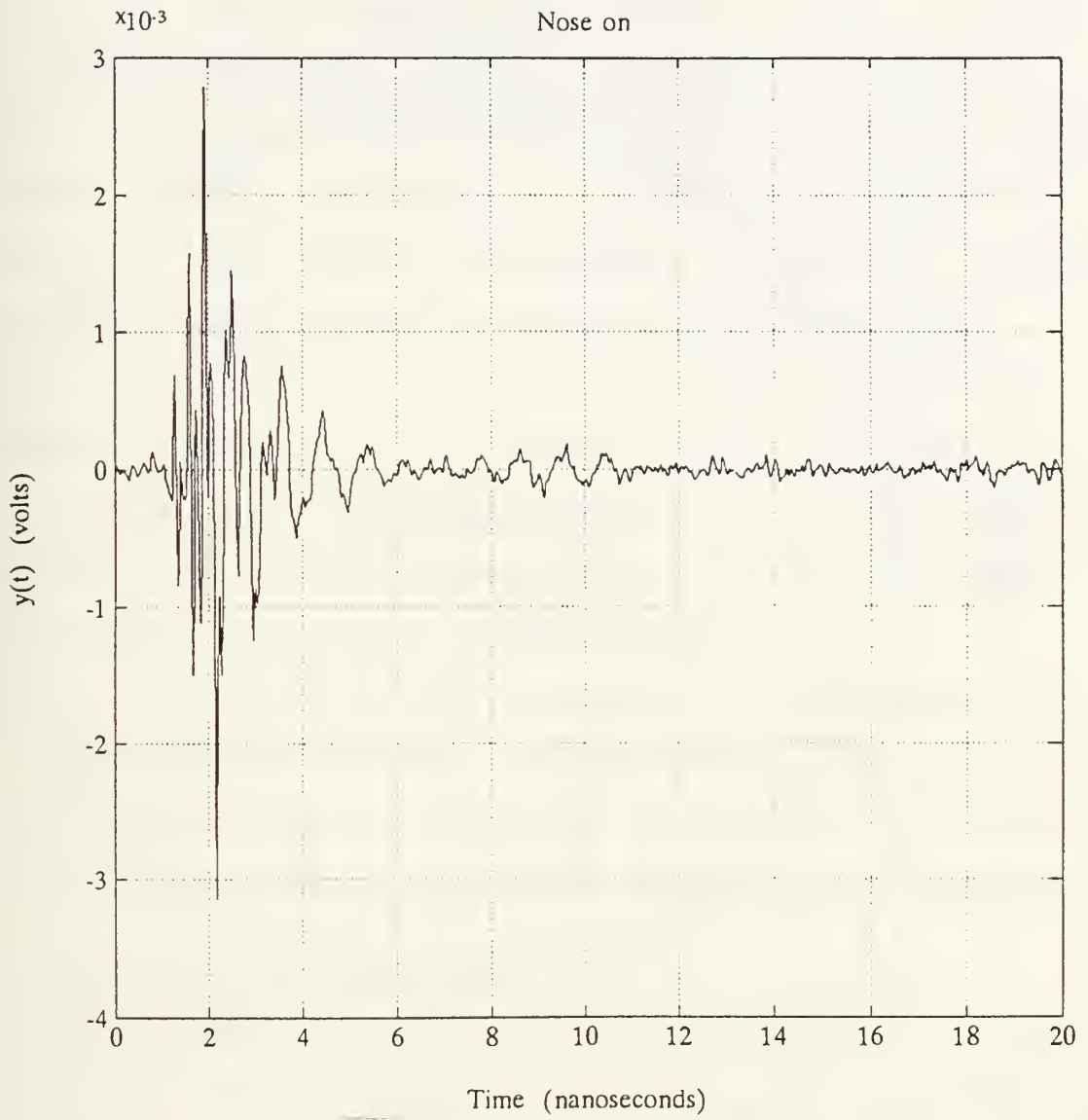


Figure 36. Target 2 Scattering, Nose on

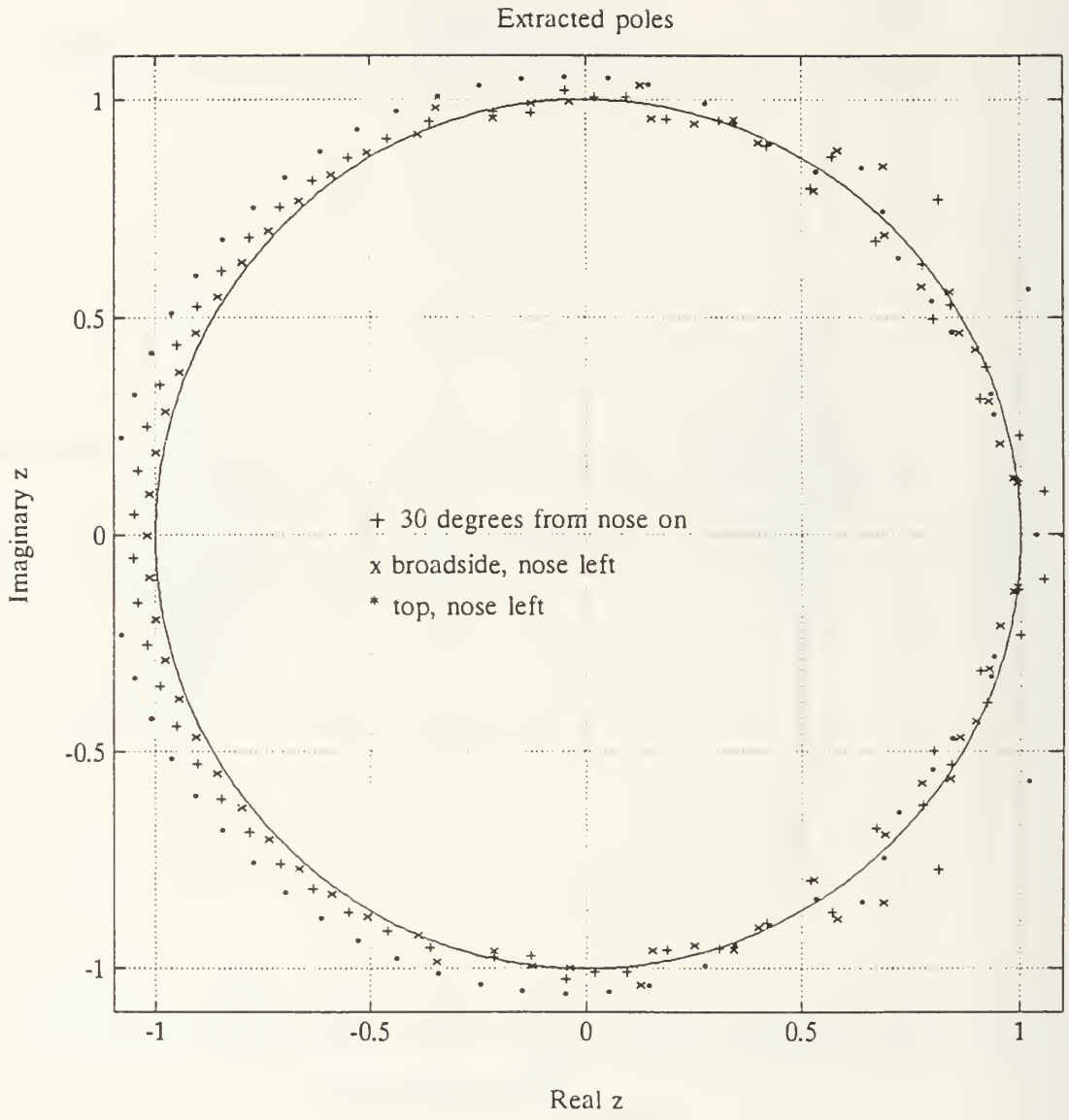


Figure 37. Kumaresan-Tufts Poles, Target 1

38. The poles extracted at all six aspects are shown in Figure 39. Only one clearly discernible cluster is present in each of the three figures. At higher frequencies, no useful information is imparted by the data. Results of similar, though slightly improved quality, were obtained from target 2. These results are presented in Figures 40 through 42 in the format of Figures 37 through 39 respectively.

Although the Kumaresan-Tufts algorithm is capable of extracting low frequency poles acceptably, the inconsistent results at higher frequencies reveals the inherent weakness in an algorithm capable of processing only the late-time portion of a target's radar response.

A side-by-side comparison of poles obtained from both aircraft by both the Kumaresan-Tufts method and the Cadzow-Solomon method is presented at the end of the chapter to illustrate the gains afforded by processing the early-time.

C. CADZOW-SOLOMON ALGORITHM

Recall from the results depicted in Figure 8 that a late transition to late-time, and the consequent reduction of signal power, caused complete breakdown of the Kumerasan-Tufts algorithm. The Cadzow-Solomon algorithm addresses this shortcoming by processing the signal at the instantaneous onset of early-time. Thus, the Cadzow-Solomon algorithm is capable of processing the earliest response of a target to

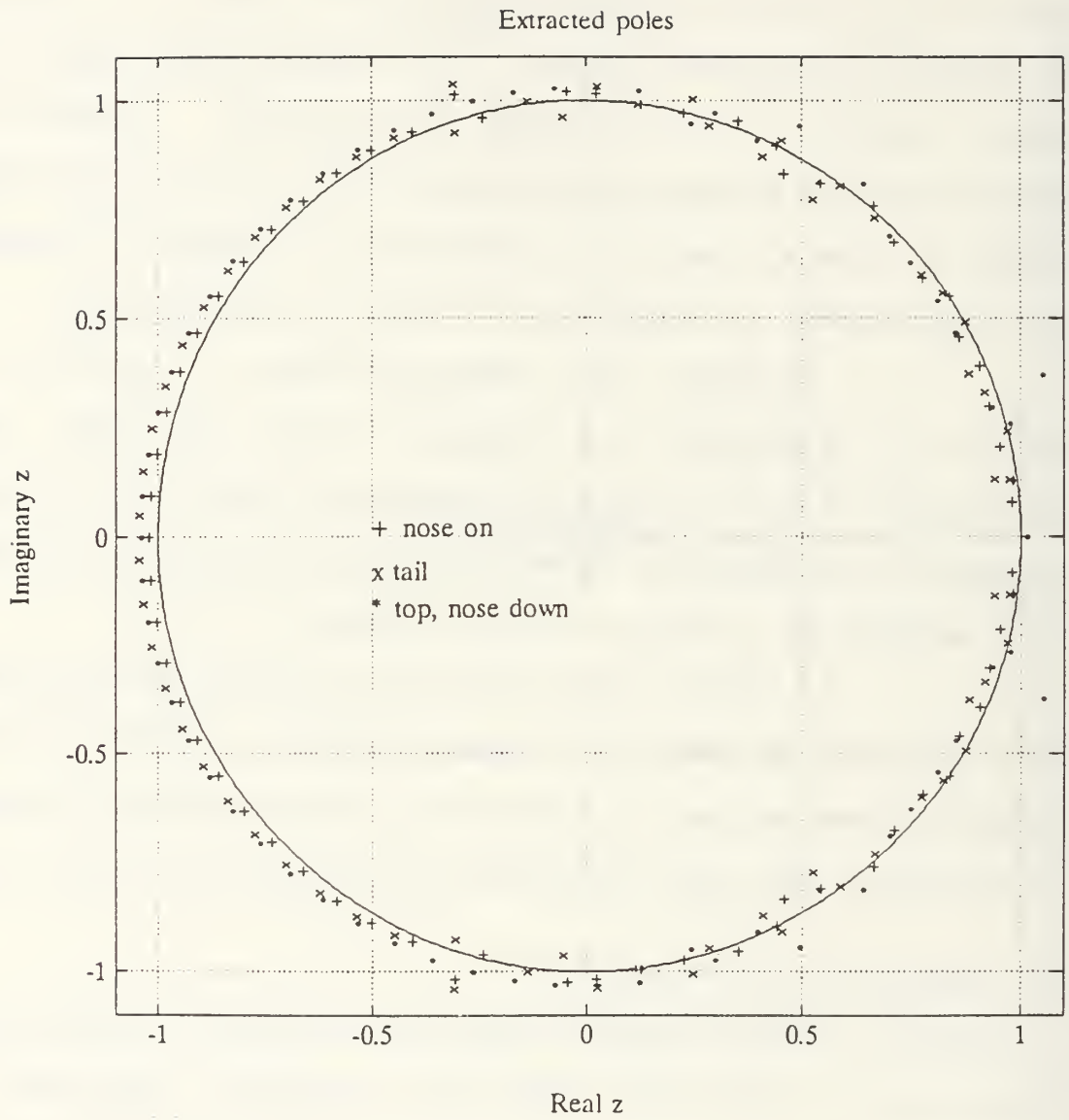


Figure 38. Kumaresan-Tufts Poles, Target 1

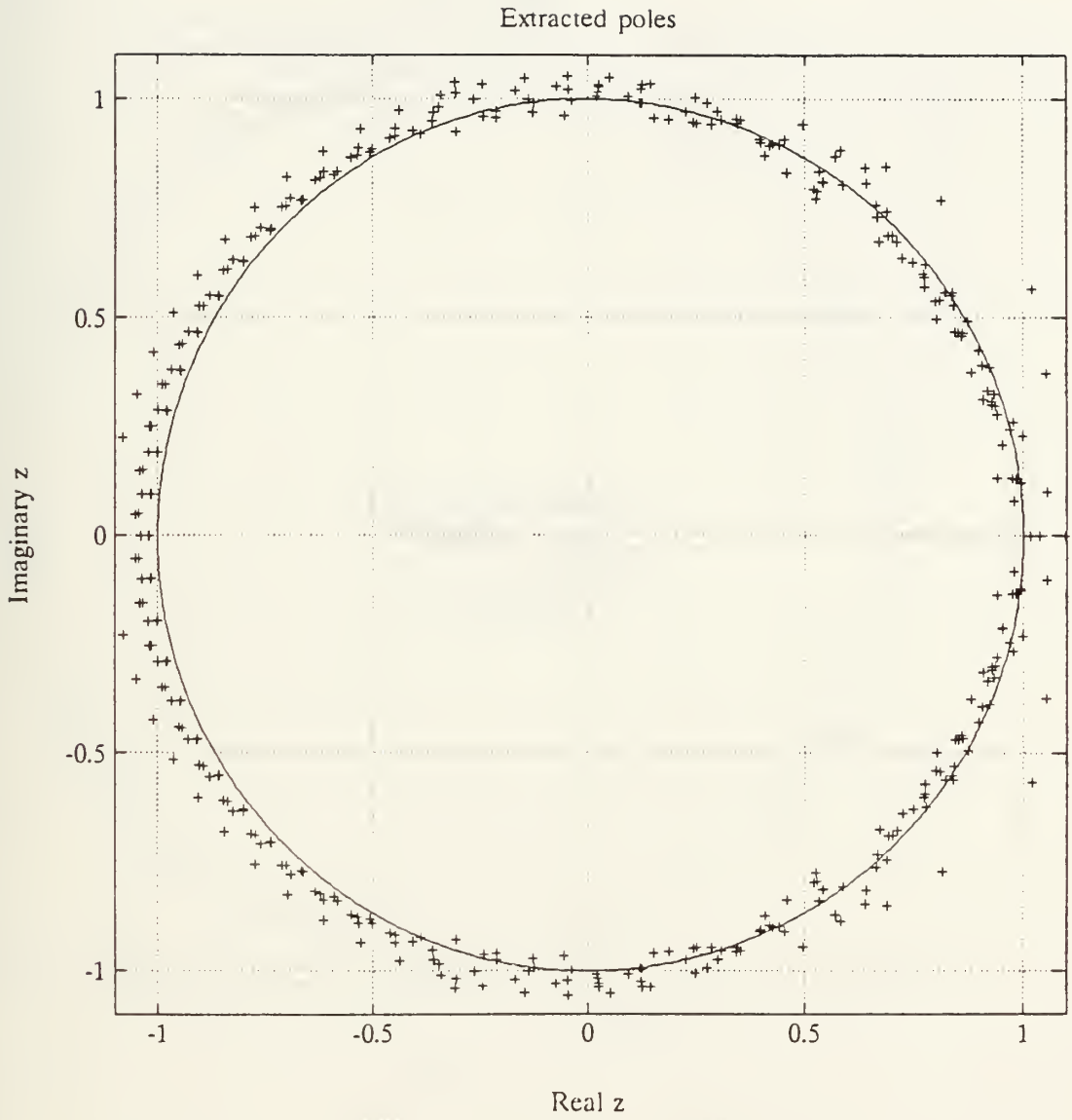


Figure 39. Kumaresan-Tufts Poles, Target 1

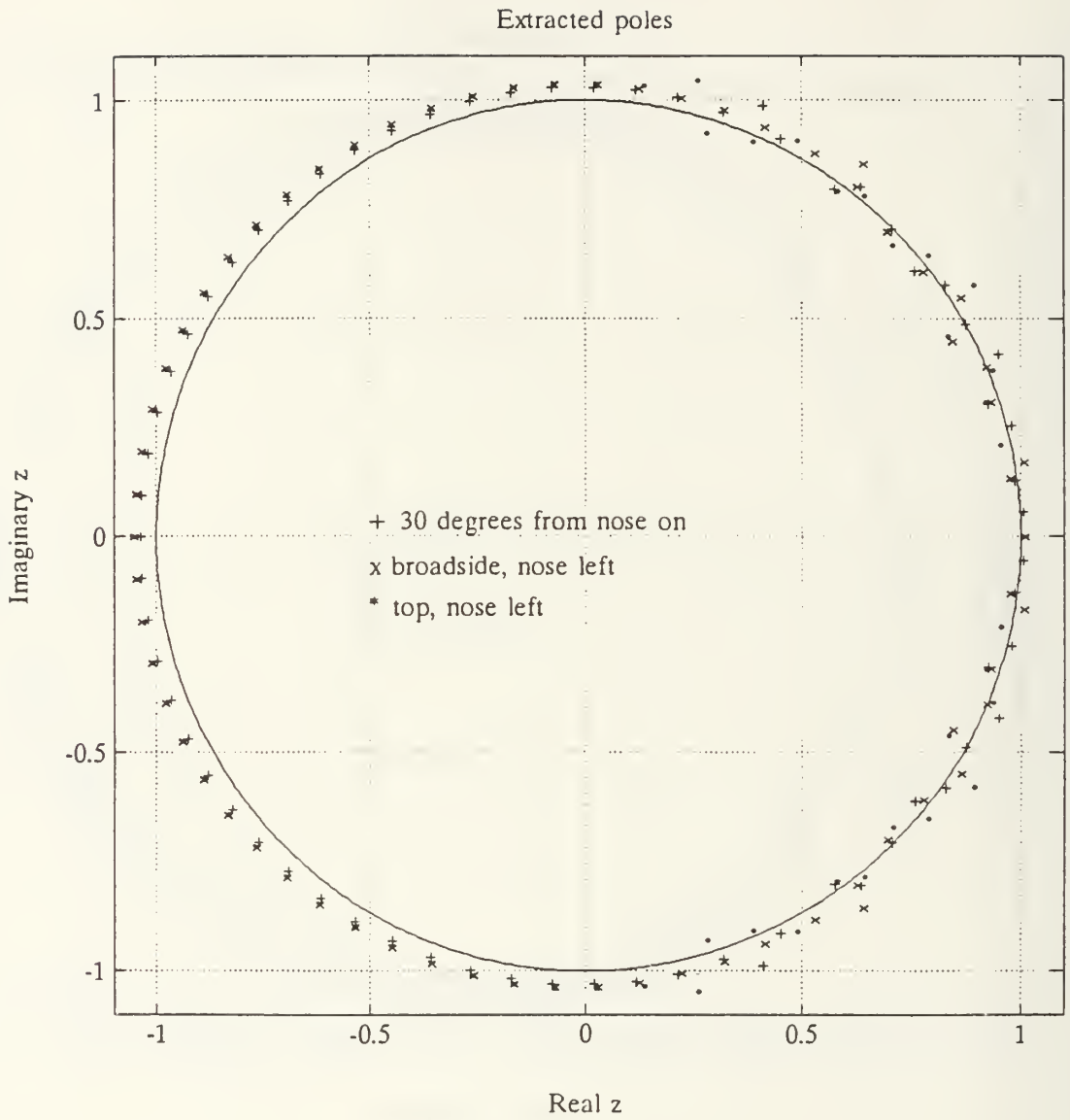


Figure 40. Kumaresan-Tufts Poles, Target 2

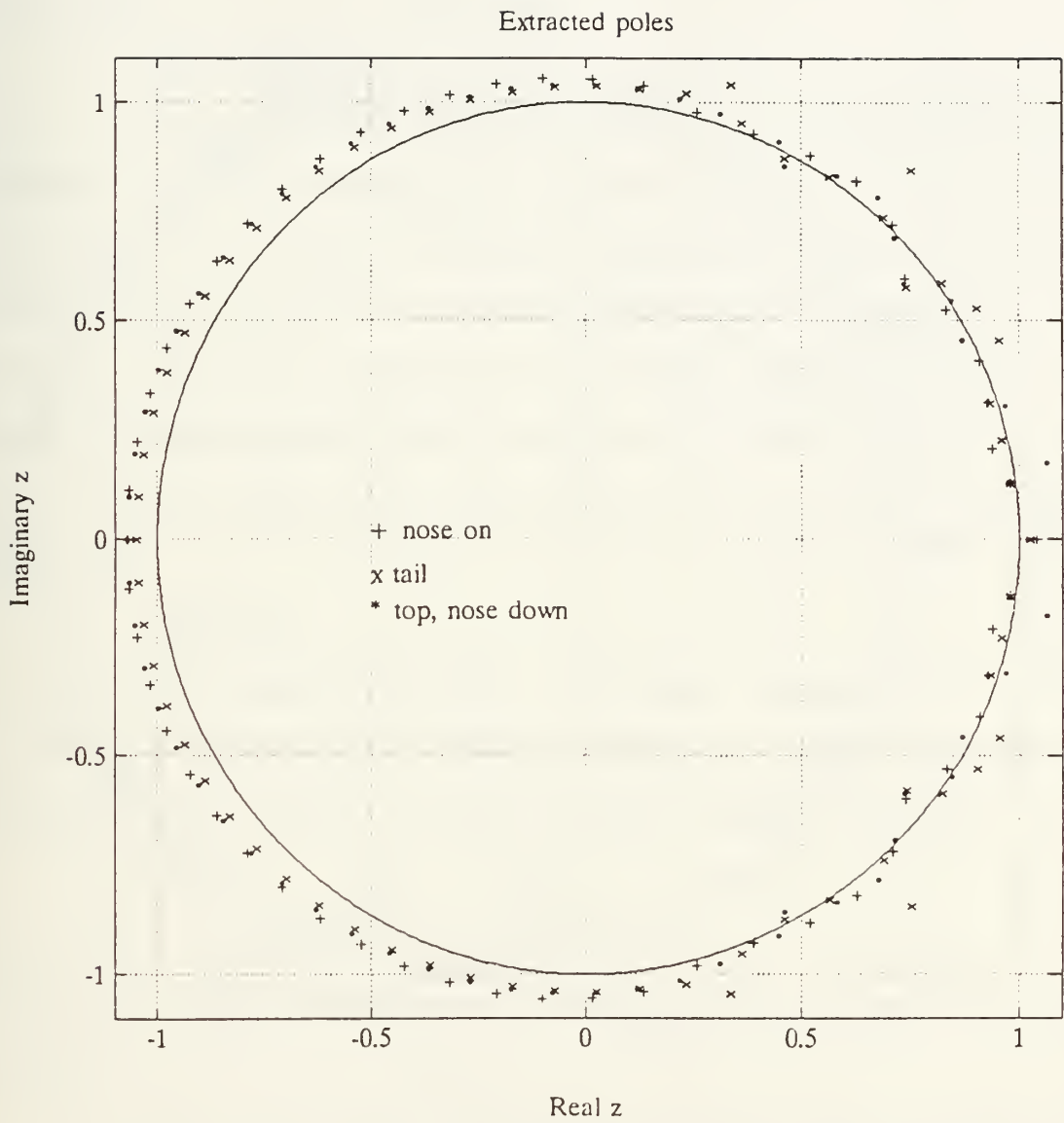


Figure 41. Kumaresan-Tufts Poles, Target 2

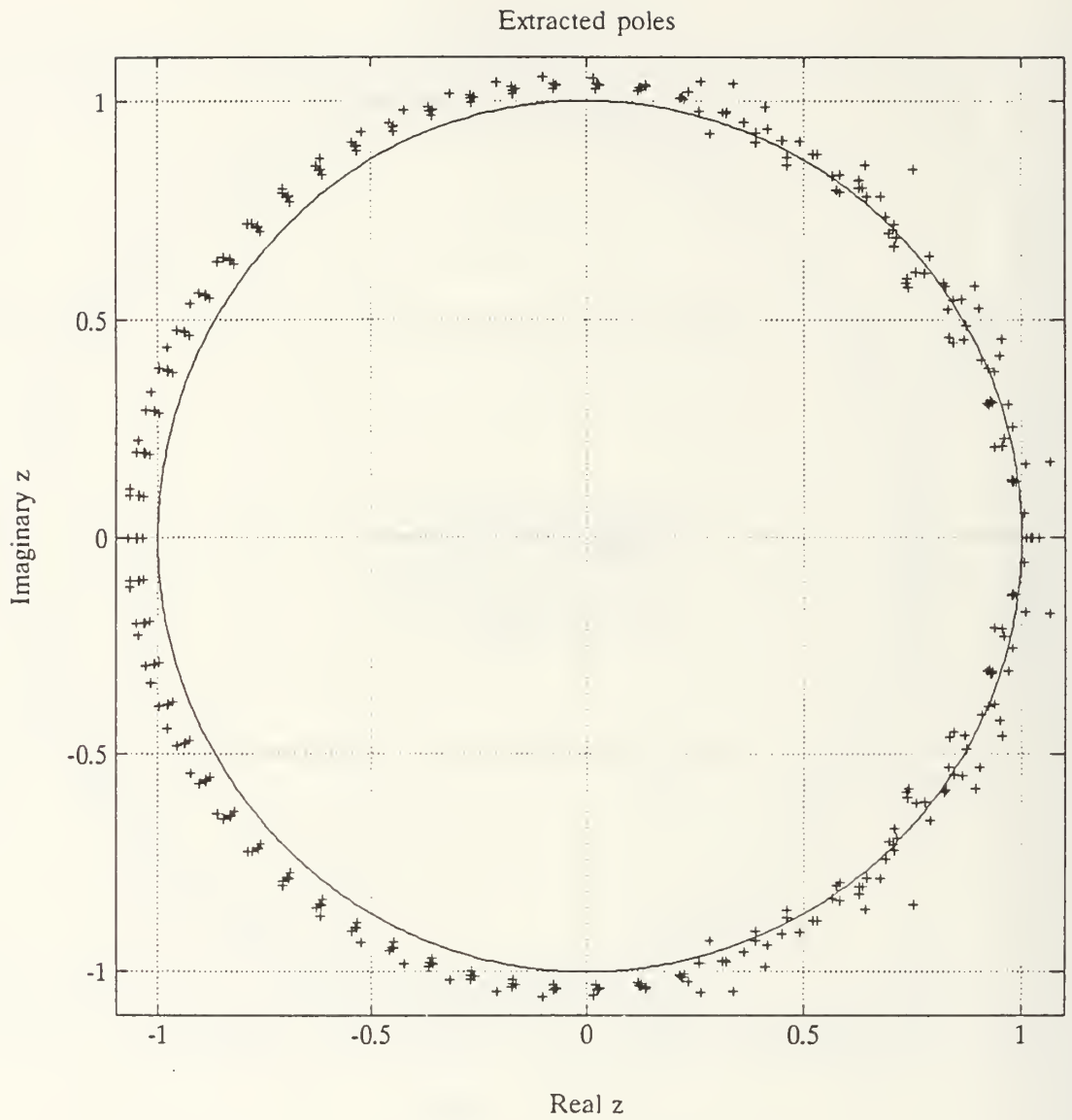


Figure 42. Kumaresan-Tufts Poles, Target 2

electromagnetic excitation where the response has the greatest magnitude.

1. Applicability

The early-time portion of a target's scattered field occurs as long as there is a driven portion of the total field. Once the field no longer contains a scattered response due, in part, to the incident excitation at points on the object, early-time ceases and late-time begins. Hence, the Cadzow-Solomon models both the system's input and output, and equivalently, the poles and zeros of the system transfer function.

2. Equations

The Cadzow-Solomon algorithm extends the autoregressive equation (9), used in Prony's method, to the more general autoregressive moving average (ARMA) equation

$$y_n = \sum_{l=1}^{K_D} b_l y_{n-l} + \sum_{l=0}^{K_N} a_l x_{n-l} \quad (23)$$

where the second summation term models the excitation to the system.

A set of M such equations in matrix form is given by

$$\begin{bmatrix} Y_0 & \cdots & Y_{K_D-1} & X_0 & \cdots & X_{K_N} \\ \vdots & & \vdots & \vdots & & \vdots \\ Y_{M-1} & \cdots & Y_{K_D+M-2} & X_{M-1} & \cdots & X_{K_N+M-1} \end{bmatrix} \begin{bmatrix} b'_{K_D} \\ \vdots \\ b'_1 \\ -\frac{1}{a_{K_N}} \\ \vdots \\ a_0 \end{bmatrix} = \begin{bmatrix} Y_{K_D} \\ \vdots \\ Y_{K_D+M-1} \end{bmatrix} \quad (24)$$

As in the Kumaresan-Tufts method, M is selected to be greater than the column dimension of the data matrix which is $K_D + K_N + 1$.

3. Excess Poles and Noise Removal

The Cadzow-Solomon method used in this thesis is a modification which incorporates the non-causal arrangement of the system equations used by Kumaresan-Tufts. This modification was first discussed by Norton in [16]. The Kumaresan approach of overestimating the system order can be used as before in a non-causal model to constrain the noise poles inside the unit circle, while SVD forces the signal poles outside the unit circle.

Since the input waveform is known, its order can be almost exactly determined. In all the work of this thesis, the input waveform used is the double Gaussian depicted in Figure 14. Approximately 25 samples defining this pulse of 0.5 nanoseconds duration makes K_N equal 25 in equation (23). Since the input is causal, the signal zeros fall inside the unit circle where they cannot be easily segregated from similarly located noise poles. However, the signal zeros impart no information about the target and need not be extracted. The inclusion of the input in the data matrix is nevertheless vital to the model of the system and the accurate determination of the signal poles.

The ARMA equation of (23) can be modified to obtain

$$y_n = \sum_{i=1}^{K_D} b'_i y_{K_D+n-1+i} + \sum_{i=0}^{K_N} a_i x_{n-1} \quad (25)$$

The recursive portion of (25) is now in a non-causal form similar to expression (12). A set of M such equations in matrix form is given by

$$\begin{bmatrix} Y_{K_N+1} & \cdots & Y_{K_N+K_D} & x_0 & \cdots & x_{K_N} \\ \vdots & & \vdots & \vdots & & \vdots \\ Y_{K_N+M} & \cdots & Y_{K_N+K_D+M-1} & x_{M-1} & \cdots & x_{K_N+M-1} \end{bmatrix} \begin{bmatrix} b'_{K_D} \\ \vdots \\ -\frac{b'_1}{a_{K_N}} \\ \vdots \\ a_0 \end{bmatrix} = \begin{bmatrix} Y_{K_D} \\ \vdots \\ Y_{K_D+M-1} \end{bmatrix} \quad (26)$$

Or, in matrix notation

$$[D_{yx}] \begin{bmatrix} -\frac{b'}{a} \end{bmatrix} = y \quad \text{where} \quad [D_{yx}] = [D_y : D_x] \quad (27)$$

4. Singular Value Decomposition

Like the system equations of the Kumaresan-Tufts model, the system equations in (26) are processed using singular value decomposition. The coefficient vector is again the minimum-norm solution, which constrains the extraneous poles and extraneous zeros to be inside the unit circle.

5. Bias Compensation in the Cadzow-Solomon Formulation

By compensating the eigenvalues of the Σ matrix in (16), the performance of the Kumaresan-Tufts algorithm is significantly improved in the presence of noise. Cadzow-Solomon have shown [5] that if the actual orders K'_D and K'_N

are overestimated to be K_D and K_N , $\min(K_D - K'_D, K_N - K'_N)$ singular values are zero in noiseless data. Since the input data is known, the eigenvalues of the data matrix may be compensated in the same manner as in the Kumaresan-Tufts algorithm for noiseless data.

To understand the compensation required in noisy data, an analysis of additive noise is required. As given by Norton [16], if the input data noise is w_1 and the output data noise is v_1 , the data matrix may be modeled as

$$[D_{yx}] = [D_y : D_x] = S_{yx} + N_{yx} \quad (28)$$

where

$$[N_{yx}] = [N_y : N_x] \quad (29)$$

and

$$N_x = \begin{bmatrix} 1 & & K_D \\ \vdots & & \vdots \\ w_M & \dots & w_{M+K_D} \end{bmatrix} \quad N_y = \begin{bmatrix} v_1 & \dots & v_{K_D} \\ \vdots & & \vdots \\ v_M & \dots & v_{M+K_D} \end{bmatrix} \quad (30)$$

The expected value of $D_{yx} D_{yx}^T$ is then

$$E[D_{yx} D_{yx}^T] = S_{yx} S_{yx}^T + E[N_{yx} N_{yx}^T] \quad (31)$$

If the input and output noise variances are not equal, the eigenvalue shifting theorem used in Kumaresan-Tufts cannot be used to analytically predict the requisite eigenvalue compensation of $D_{yx} D_{yx}^T$. Nevertheless, when the input and output variances were assumed equal, and eigenvalue compensation similar to that used in Kumaresan-Tufts was

performed, the results were consistently superior to those obtained without compensation. Therefore, the results of Cadzow-Solomon signal processing presented in this thesis were obtained using eigenvalue compensation and the assumption of equal noise variance.

6. Performance

The Cadzow-Solomon algorithm was programmed in Fortran and tested on the same data used for evaluating the Kumaresan-Tufts algorithm. Note that the Cadzow-Solomon algorithm can use the early-time portion of the data that the Kumaresan-Tufts algorithm can not use. The program appears in Appendix B.

a. Synthetically Generated Data

The starting point for evaluating the performance of the Cadzow-Solomon algorithm was with synthetically generated data of the form given by (8) plus the addition of input data required to model early time data.

1. Noise Performance

The algorithm was evaluated at various signal-to-noise ratios, ranging from 90.0 dB to 7.0 dB. Figure 43 shows the signal produced by two s-plane poles at 90.0 dB, with a late-time beginning at 10.0 nanoseconds. Figures 44 through 48 depict the poles extracted from this signal at the different signal-to-noise ratios.

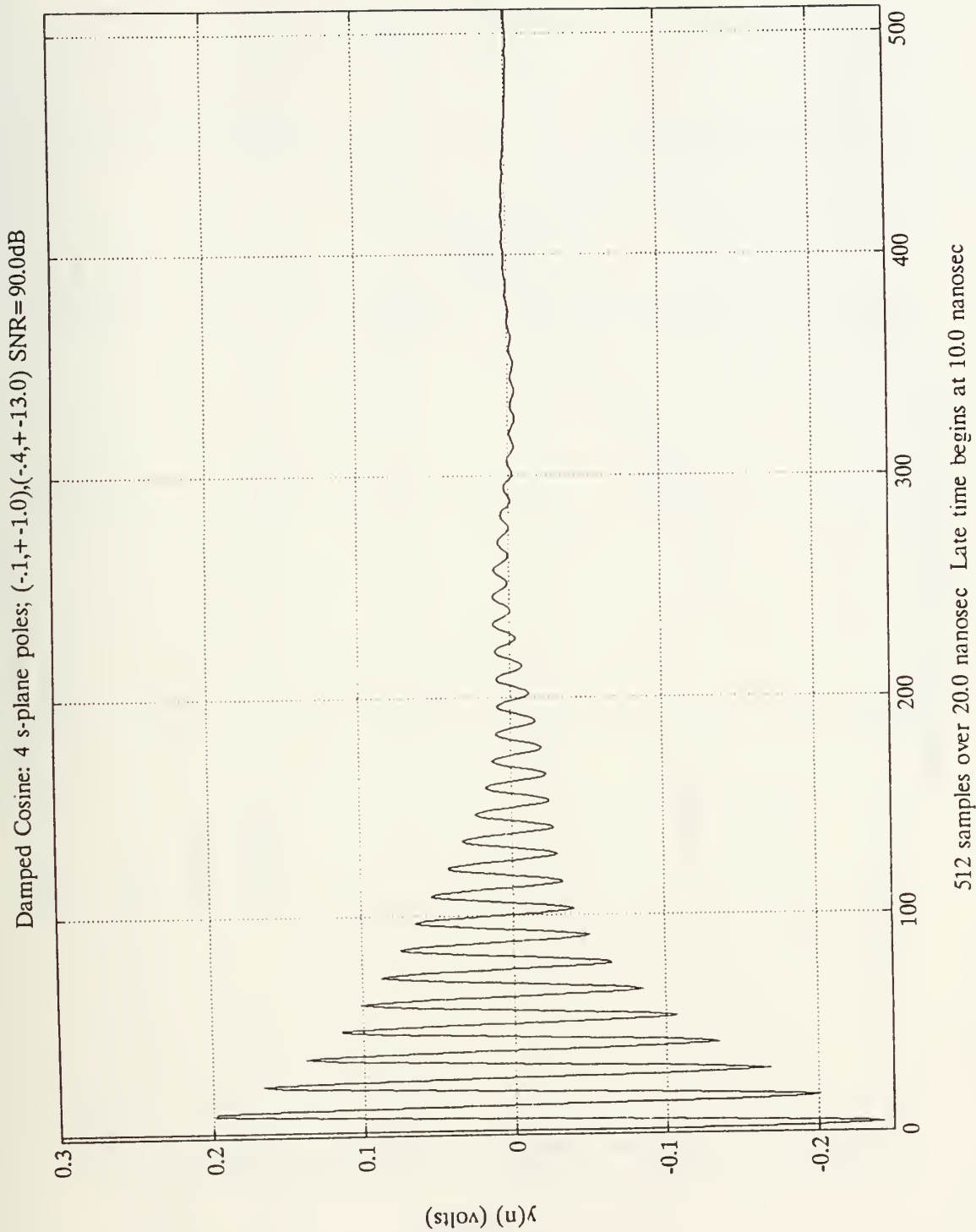


Figure 43. Signal Containing Two S-Plane Poles, 90.0 dB SNR

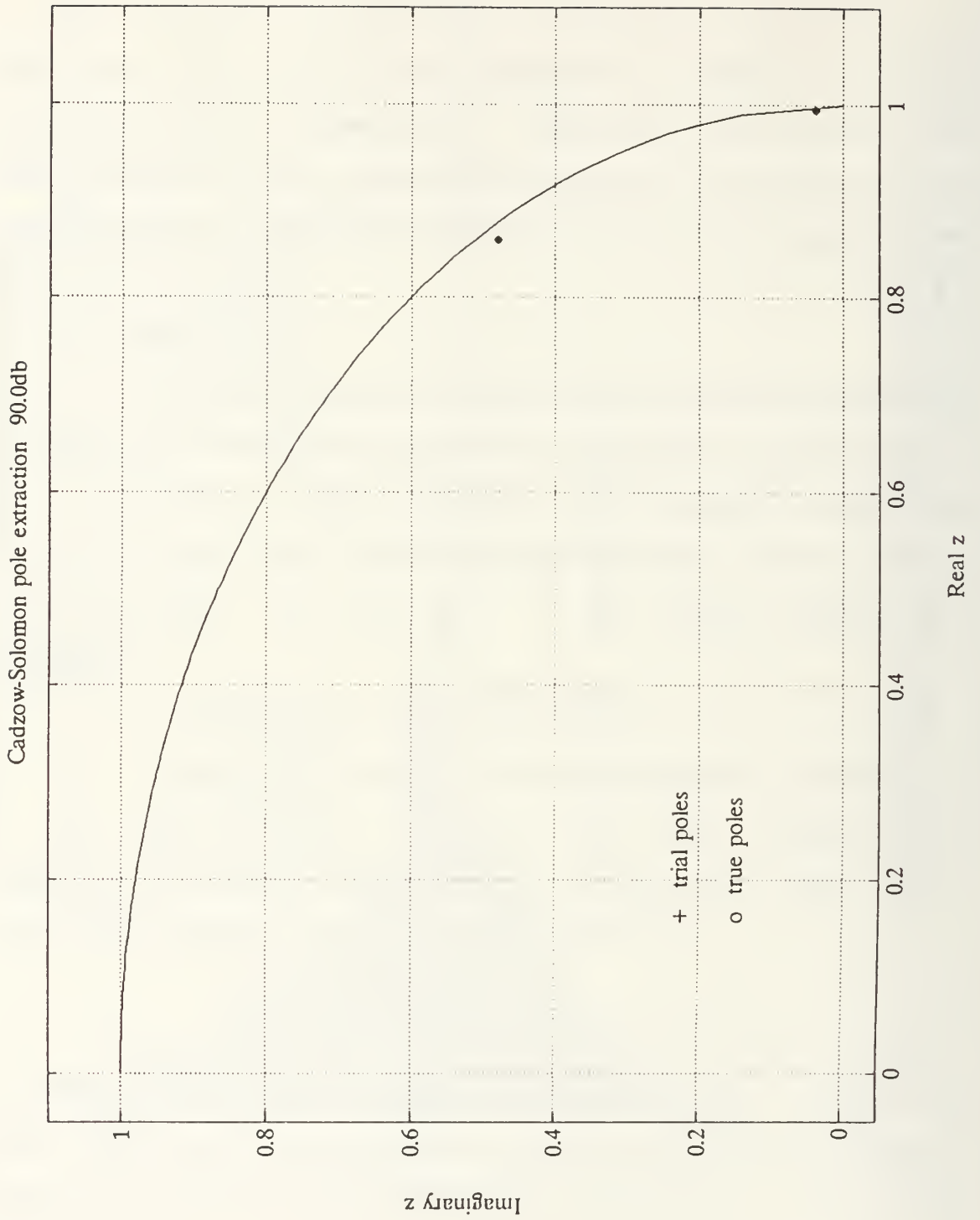


Figure 44. Cadzow-Solomon Poles, Synthetic Data, 90.0 dB SNR

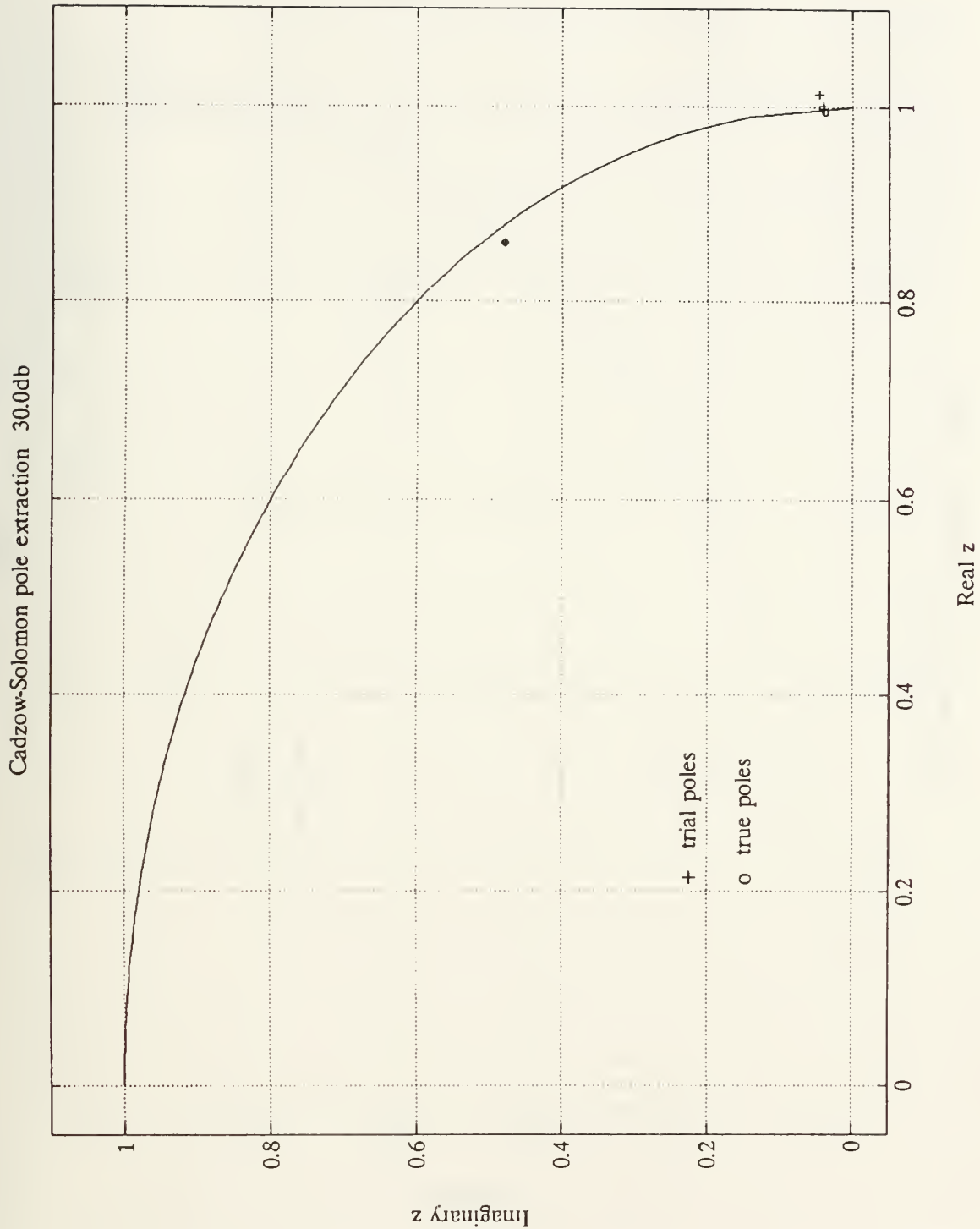


Figure 45. Cadzow-Solomon Poles, Synthetic Data, 30.0 dB SNR

Cadzow-Solomon pole extraction 20.0db

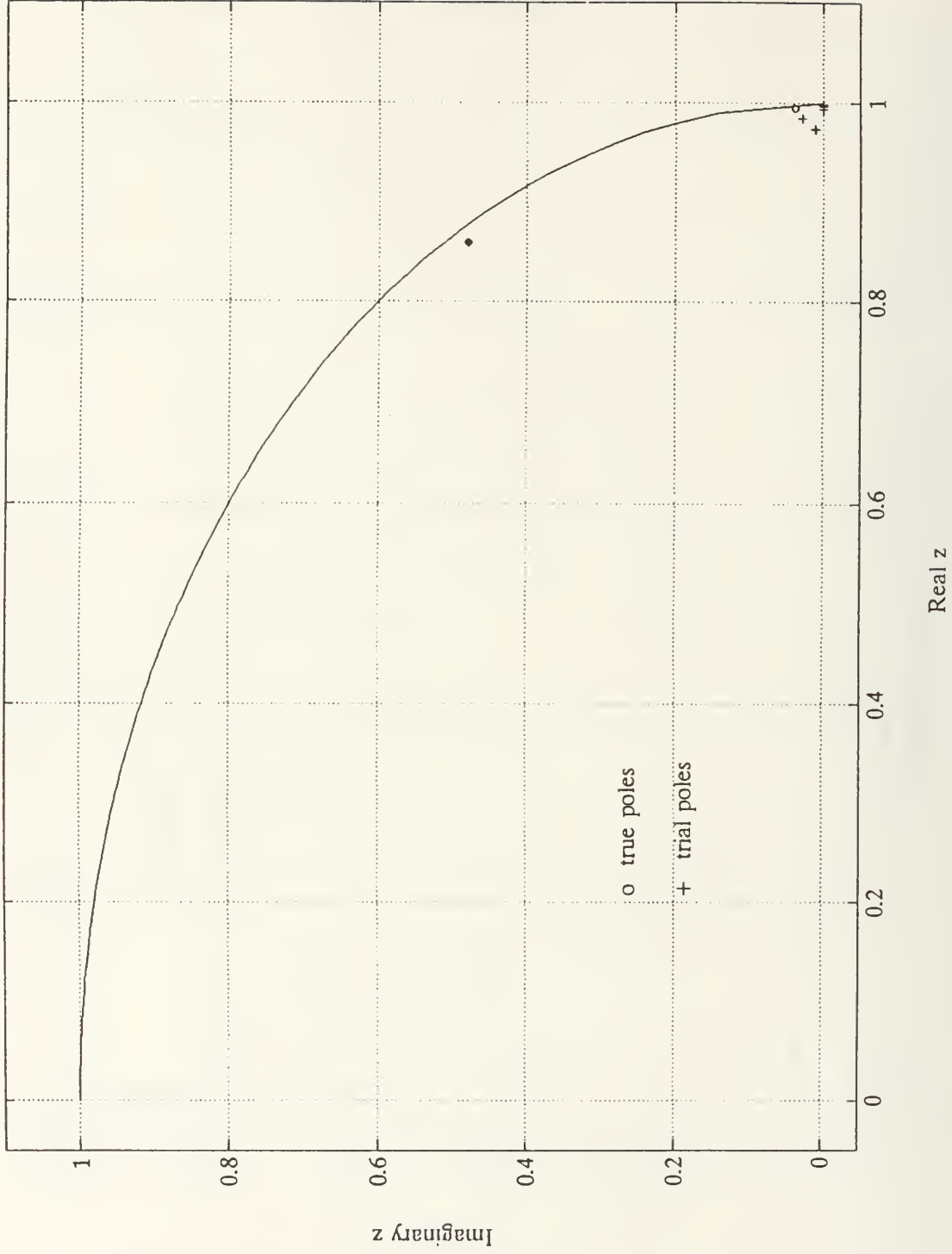


Figure 46. Cadzow-Solomon Poles, Synthetic Data, 20.0 dB SNR

Cadzow-Solomon pole extraction 10.0db

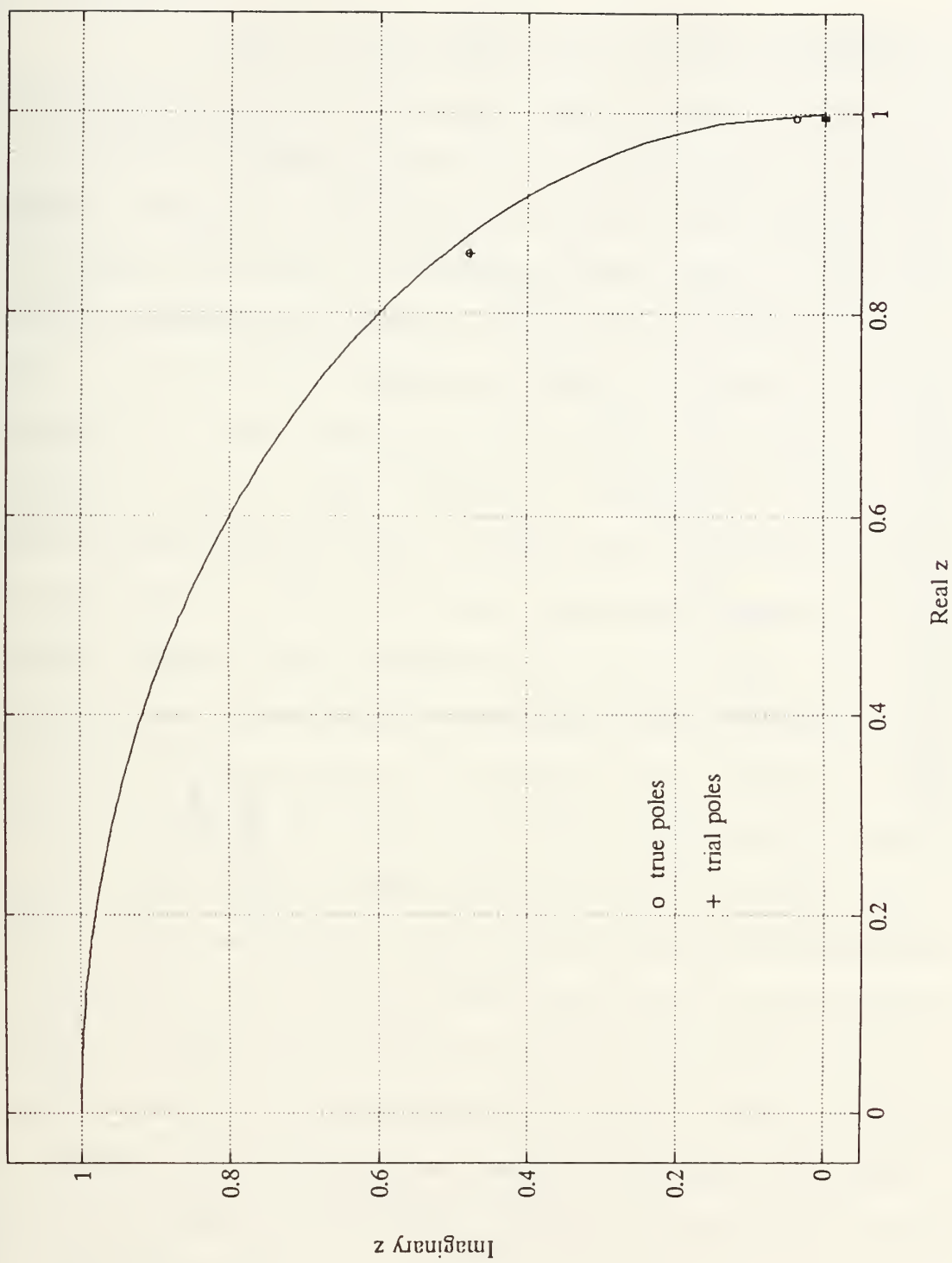


Figure 47. Cadzow-Solomon Poles, Synthetic Data, 10.0 dB SNR

Cadzow-Solomon pole extraction 7.0db

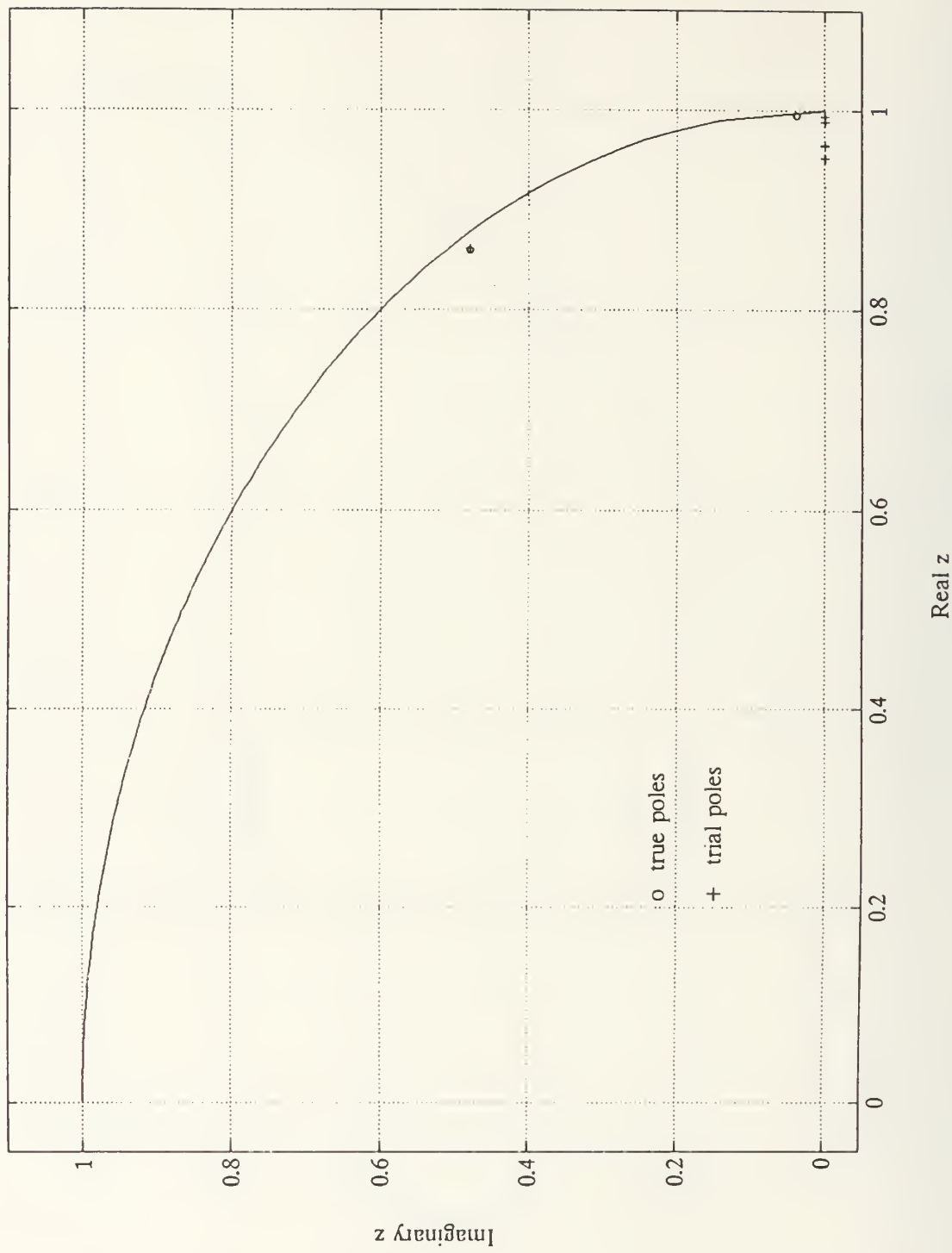


Figure 48. Cadzow-Solomon Poles, Synthetic Data, 7.0 dB SNR

The figures chart the steady degradation of the algorithm's performance with the increase of noise. At 30.0 dB, the location of the low frequency pole is already slightly displaced. More significant is the location of one of the extracted poles in the noise signal space. At 20.0 dB, the low frequency pole is located in some trials on the real axis. At 10.0 dB, all the extractions are located on the real axis and at 7.0 dB their locations there are dispersed. The extraction of the higher frequency pole is uncharacteristically more accurate than that of the low frequency pole. Even at 7.0 dB, the high frequency pole is located with excellent accuracy. The location of the low frequency pole near the real axis was chosen deliberately to illustrate the difficulty in resolving the slight frequency difference between the true pole and a noise pole located on the real axis. Also, fewer points were processed using the Cadzow-Solomon method than were processed using the Kumaresan-Tufts method, since the largest data matrix allowed by the programs in Appendices A and B contain fewer data points in the Cadzow-Solomon data matrix than in the Kumaresan-Tufts data matrix. The results demonstrate the need to process a substantial number of points in order to accurately extract low frequency poles.

b. Thin Wire Integral Equation Generated Data

The performance of the Cadzow-Solomon algorithm was evaluated using the same set of data tested by the Kumaresan-Tufts algorithm. The results are presented in Figure 49. Tight clusters appear at frequencies higher than those obtained with the Kumaresan-Tufts algorithm. Figure 50 depicts the poles extracted from the same signal at a 20.0 dB SNR. The clustering at this SNR is comparable to the results obtained by the Kumaresan-Tufts method with the noiseless data. Further angle-by-angle comparisons of the poles extracted from the noiseless data and the 20.0 dB data are depicted in Figures 51 through 54. Note the small number of poles in Figure 54 due to the unexcited odd-symmetric poles at 90° aspect.

One further test was conducted on computed data at a 7.0 dB SNR. The results are depicted in Figure 55. Even at 7.0 dB, discernible clusters are present. Angle-by-angle comparisons of the poles obtained in 7.0 dB data and those obtained in noiseless data are presented in Figures 56 through 59.

c. Scale Models

The same scale models used to evaluate the Kumaresan-Tufts algorithm were used to evaluate the Cadzow-Solomon algorithm.

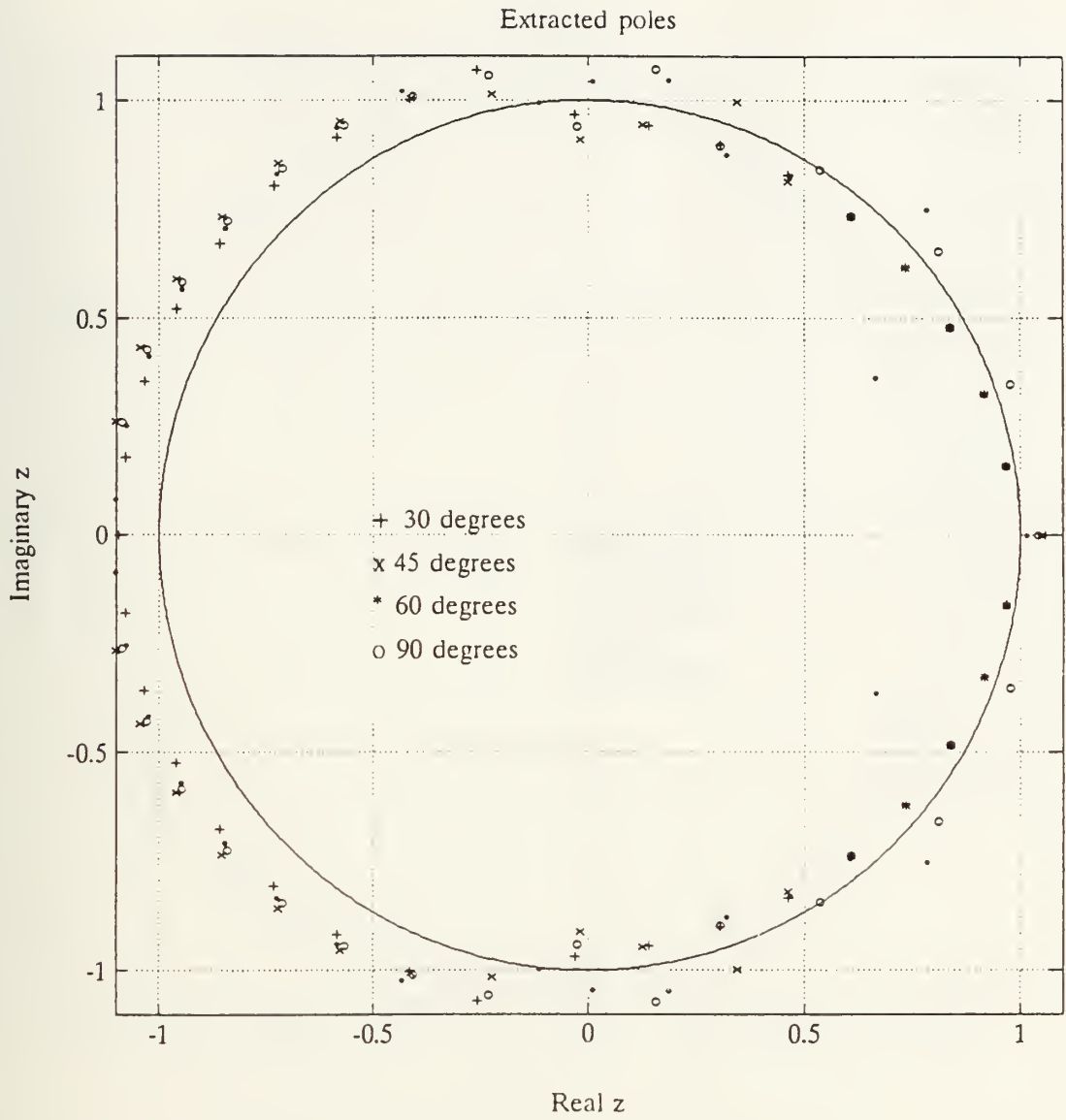


Figure 49. Cadzow-Solomon Poles, Noiseless Thin Wire Data

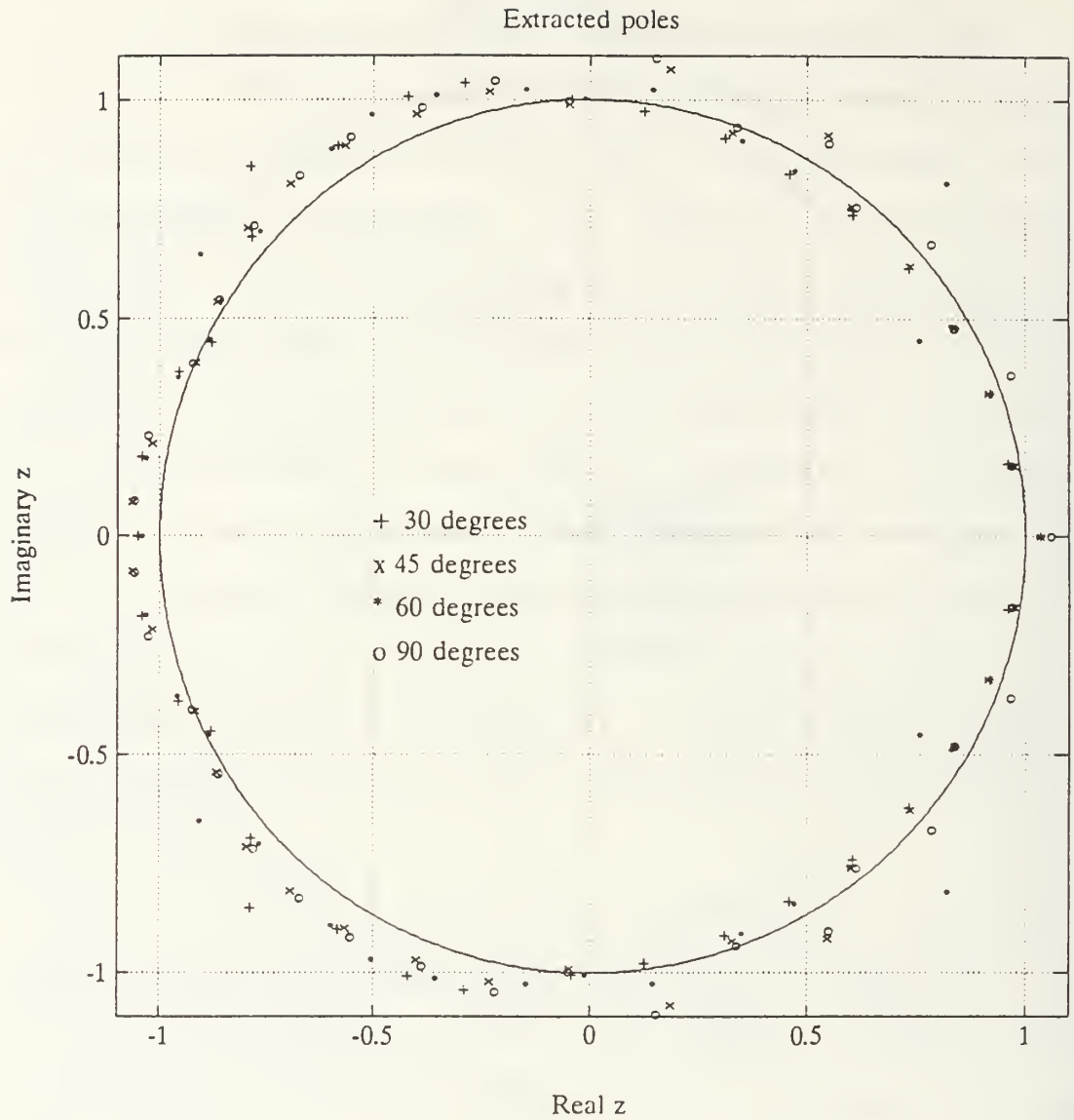


Figure 50. Cadzow-Solomon Poles, 20.0 dB SNR

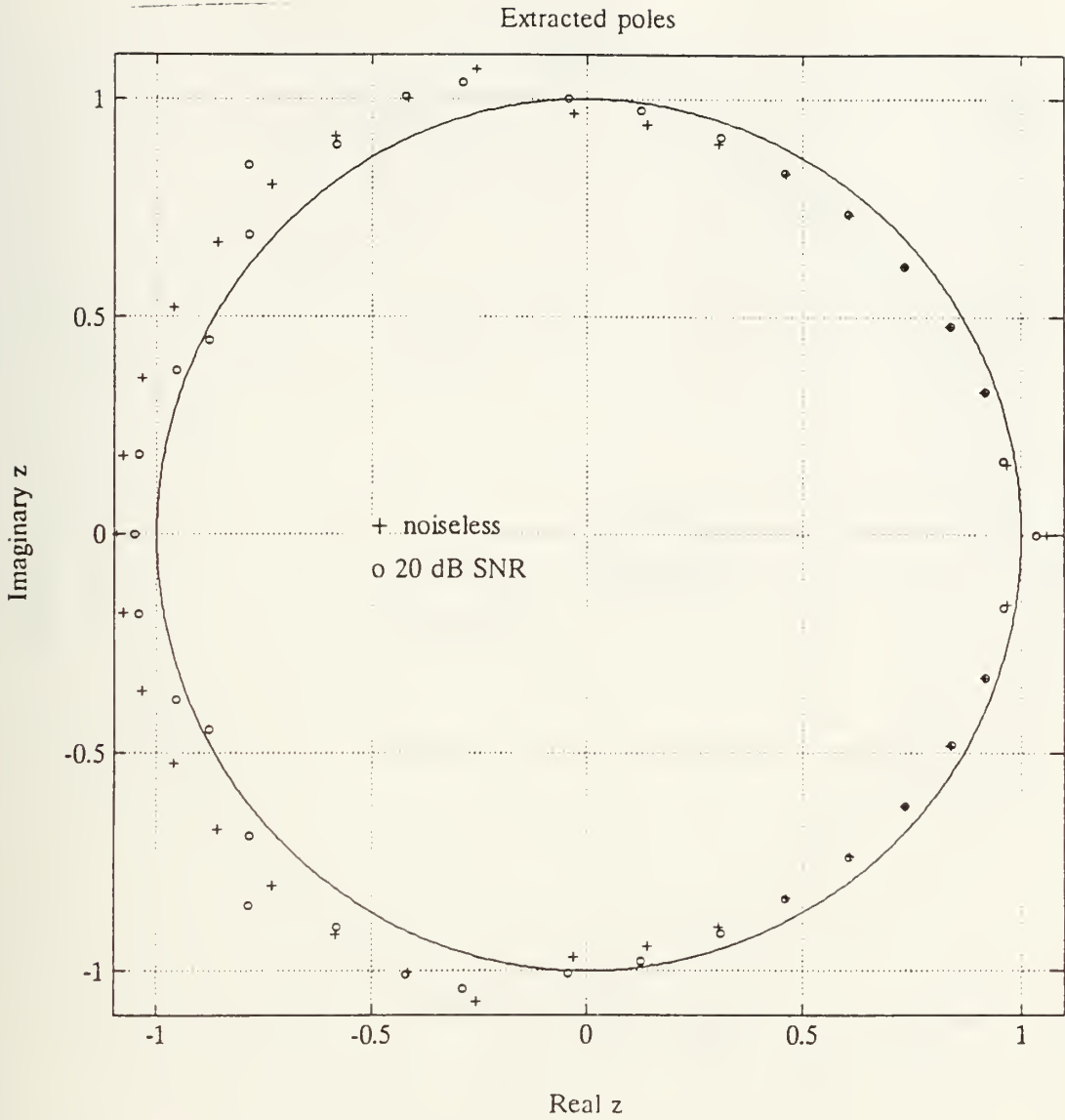


Figure 51. Integral Equation Thin Wire Comparison, Noiseless vs. 20.0 dB SNR, 30 Degree Aspect

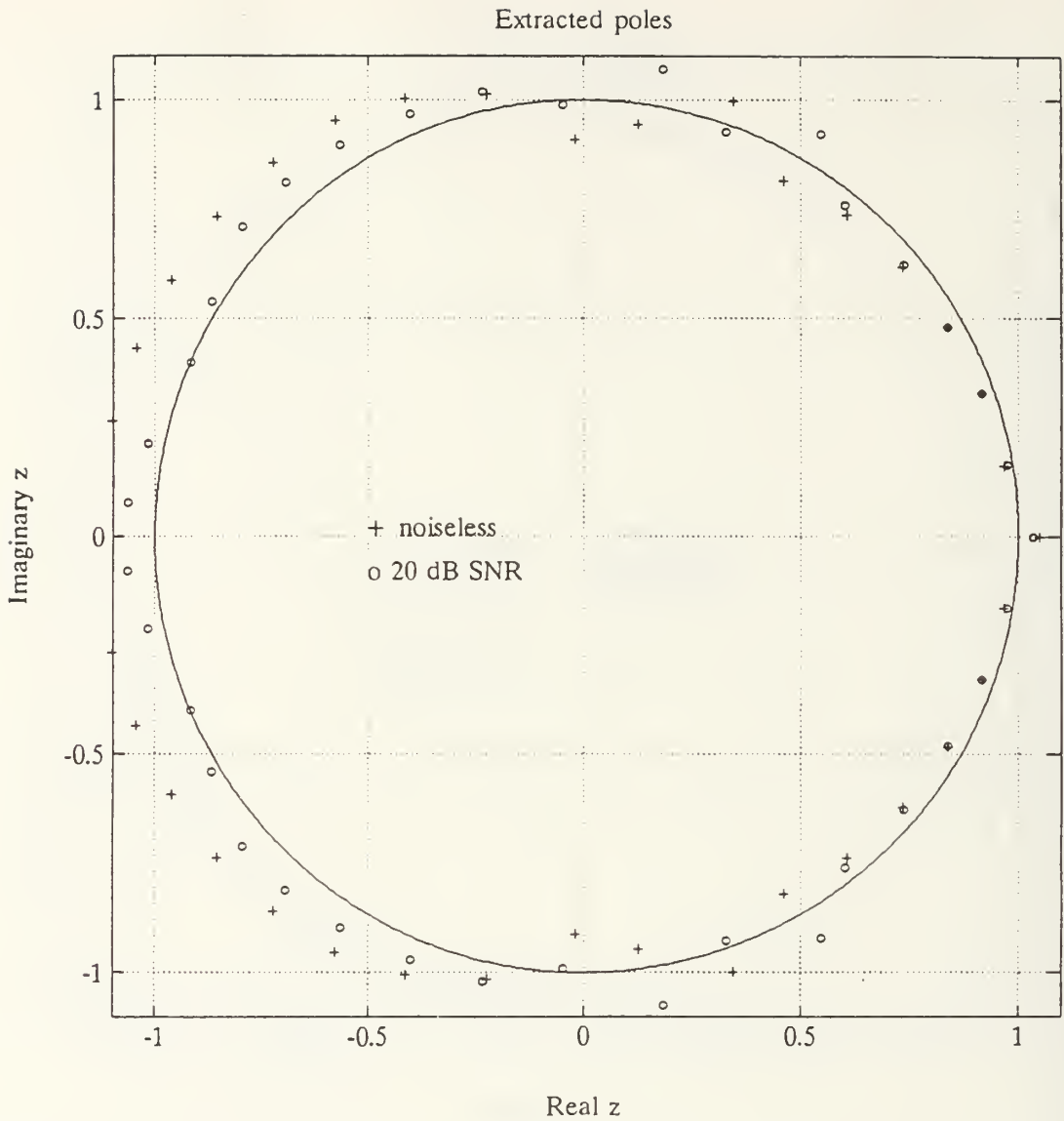


Figure 52. Integral Equation Thin Wire Comparison, Noiseless vs. 20.0 dB SNR, 45 Degree Aspect

Extracted poles

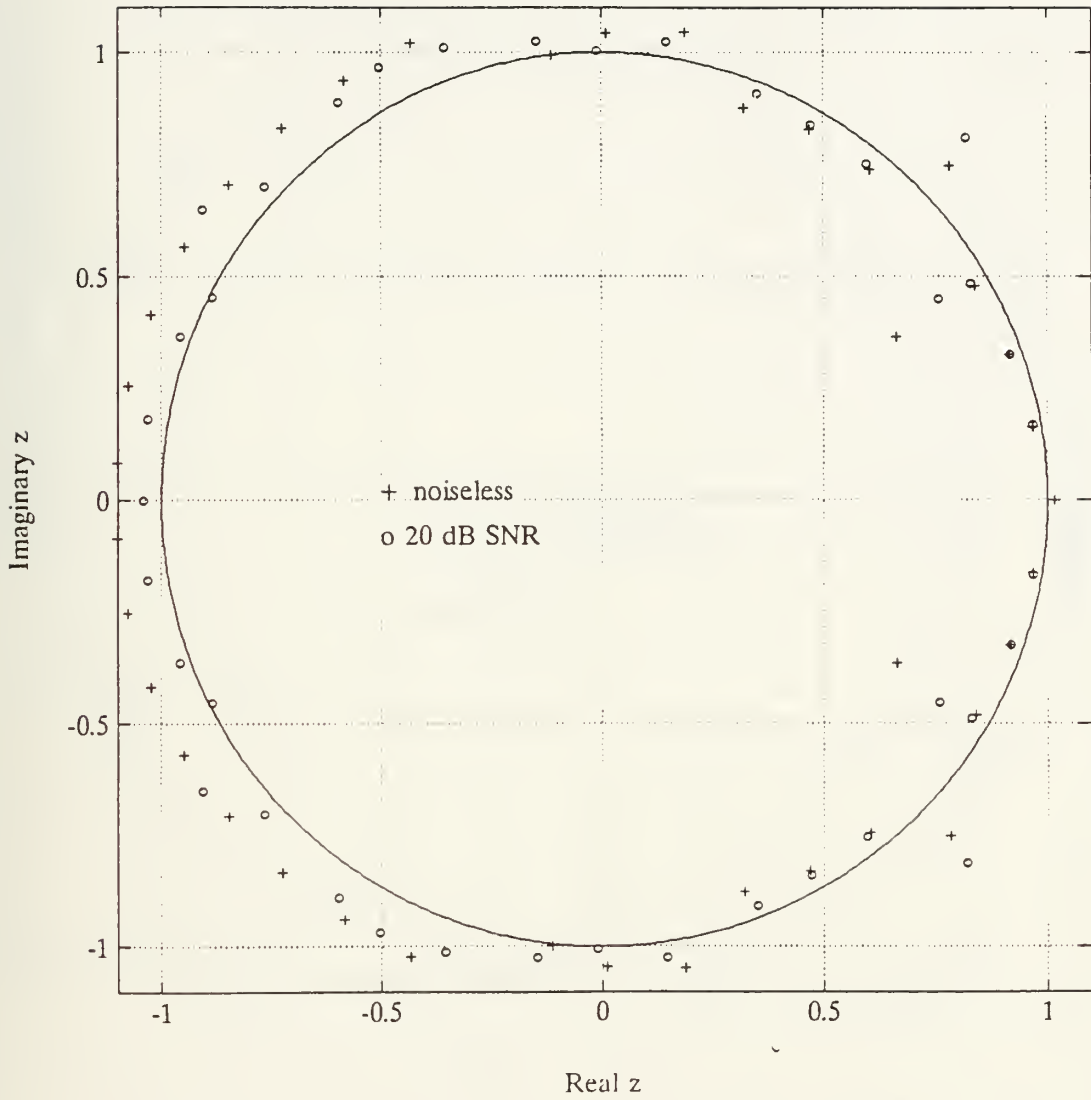


Figure 53. Integral Equation Thin Wire Comparison, Noiseless vs. 20.0 dB SNR, 60 Degree Aspect

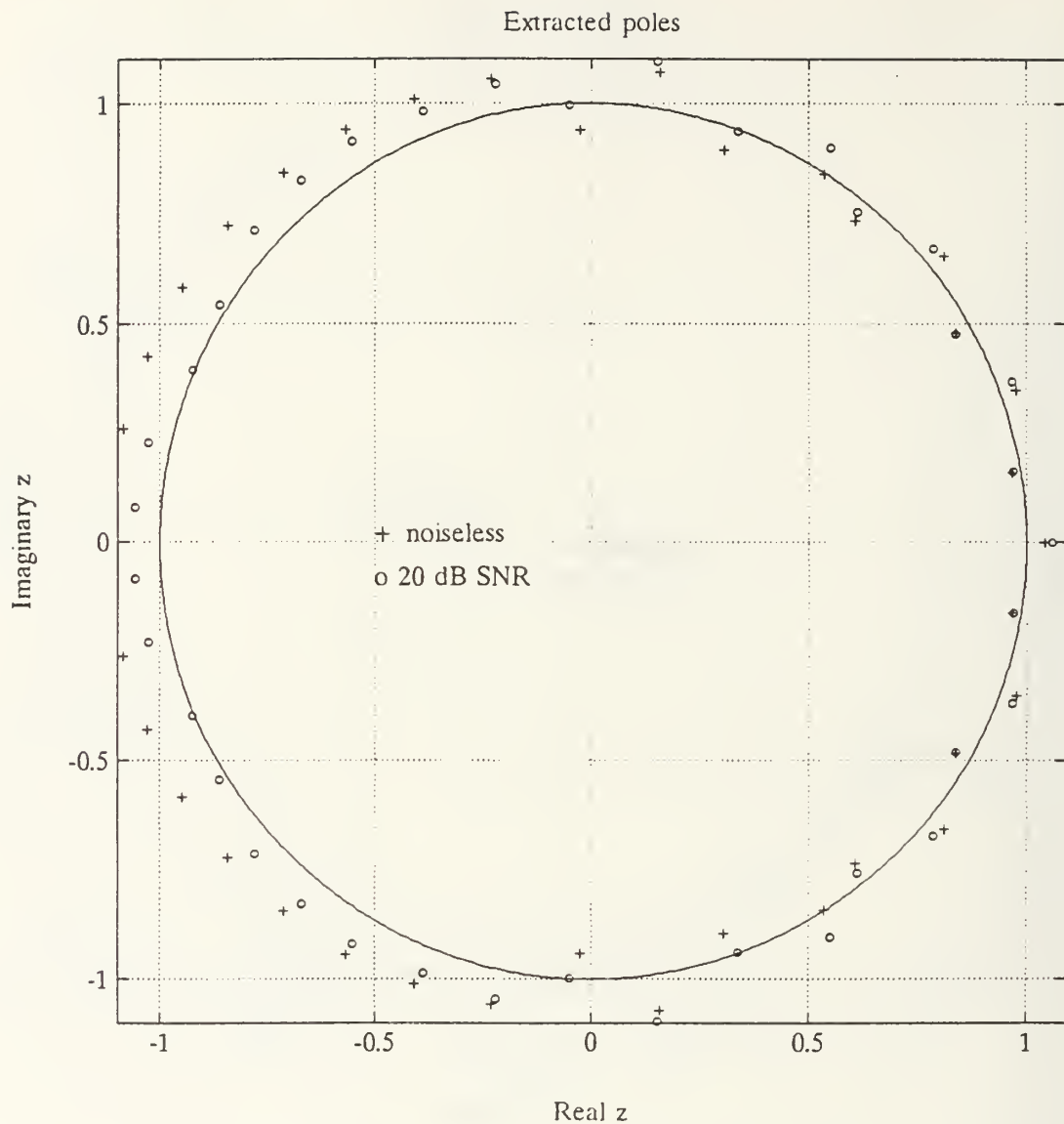


Figure 54. Integral Equation Thin Wire Comparison, Noiseless vs. 20.0 dB SNR, 90 Degree Aspect

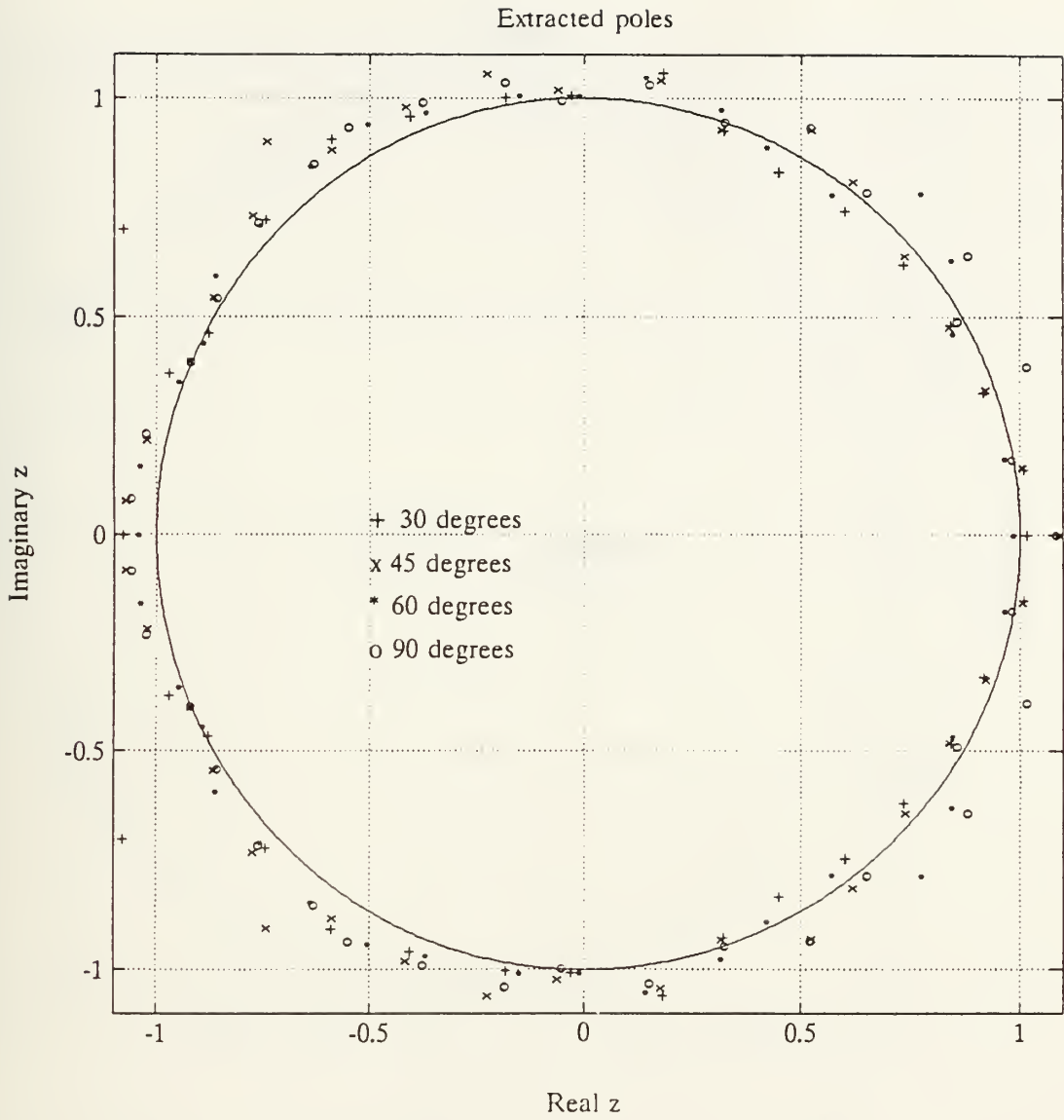


Figure 55. Cadzow-Solomon Poles, 7.0 dB SNR

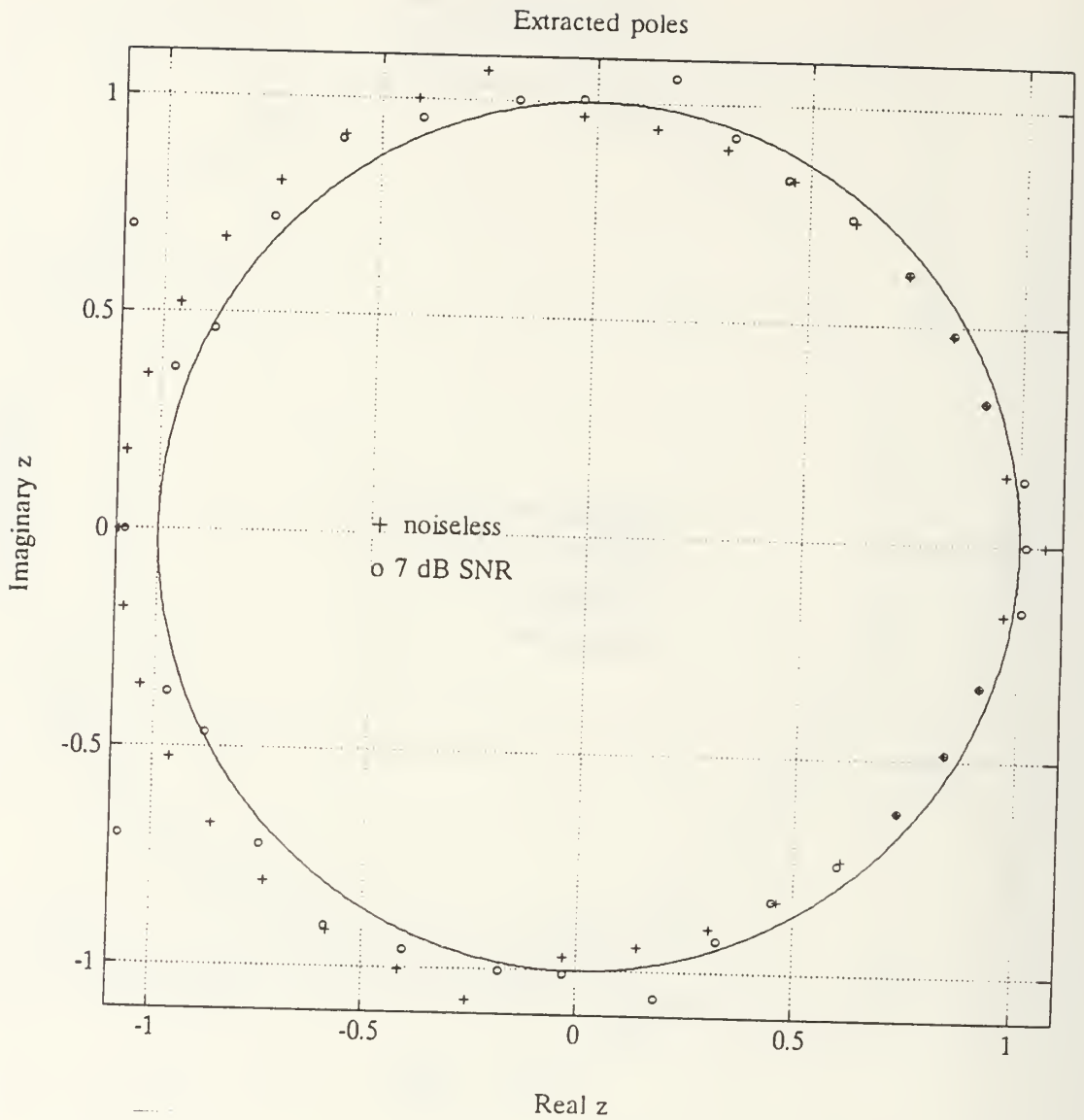


Figure 56. Integral Equation Thin Wire Comparison, Noiseless vs. 7.0 dB SNR, 30 Degree Aspect

Extracted poles

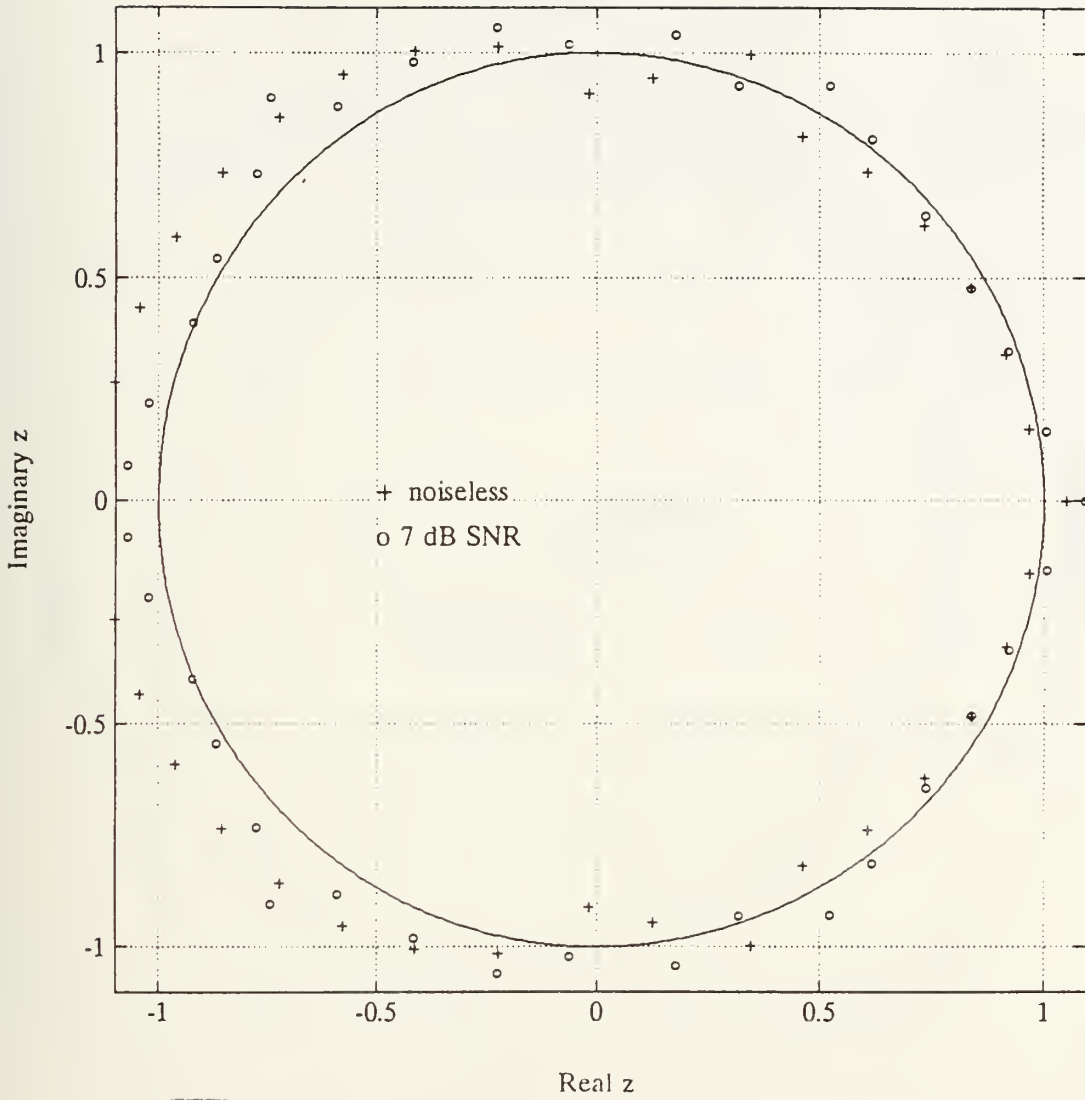


Figure 57. Integral Equation Thin Wire Comparison, Noiseless vs. 7.0 dB SNR, 45 Degree Aspect

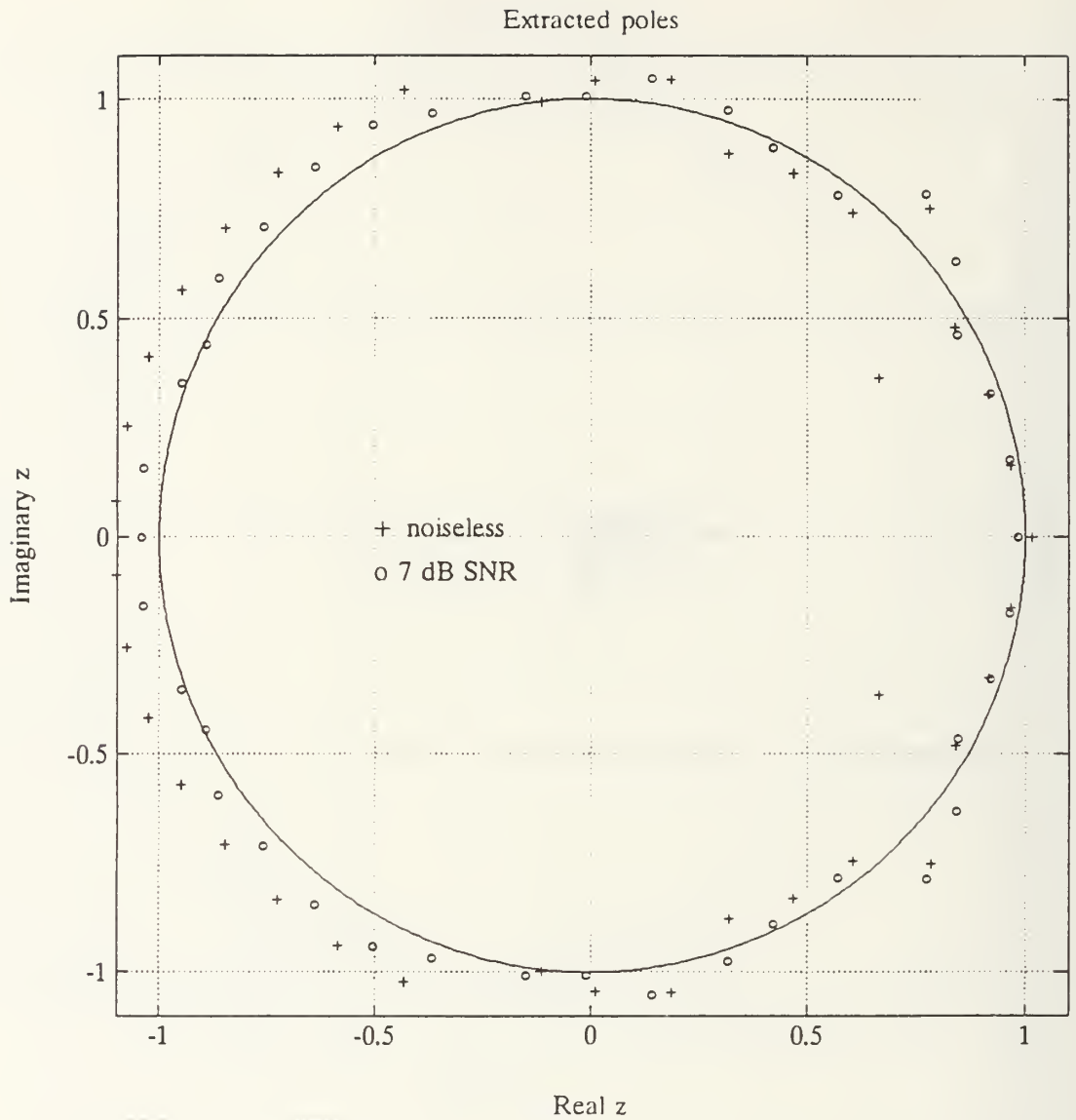


Figure 58. Integral Equation Thin Wire Comparison, Noiseless vs. 7.0 dB SNR, 60 Degree Aspect

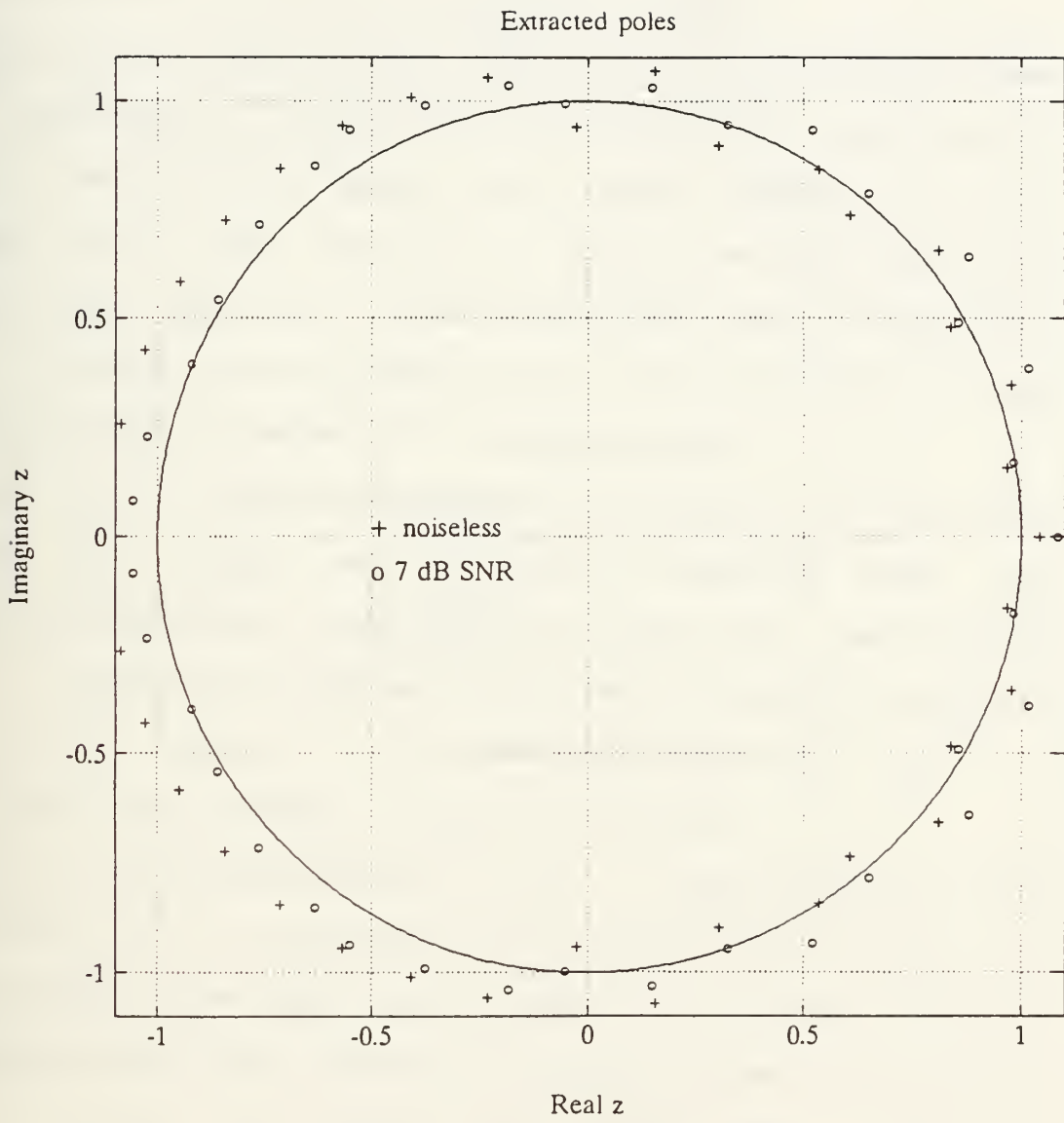


Figure 59. Integral Equation Thin Wire Comparison, Noiseless vs. 7.0 dB SNR, 90 Degree Aspect

1. Wire Targets

Figure 60 depicts the poles extracted from measurements of a 0.1 meter wire. Three tight clusters appear at the lowest frequencies and at the highest frequencies. The poles in between can not be easily discriminated. The dispersion of these poles is apparently due to the aspect dependence of their measurable power. In other words, these poles are excited more at some aspects than at others.

Figure 61 depicts the comparison between poles extracted from computed data and measured data. As in Figure 60, close agreement exists at the highest and lowest frequencies. The results are much more favorable than those similarly obtained by the Kumaresan-Tufts algorithm.

2. Model Aircraft

Figures 62 through 64 depict poles extracted from aircraft target 1. As in the Kumaresan-Tufts testing, the Cadzow-Solomon testing was conducted at six different aspects. Results for target 2 are depicted in Figures 65 through 67. The results of both targets show clearly defined clusters. The first two clusters of target 2 are exceptionally tight. However, the mid-frequency clusters of target 2 are not as clearly formed as those of target 1.

Comparisons of poles obtained with each method for target 1 and 2 are depicted in Figure 68 and 69 respectively. These two figures graphically depict the clear

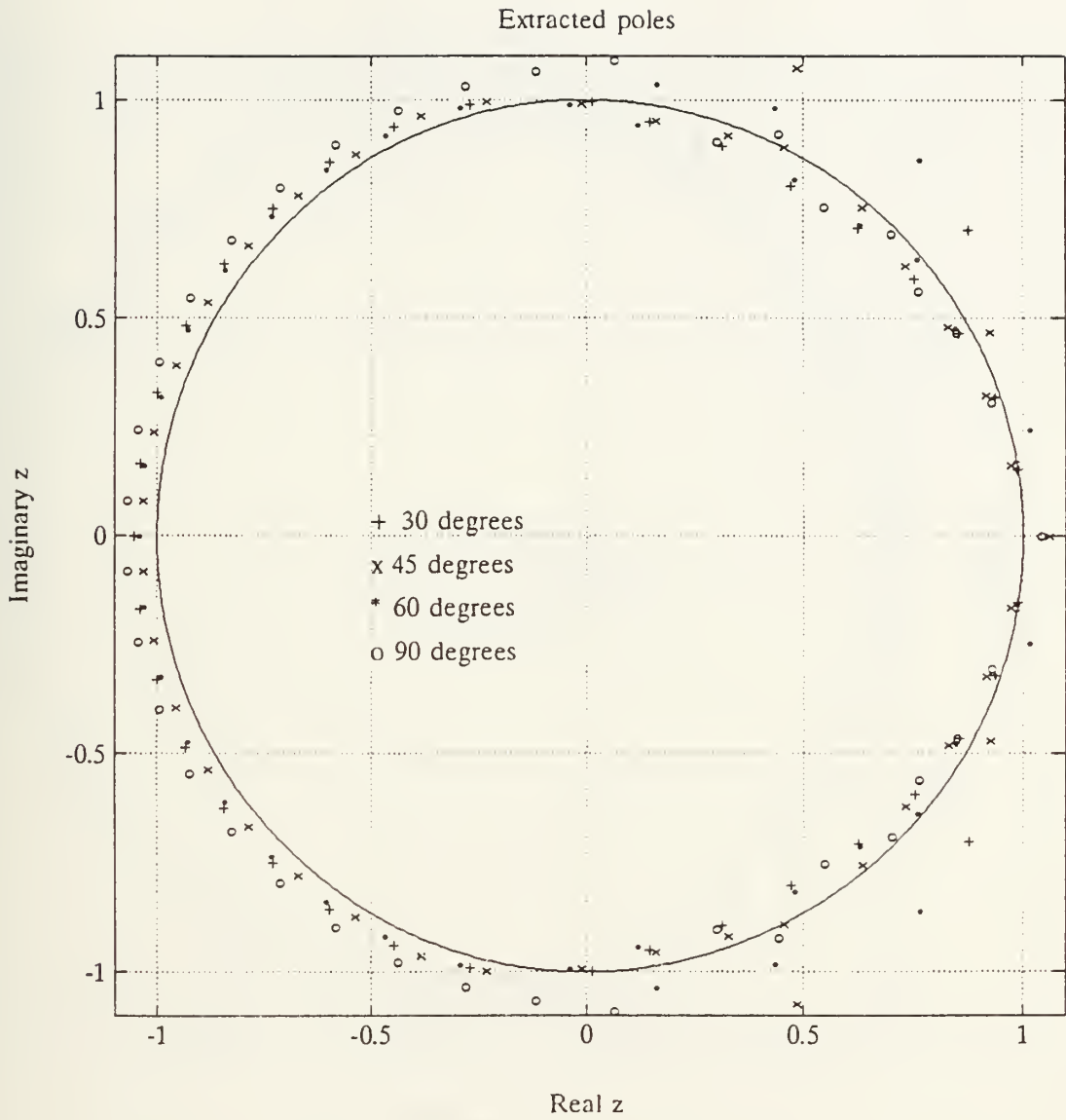


Figure 60. Cadzow-Solomon Poles, Measured Thin Wire

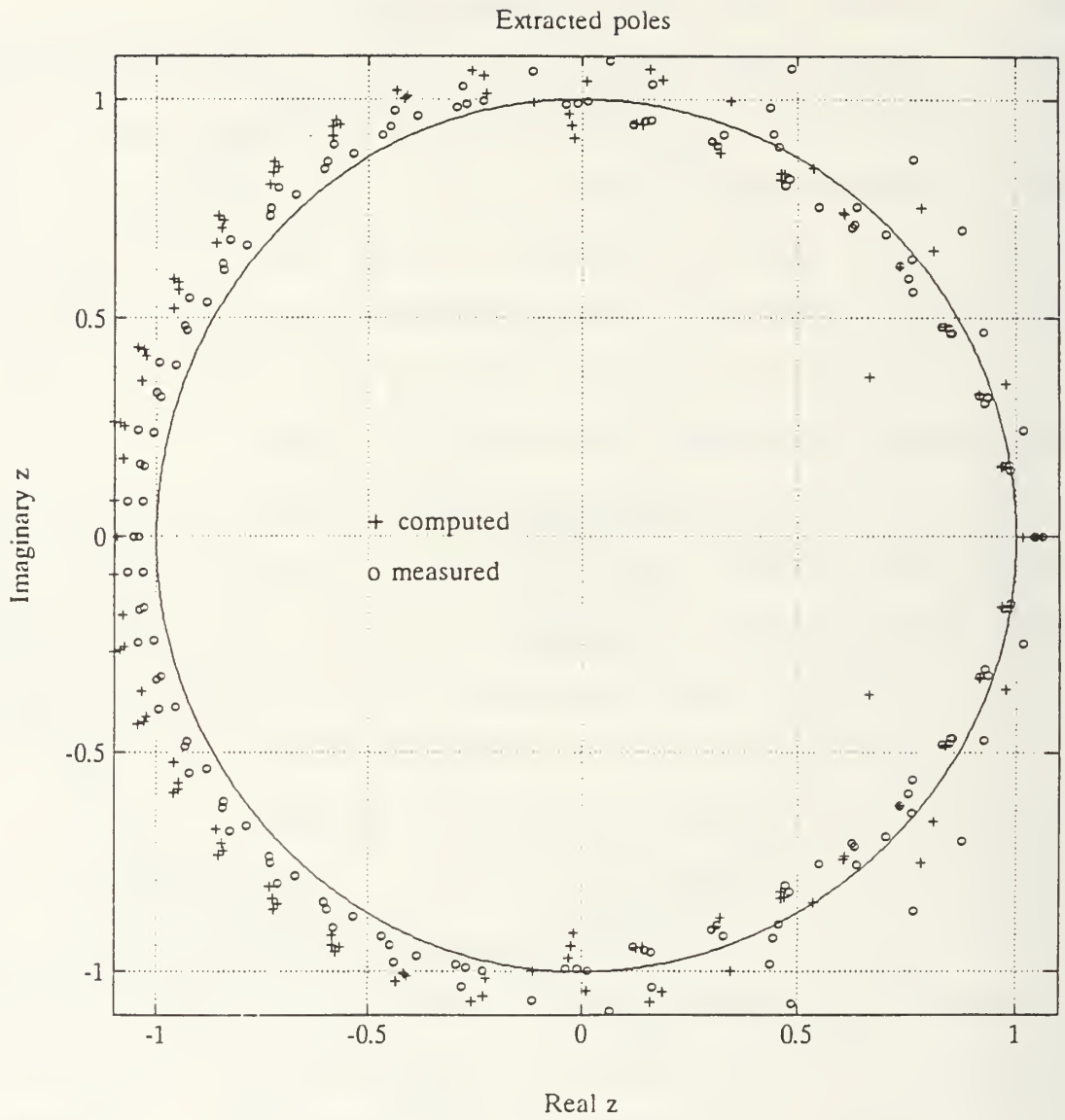


Figure 61. Thin Wire Comparison, Measured vs. Integral Equation

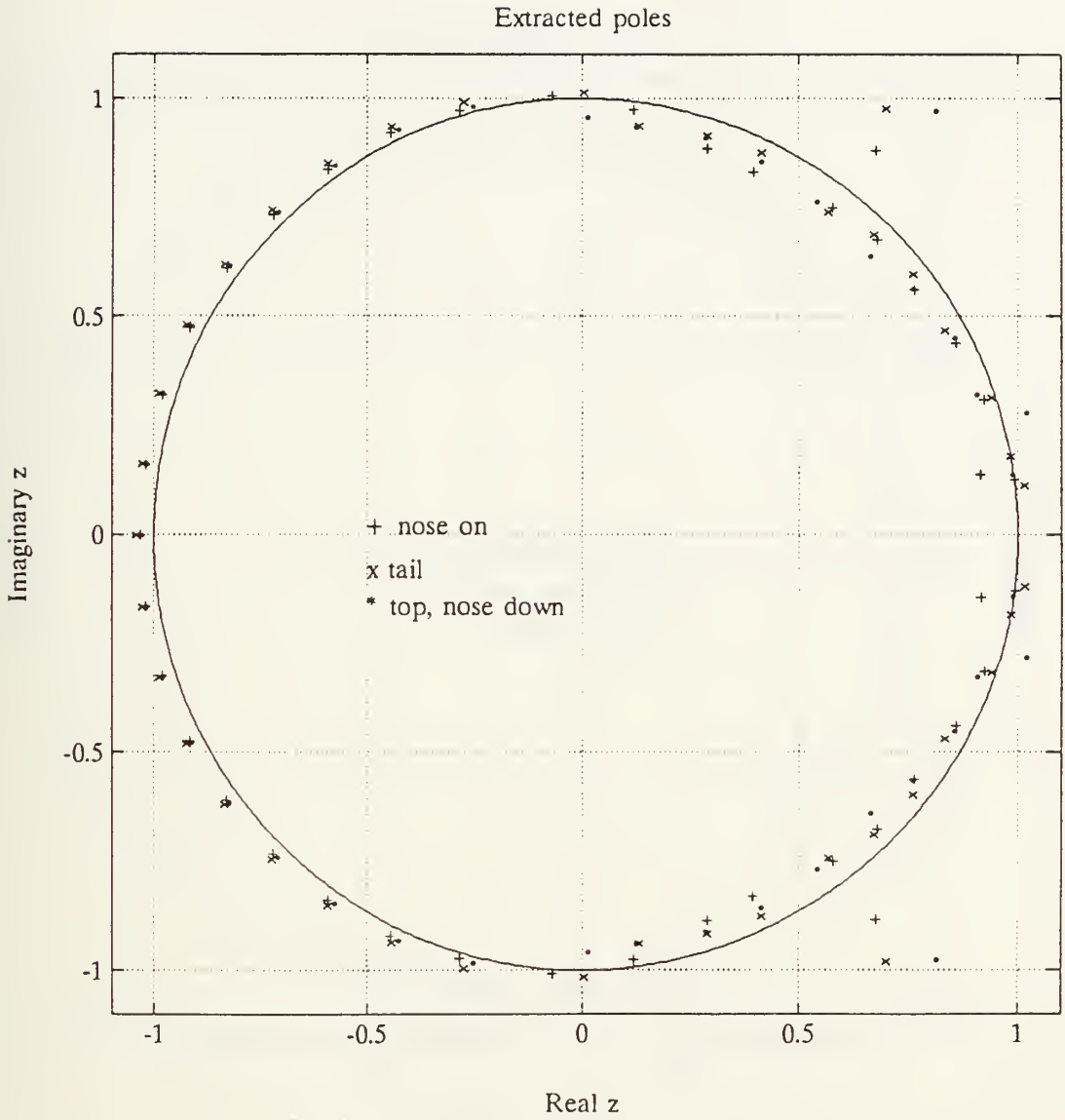


Figure 62. Cadzow-Solomon Poles Target 1, Three Aspects

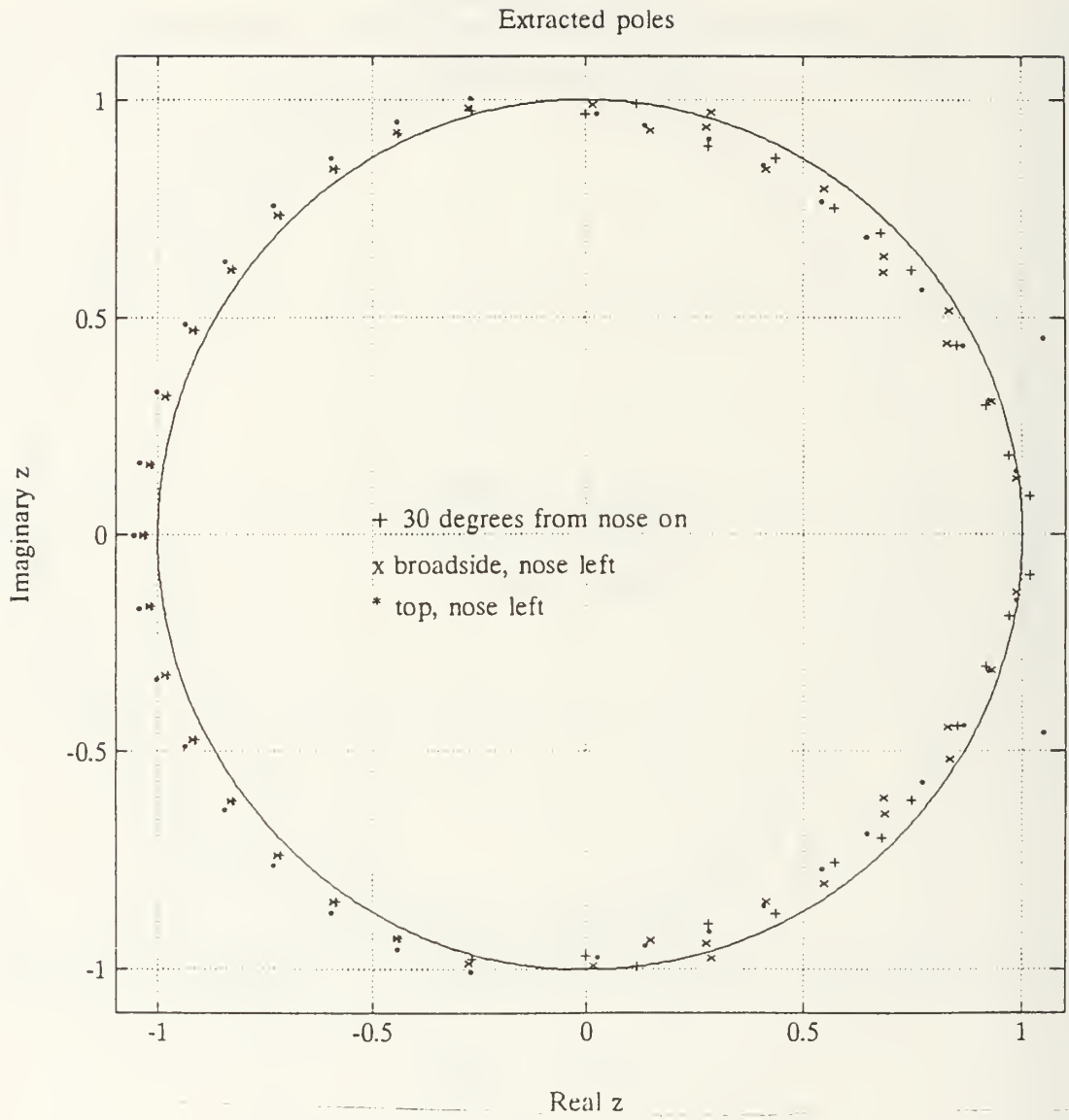


Figure 63. Cadzow-Solomon Poles Target 1, Three Aspects

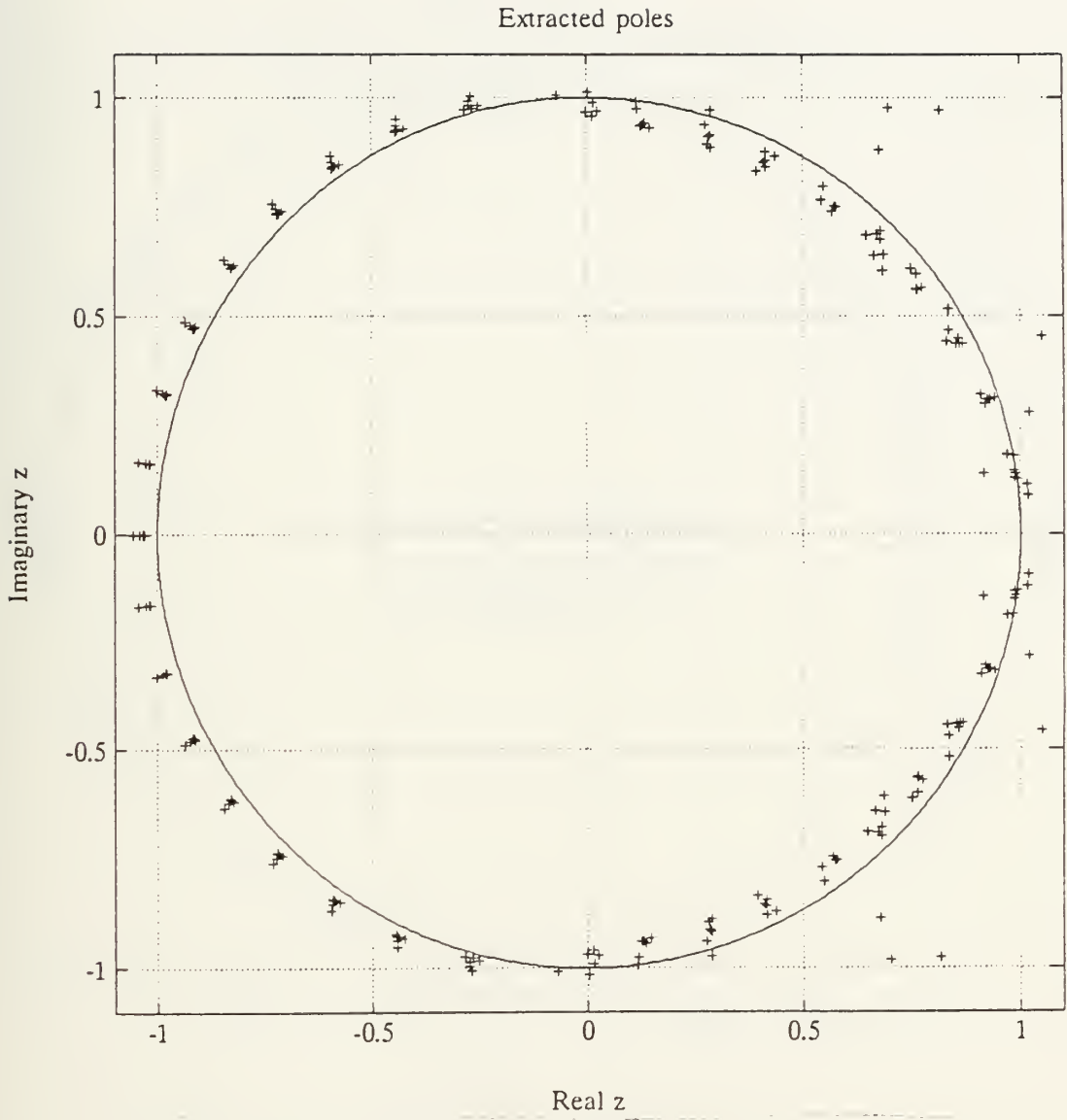


Figure 64. Cadzow-Solomon Poles Target 1, All Six Aspects

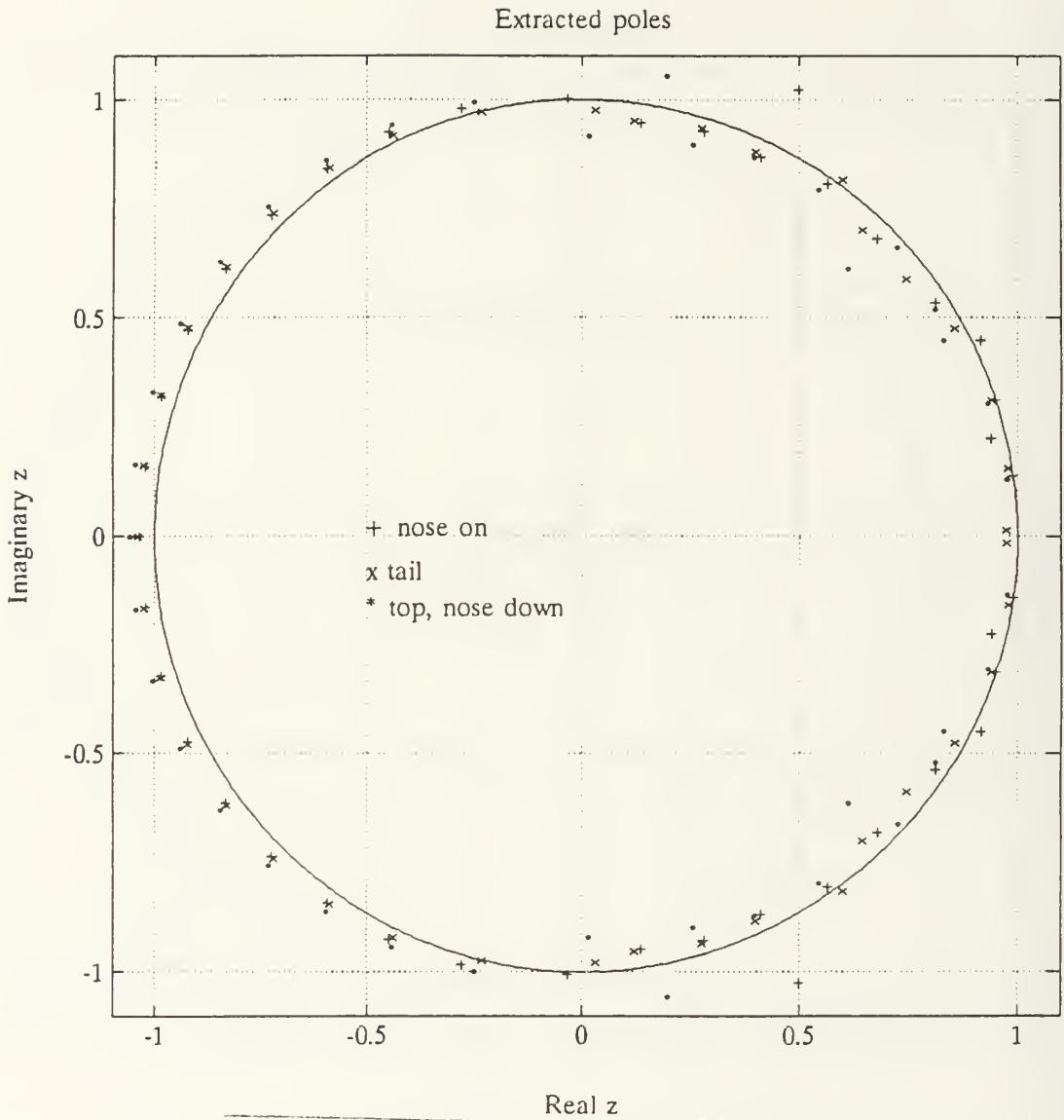


Figure 65. Cadzow-Solomon Poles Target 2, Three Aspects

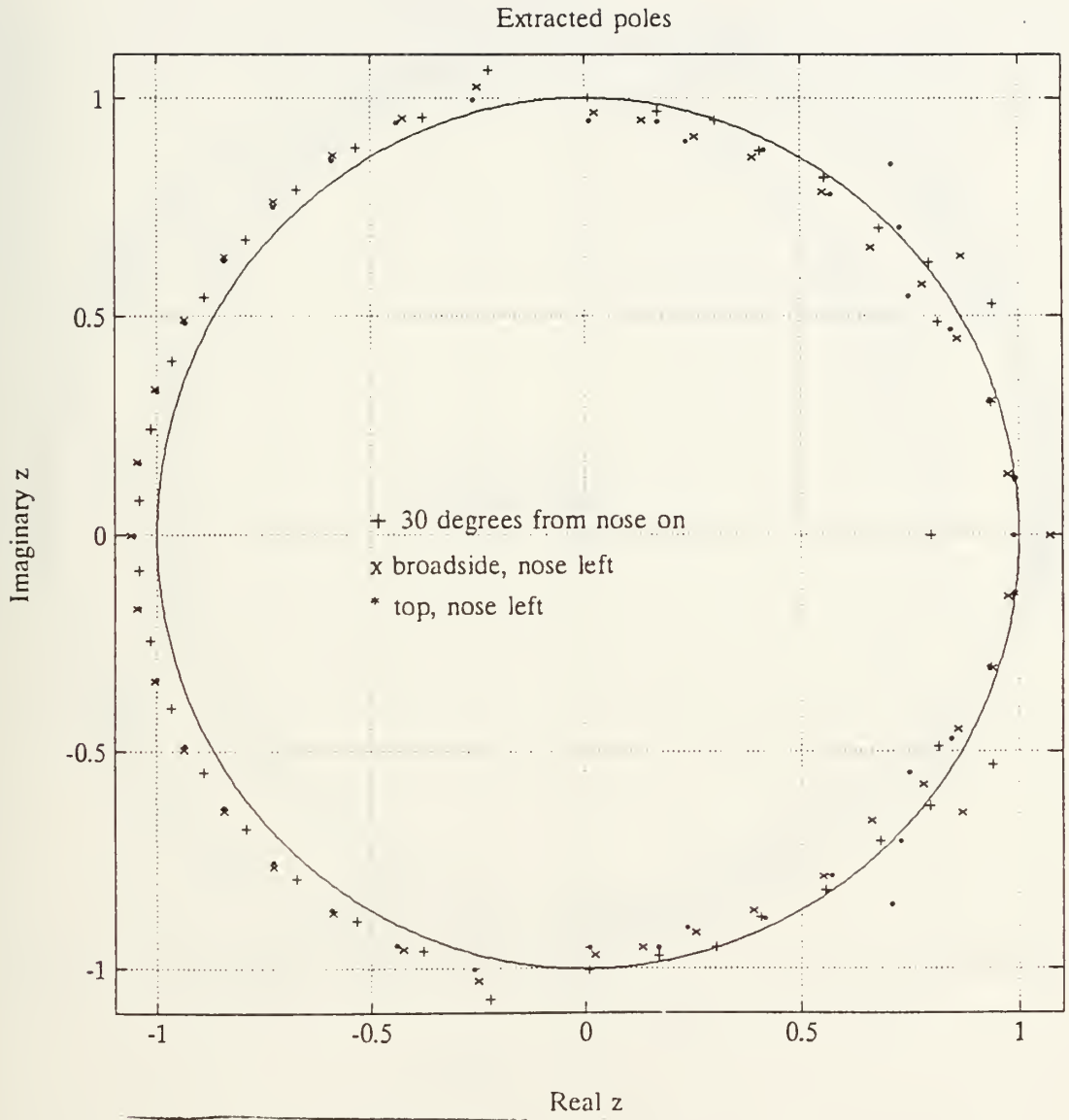


Figure 66. Cadzow-Solomon Poles Target 2, Three Aspects

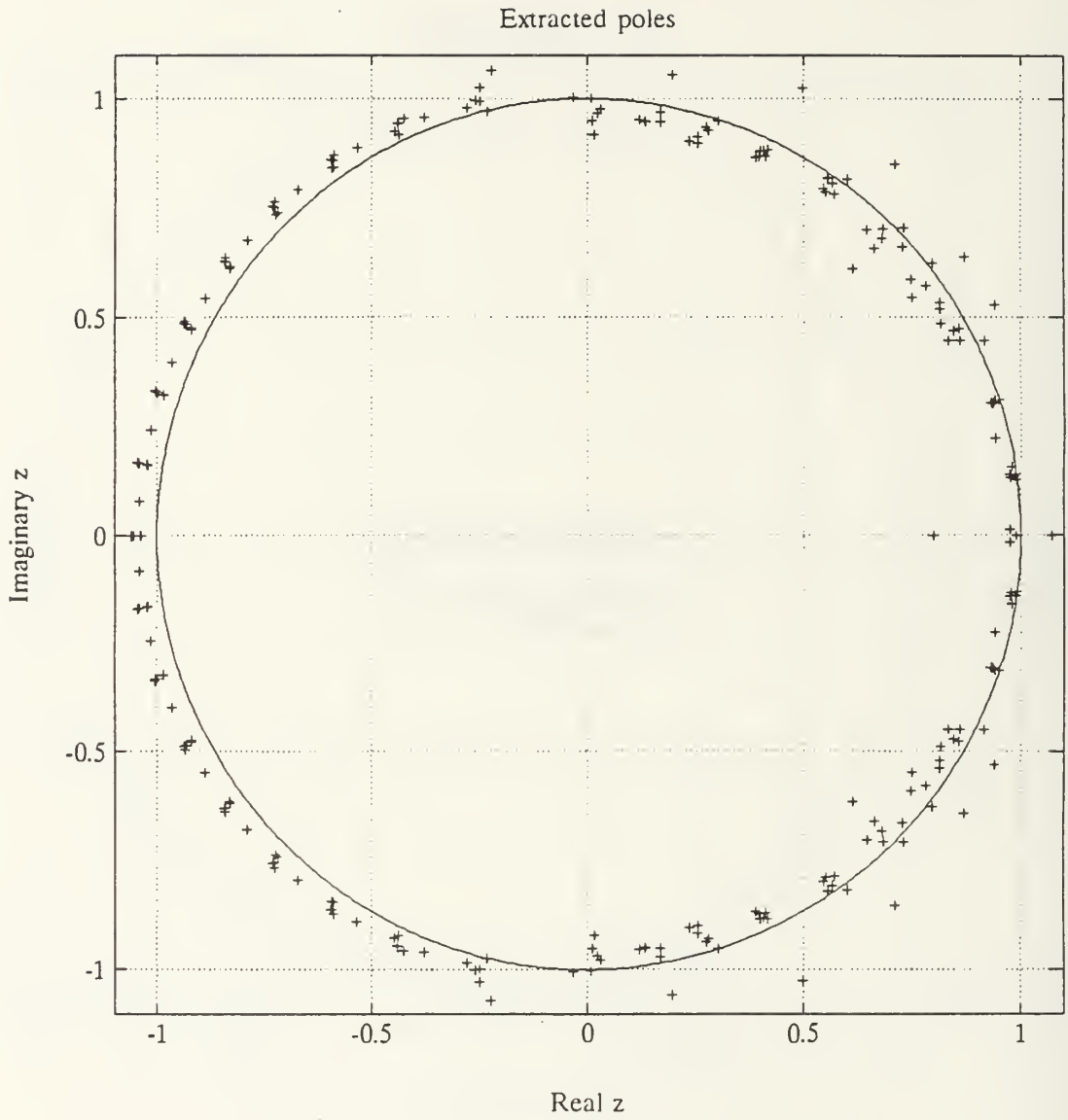


Figure 67. Cadzow-Solomon Poles Target 2, All Six Targets

Extracted poles

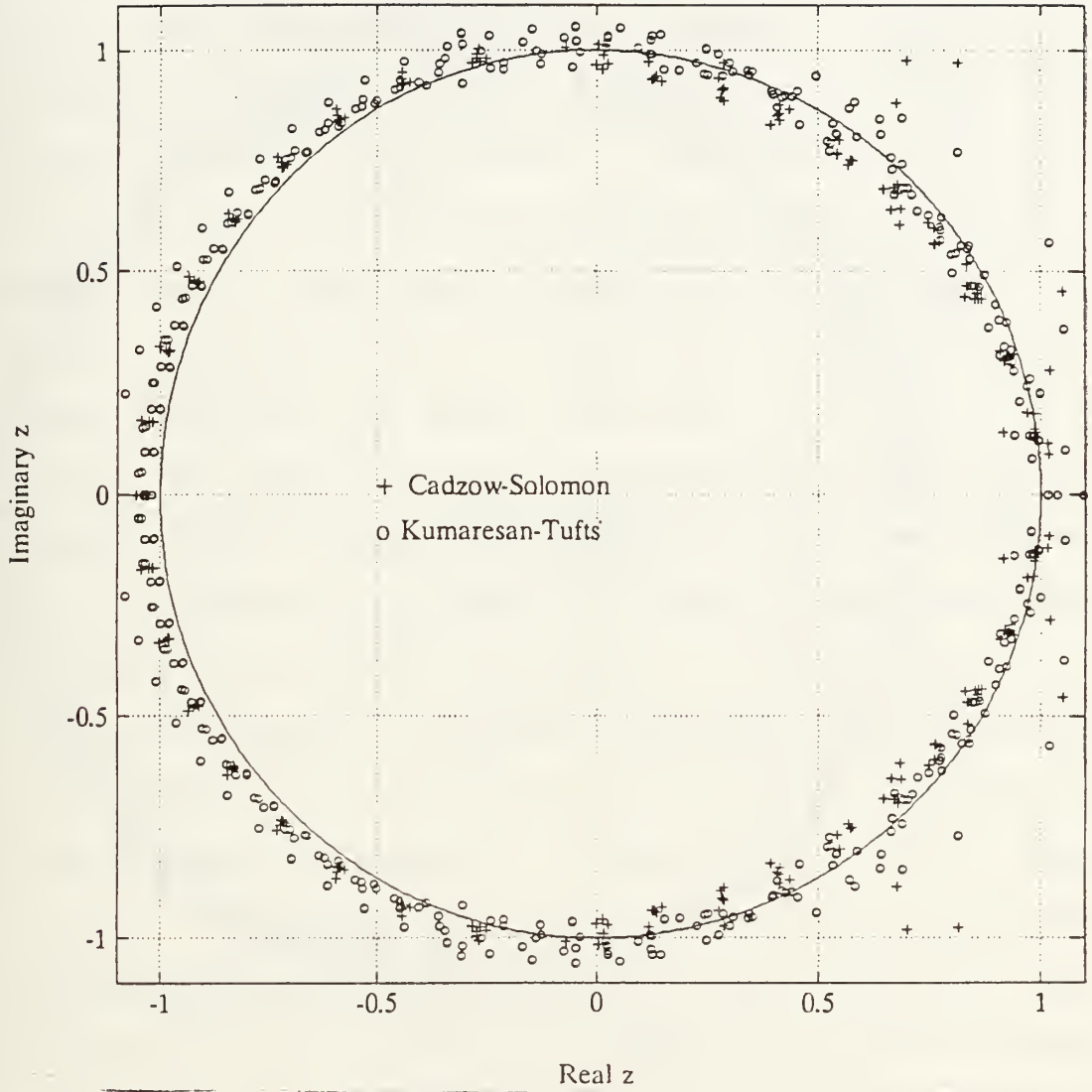


Figure 68. Pole Comparisons, Target 1, All Six Targets

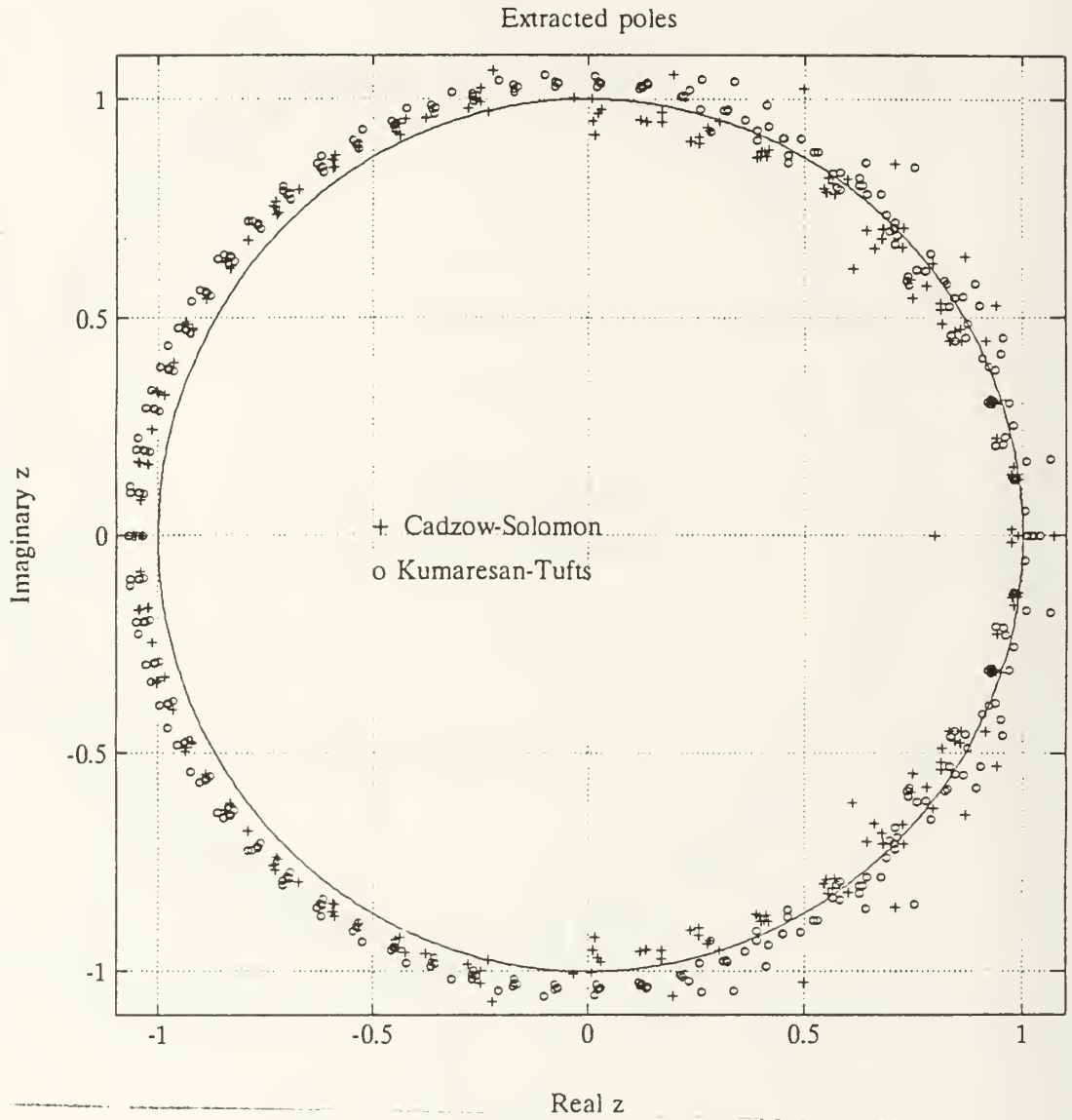


Figure 69. Pole Comparisons, Target 2, All Six Aspects

superiority of the Cadzow-Solomon algorithm over the Kumaresan-Tufts algorithm.

In order to obtain an initial indication of the possibility for target classification through pole extraction, nose-on measurements of two additional aircraft models were made, processed and compared with the results of targets 1 and 2. The nose-on measurements of targets 3 and 4 appear in Figures 70 and 71 respectively. A comparison plot of poles extracted from each of the four targets is depicted in Figure 72. Each of the four aircraft measured are fighters of similar size and shape (see Table 1). The poles for each target are sufficiently different in this single measurement to identify each aircraft individually. However, some of the poles are arranged in clusters which appear with a harmonic pattern similar to that obtained for either of the first two aircraft at various aspects. In order to more fully assess the target classification capability of pole extraction, several measurements should be made of a given aircraft model. A plot of the poles extracted from each of these measurements would form clusters at the locations of the true poles. The centroid of each of these clusters would then be compared against the centroid poles similarly obtained from other aircraft. Although several poles of different aircraft might be similar, the set of poles belonging to an aircraft could form the basis for classification if that set was unique among

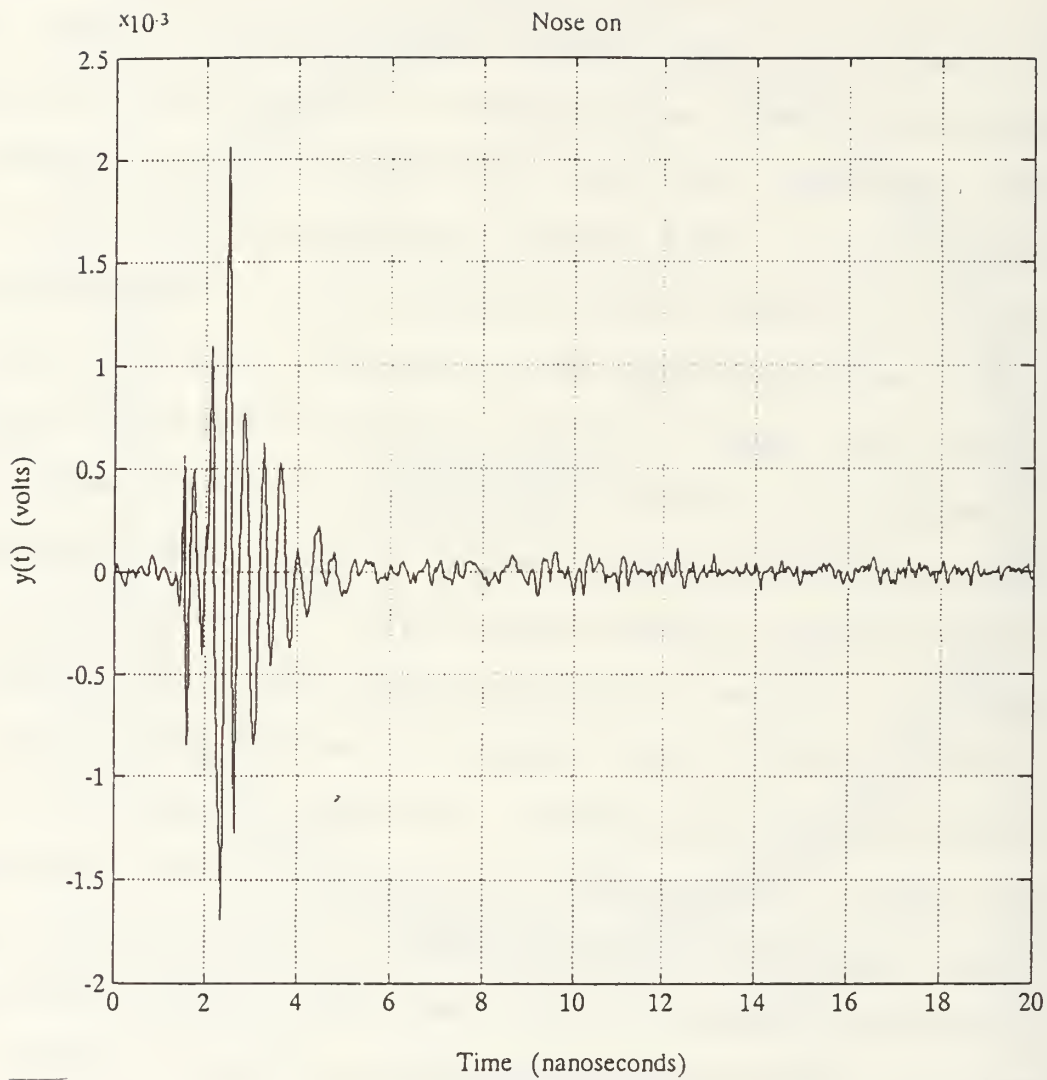


Figure 70. Target 3 Scattering, Nose-on

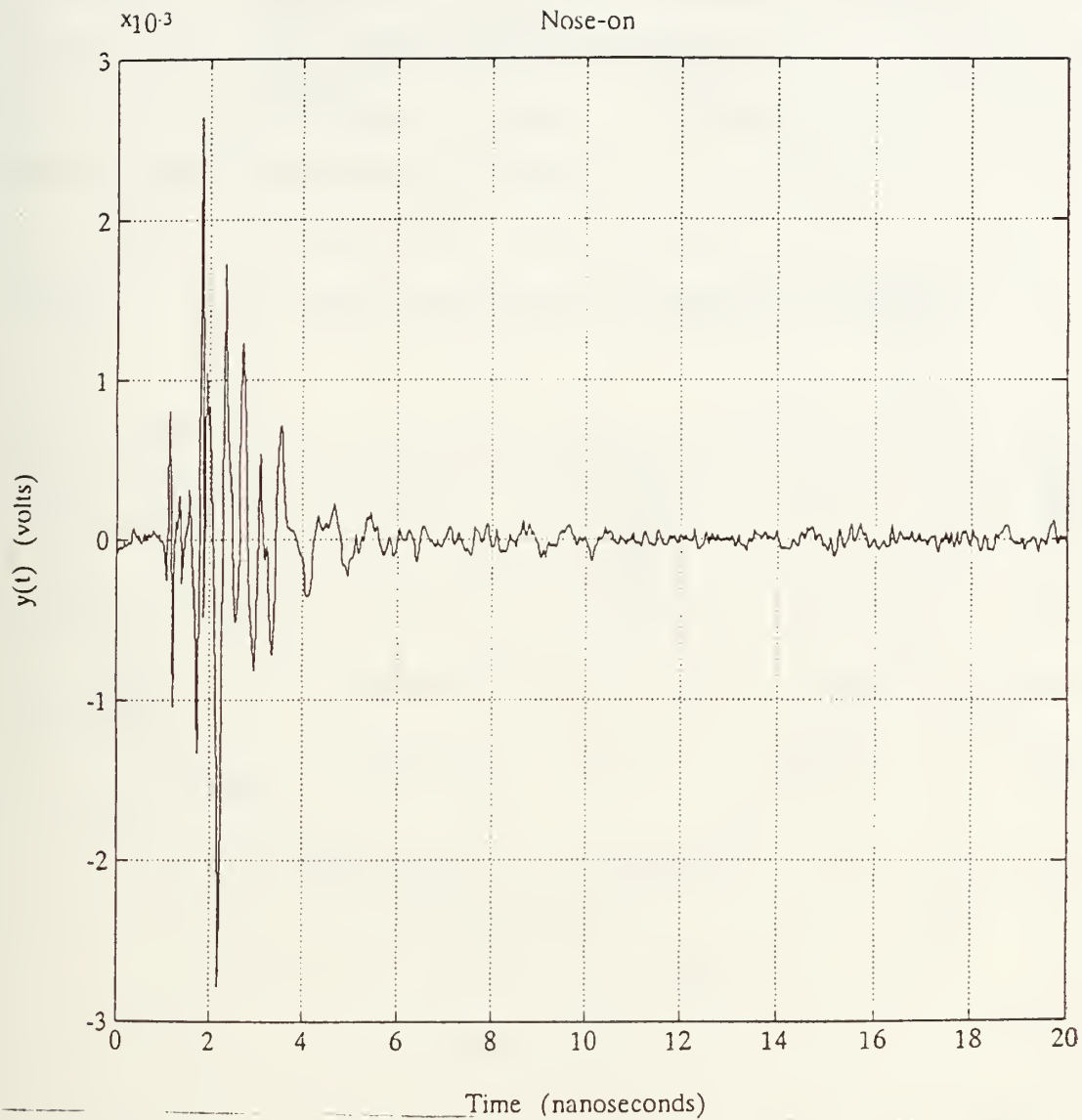


Figure 71. Target 4 Scattering, Nose-on

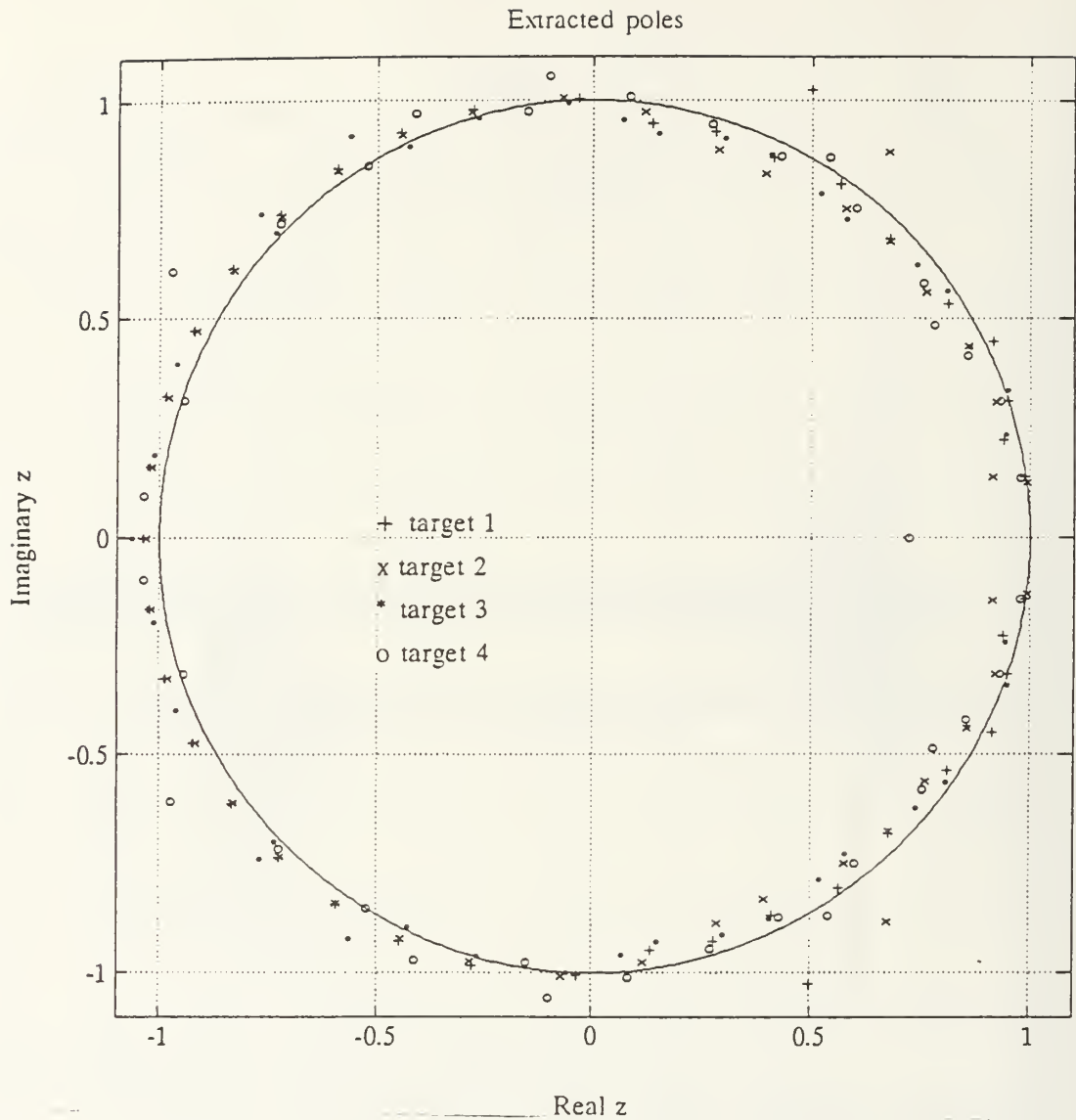


Figure 72. Cadzow- Solomon Pole Comparisons, 4 Targets, Nose-on

the sets belonging to all other measured aircraft. The results in Figure 72 demonstrate the possibility of using the Cadzow-Solomon pole extraction algorithm to aid in the classification of aircraft, perhaps by use of the extracted poles in constructing annihilation filters.

TABLE 1. FULL SIZE DIMENSIONS OF TARGETS RECORDED

Target number	1	2	3	4
Overall length (meters)	12.20	15.03	16.94	16.00
Overall height (meters)	3.35	5.09	4.51	4.80
Wingspan (meters)	10.96	10.00	11.43	13.95
Tailplane span (meters)	Unknown	5.58	6.92	5.75

III. SUMMARIES AND CONCLUSIONS

In this chapter, a step-by-step guide through each algorithm is presented. At each step, techniques and lessons learned are discussed together with general observations. Conclusions are presented at the end of the chapter.

A. KUMARESAN-TUFTS

The first step in processing a signal with the Kumaresan-Tufts algorithm is to determine the beginning of early-time. The objective is to pick the earliest possible starting point without entering into the latter part of early-time. If the starting point for processing is improperly chosen to include the early-time, the results will be completely unreliable since the signal no longer satisfies the late time model. If the starting point is chosen too late, the signal may not be sufficiently strong in the presence of measurement noise. Since the signal is the sum of exponentially damped sinusoids, the optimum starting point is at the precise instant of transition into late-time. The key to determining the beginning of late-time is in determining the beginning of early time. Determining the first response of the target to excitation cannot usually be done by a simple visual inspection of measurement data. Unless the exact distance to

the target is known, the most accurate method attempted by the author for determining the beginning of early-time is to process the signal using the Cadzow-Solomon algorithm. This is discussed in the next section. However, the reliance of the Kumaresan-Tufts algorithm on information provided by the Cadzow-Solomon algorithm is an obvious disadvantage of the former method.

Once the starting point for processing has been selected, the next step is to determine the dimensions of the data matrix and, consequently, the number of points in the signal to be processed. In trials conducted on noiseless synthetic data, the accuracy of pole extraction increased steadily with the increase in the data matrix dimensions. These trials were conducted up to the limit of the array dimensions defined in the computer program of Appendix A. The number of points processed in measurement data should be as large as possible, while still meeting the following two constraints. First, incorporate as many cycles of the data as possible. Usually, visual inspection of the data reveals a repeating pattern which should be entirely incorporated into the window of points to be processed. When only portions of these patterns are selected, a disproportionate weighting tends to be placed on certain poles. Second, signal portions late in the response which are no longer distinguishable in the presence of measurement noise should not be selected.

The final step involves determining the number of true poles in the system. The following approach has proven to be the most successful. First, process the signal without any eigenvalue compensation to establish an upper bound on the order of the system. In most cases, the number of poles outside the unit circle will be less than the overestimated order of the system. If not, increase the row dimension of the data matrix in order to increase the estimated order of the system, and repeat. When the number of poles is less than the estimated order of the system, then one should gradually increase the number of eigenvalues compensated in successive trials, while closely observing the effects induced on the poles outside the unit circle. As the number of eigenvalues compensated is steadily increased, noise poles and weak signal poles will move inside the unit circle. The programs in Appendix A and B allow the user to compare the results of successive trials, by generating overlays for each plot. If N poles are in the signal space, at least the first N eigenvalues must not be compensated, or true poles may be lost. As the actual order of the system is approached by compensation, the user will notice an orderly, even arrangement assumed by the noise poles. If certain poles still remain suspect after compensation, vary slightly the other parameters, such as the starting point and the

dimensions of the data matrix. Generally, only true signal poles will repeatedly assert themselves under varying parameters.

B. CADZOW-SOLOMON

The techniques and general observations offered in the preceding section apply equally to the Cadzow-Solomon algorithm. An important consideration in this method, not discussed above, is the selection of the beginning of early-time. Candidates for a starting point are usually at or near zero crossings within approximately thirty points of the object's first definite response to electromagnetic excitation. Begin processing at the chosen point while varying parameters in successive trials. Select the point whose successive results are the most consistent under varying parameters.

The selection of the starting point for beginning of early-time can be very critical. For example, not a single pole could be extracted in one trial wherein the starting point occurred only ten points after the actual starting point. Additionally, in most cases observed, the late-time start given by the selected early-time occurred within less than two points from a zero crossing. If this observation proves to be generally true in later research, it may serve

as a way to check the starting point selected for one algorithm in terms of the other.

C. CONCLUSIONS

Both the Kumaresan-Tufts and the Cadzow-Solomon algorithms can effectively extract poles from the scattering response of a radar target. Because both algorithms obtain a least-squares solution to the system model, both perform acceptably in the presence of noise. Although eigenvalue compensation is not analytically justified in the Cadzow-Solomon algorithm, the results obtained through eigenvalue compensation in this method were generally superior to those similarly obtained in the Kumaresan-Tufts method. The results demonstrated the inherent advantages of an algorithm capable of processing a target's strongest response in the early time. The Kumaresan-Tufts method compared favorably with the Cadzow-Solomon only in responses with a long late-time.

APPENDIX A. THE KUMARESAN-TUFTS POLE EXTRACTION ALGORITHM

The following program implements the Kumaresan-Tufts algorithm as described in Chapter 2 of this thesis. The program is written in Fortran 77. The SVD and root-finding subroutines called by this program are found in the EISPACK library [18]. The SVD subroutine is a translation from ALGOL as given in [19]. The matrix multiplication and graphics subroutines, also called by this program, are found in Appendix C and D respectively.

```

INTEGER IERR,Kd,M,MN,MAGPOL,NSTRPT,DELTA
INTEGER IER,NCAUS,NMENU,L/1/
INTEGER*2 KdPLT
REAL*8 A(70,70),W(70),U(70,70),V(70,70),RV1(70)
REAL*8 VS(70,70),UT(70,70),AINV(70,70),X(70)
REAL*8 XP(70),B(70),SIGMA(70,70),SIG(70,70)
REAL*8 COF(70),ROOTR(70),ROOTI(70)
REAL*8 D(1024),AVG,MACHEP/1.0E-16/,Dy(140)
COMPLEX*16 S(70)
LOGICAL MATU/.TRUE./,MATV/.TRUE./,CAUSAL/.TRUE./,LONG/.TRUE./
LOGICAL DSET/.FALSE./,NUFILE/.TRUE./
CHARACTER TITL*16,HEADER*64,YN*1,DC*1,TITLER*16,TITL*16
CHARACTER TITL*16

```

C Enter parameters for processing

```

11 IF (DSET) CLOSE(10)
NOVERLAY=0
OPEN(10,FILE='PLOT')
IF (DSET) GO TO 85
WRITE (*,*) 'Welcome to signal processing using the'
WRITE (*,*) 'Kumaresan-Tufts method'
WRITE (*,*) ' '
WRITE (*,*) 'Do you want '
WRITE (*,*) ' '
WRITE (*,*) '1. The long version for beginners'
WRITE (*,*) '2. The short version for pros'
WRITE (*,*) ' '

```

```

15  WRITE (*,*) 'Please enter 1 or 2 '
    READ (*,*) N
    IF (N .EQ. 1) THEN
    LONG=.TRUE.
    ELSEIF (N .EQ. 2) THEN
    LONG=.FALSE.
    ELSE
    GO TO 15
    ENDIF

    WRITE (*,*) 'Session will begin with entry of parameters needed for processing'
    WRITE (*,*)
    WRITE (*,*) 'Do you want to enter parameters from'
    WRITE (*,*) ' '
    WRITE (*,*) '1. The keyboard'
    WRITE (*,*) '2. A previously created file of parameters'
    WRITE (*,*) ' '
16  WRITE (*,*) 'Please enter 1 or 2 '
    READ (*,*) N
    IF (N .EQ. 1) THEN
    GO TO 1
    ELSEIF (N .EQ. 2) THEN
10  WRITE (*,*) 'Enter title of file containing parameters'
    READ (*,105) TTTL
    OPEN(1,FILE=TTTL)
    READ(1,105) TITLE
    READ(1,110) NPTS
    READ(1,110) NRT
    READ(1,110) Kd
    READ(1,110) M
    READ(1,110) DELTAY
    READ(1,110) NSTRTPT
    READ(1,110) NCAUS
    CLOSE(1)
    GO TO 85
    ELSE
    GO TO 16
    ENDIF
    WRITE (*,*) ' '

1  NUFIL=.TRUE.
    IF (.NOT. DSET) NSTRTPT=1
    WRITE (*,*) 'Enter title of data file to be read'
    READ (*,105) TITLE
    OPEN(1,FILE=TITLE)
    READ(1,105) HEADER
    READ(1,110) NPTS
    IF (NPTS .GT. 1024) THEN
    WRITE (*,*) 'Number of points in data file exceeds the dimension'
    WRITE (*,*) 'of the array used in the program to store the file'

```

```

STOP
ENDIF
CLOSE(1)

IF (DSET) THEN
IF (NSTRTPT+(Kd+M-1)*DELTAY .LE. NPTS) GO TO 85
ENDIF

3 IF (NUFILE) THEN
WRITE (*,*) 'Enter Kd, >= the estimated order of the system '
READ (*,*) Kd
IF (Kd .GT. 69) THEN
WRITE (*,*) 'Kd must be less than 70, or dimension statements'
WRITE (*,*) 'in this program must changed by the user'
GO TO 3
ELSEIF (Kd .LT. 2) THEN
WRITE (*,*) 'Kd must be at least 2'
GO TO 3
ENDIF
IF (2*Kd .GT. NPTS) THEN
WRITE (*,*) 'Kd must be less than or equal to ',NPTS/2
GO TO 3
ELSEIF (2*Kd .EQ. NPTS) THEN
WRITE (*,*) 'Kd equals',Kd
WRITE (*,*) 'M must be',Kd
M=Kd
WRITE (*,*) 'since there are a total of',NPTS
WRITE (*,*) 'points in ',TITLE
GO TO 45
ENDIF
GO TO 4
ELSEIF (DSET) THEN
N=M
20 IF (NSTRTPT+(N+M-1)*DELTAY .LE. NPTS) THEN
WRITE (*,*) 'Given the other parameters chosen thus far,'
25 WRITE (*,*) 'Kd may range from ',NRT
WRITE (*,*) ' to',N
WRITE (*,*) 'Enter Kd'
READ (*,*) Kd
IF (Kd .GE. NRT .AND. Kd .LE. N) GO TO 85
GO TO 25
ELSE
N=N-1
GO TO 20
ENDIF
ENDIF

4 IF (NUFILE) THEN
WRITE (*,*) 'Enter M, the row dimension of the data matrix'
IF (.NOT. DSET .AND. LONG) THEN

```

```

WRITE (*,*) ' '
WRITE (*,*) 'Note: Kd+M points in ',title
WRITE (*,*) '      will be processed '
WRITE (*,*) ' '
ENDIF
30  WRITE (*,*) 'M may range from',Kd
    IF (NPTS-Kd .GT. 69) THEN
WRITE (*,*) '      to      69'
    ELSE
WRITE (*,*) '      to',NPTS-Kd
    ENDIF
    READ (*,*) M
    IF (M .GT. 69) THEN
WRITE (*,*) 'M must also be less than 70'
GO TO 30
    ELSEIF (M .LT. Kd) THEN
WRITE (*,*) 'M must be greater than or equal to Kd, Kd= ',Kd
GO TO 30
    ELSEIF (Kd+M .GT. NPTS) THEN
WRITE (*,*) 'Kd+M must be less than or equal to',NPTS,' '
WRITE (*,*) 'the number of data points in',TITLE
WRITE (*,*) ' '
GO TO 30
    ENDIF
    ELSE
    N=Kd
35  IF (NSTRTPT+(Kd+N-1)*DELTAY .LE. NPTS) THEN
        N=N+1
        GO TO 35
        ELSE
        N=N-1
        ENDIF
        IF (N .EQ. Kd) THEN
WRITE (*,*) 'M must equal',Kd
        M=Kd
        GO TO 85
        ENDIF
        IF (N .GT. 69) N=69
40  WRITE (*,*) 'M may range from',Kd
    WRITE (*,*) '      to',N
    WRITE (*,*) 'Enter M'
    READ (*,*) M
    IF (M .GE. Kd .AND. M .LE. N) GO TO 85
    GO TO 40
    ENDIF

45  IF (.NOT. NUFIL) GO TO 85

5   N=1
50  IF (NSTRTPT+N*(Kd+M-1) .LE. NPTS) THEN

```

```

N=N+1
GO TO 50
ELSE
N=N-1
ENDIF
IF (N .EQ. 1) THEN
WRITE (*,*) 'Given the other parameters chosen thus far,'
WRITE (*,*) 'Spacing can only be 1'
DELTAY=1
  IF (NUFILE) THEN
    GO TO 60
  ELSE
    GO TO 85
  ENDIF
ENDIF
IF (.NOT. DSET .AND. LONG) THEN
WRITE (*,*) 'Enter spacing between the ',Kd+M
WRITE (*,*) 'data points of ',TITLE
WRITE (*,*) 'to be processed '
WRITE (*,*) ' '
WRITE (*,*) 'If, for example, one is chosen, then ',Kd+M
WRITE (*,*) 'consecutive points in ',TITLE
WRITE (*,*) 'will be processed '
WRITE (*,*) ' '
ENDIF
55 WRITE (*,*) 'Spacing may range from          1 '
   WRITE (*,*) '                to',N
   READ (*,*) DELTAY
   IF (DELTAY .GE. 1 .AND. DELTAY .LE. N) THEN
     IF (NUFILE) THEN
       GO TO 60
     ELSE
       GO TO 85
     ENDIF
   ELSE
     GO TO 55
   ENDIF

60 WRITE (*,*) 'Do you wish to adjust eigenvalues? (y/n)'
   READ (*,120) YN
   IF (YN .EQ. 'N' .OR. YN .EQ. 'n') THEN
     IF (NUFILE) GO TO 6
     GO TO 85
   ENDIF
   IF (YN .NE. 'Y' .AND. YN .NE. 'y') GO TO 60
2  WRITE (*,*) 'Discard or compensate eigenvalues? (d/c)'
   READ (*,120) DC
   IF (DC .EQ. 'D' .OR. DC .EQ. 'd') GO TO 65
   IF (DC .NE. 'C' .AND. DC .NE. 'c') GO TO 2
   WRITE (*,*) 'Enter estimate of the actual order of the system'

```



```

WRITE (*,*) ' '
IF (LONG) THEN
WRITE (*,*) 'This estimate will be used to determine the '
WRITE (*,*) 'number of eigenvalues compensated or discarded '
ENDIF
65 WRITE (*,*) 'the estimate may range from           2'
WRITE (*,*) '                                     to',Kd-1
READ (*,*) NRT
IF (NRT .GT. Kd .OR. NRT .LT. 2) THEN
GO TO 65
ELSEIF (.NOT. NUFILE) THEN
GO TO 85
ENDIF

6   NSTRIPT=1
70  IF (NSTRIPT+(Kd+M-1)*DELTAY .LE. NPTS) THEN
    NSTRIPT=NSTRIPT+1
    GO TO 70
  ELSE
    NSTRIPT=NSTRIPT-1
  ENDIF
  IF (NSTRIPT .EQ. 1) THEN
    WRITE (*,*) 'Given the other parameters chosen thus far,'
    WRITE (*,*) 'the starting point for processing the data'
    WRITE (*,*) 'must be the first point in the data file'
    GO TO 85
  ENDIF
  WRITE (*,*) 'Enter desired starting point in data file'
  IF (.NOT. DSET .AND. LONG) THEN
    WRITE (*,*) '1 indicates the first point in the data file '
  ENDIF
  WRITE (*,*) ' '
  WRITE (*,*) 'Given the other parameters chosen thus far,'
75  WRITE (*,*) 'the starting point may range from           1'
  WRITE (*,*) '                                     to',NSTRIPT
  READ (*,*) N
  IF (N .GE. 1 .AND. N .LE. NSTRIPT) THEN
    NSTRIPT=N
  ELSE
    WRITE (*,*) 'Enter starting point again'
    WRITE (*,*) ' '
    GO TO 75
  ENDIF
  IF (.NOT. NUFILE) GO TO 85

7   WRITE (*,*) 'Do you want the data matrix arrangement to be'
    WRITE (*,*) ' '
    WRITE (*,*) '1. Causal'
    WRITE (*,*) '2. Non-causal'
    WRITE (*,*) ' '

```

```

80  WRITE (*,*) 'Please enter 1 or 2 '
    READ (*,*) NCAUS
    IF (NCAUS .EQ. 1) THEN
    CAUSAL=.TRUE.
    ELSEIF (NCAUS .EQ. 2) THEN
    CAUSAL=.FALSE.
    ELSE
    GO TO 80
    ENDIF
    GO TO 85
9   WRITE (*,*) 'Enter title of file to contain parameters'
    READ (*,105) TTTL
    OPEN(1,FILE=TTTL)
    WRITE(1,105) TITLE
    WRITE(1,110) NPTS
    WRITE(1,110) NRT
    WRITE(1,110) Kd
    WRITE(1,110) M
    WRITE(1,110) DELTAY
    WRITE(1,110) NSTRTPT
    WRITE(1,110) NCAUS
    CLOSE(1)
    IF (DSET) GO TO 85

12  IF (DSET) THEN
    CLOSE(2)
    CLOSE(3)
    CALL SUBPLT(NOVERLAY)
    ENDIF

85  DSET=.TRUE.
    NUFILE=.FALSE.
    WRITE(*,*) ' '
    WRITE(*,*) '1. Data file to be processed          ',T
+TITLE
    WRITE(*,*) '   Number of data points in data file          ',NPTS
    WRITE(*,*) '2. Estimated order of the system          ',NRT
    WRITE(*,*) '3. Kd, the number of columns in the data matrix',Kd
    WRITE(*,*) '4. M, the number of rows in the data matrix',M
    WRITE(*,*) '5. Spacing between data points being processed ',DELTA
+Y
    WRITE(*,*) '6. First point in the data file to be processed',NSTRT
+PT
    WRITE(*,*) '   Last point in the data file to be processed',NSTRT      IF

+PT+Kd+M-1
    IF (NCAUS .EQ. 1) THEN
    WRITE(*,*) '7. Data matrix arrangement for processing      CA
+USAL '
    ELSE

```



```

WRITE(*,*) '7. Data matrix arrangement for processing      NON-CA
+USAL '
ENDIF
WRITE(*,*) ' '
WRITE(*,*) '8. Begin processing using above settings'
WRITE(*,*) '9. Store parameters 1-7 in a file'
WRITE(*,*) '10. Retrieve parameters 1-7 from a previously created
+file'
WRITE(*,*) '11. Reset overlays'
WRITE(*,*) '12. Re-plot overlays'
WRITE(*,*) '13. End this session of Kumaresan-Tufts signal process
+ing'
WRITE(*,*) ' '
WRITE(*,*) 'Enter an integer from 1 to 12 to make changes as often
+ as you desire'
90  READ (*,*) NMENU
    IF (NMENU .LT. 1 .OR. NMENU .GT. 13) THEN
        WRITE(*,*) 'Enter an integer from 1 to 13'
        GO TO 90
    ENDIF

    GO TO (1,2,3,4,5,6,7,8,9,10,11,12,13),NMENU

8   OPEN(1,FILE=TITLE)
    READ(1,105) HEADER
    READ(1,110) NPTS
    READ(1,115) XQ
    READ(1,115) XQ
    DO 95 I=1,NPTS
    READ(1,115) D(I)
95  CONTINUE
    CLOSE(1)
    KdPLT=Kd
    WRITE(*,*) 'Enter title of file to contain real part of poles'
    READ(*,105) TITLER
    OPEN(2,file=TITLER)

    WRITE(*,*) 'Enter title of file to contain imaginary part of poles'
    READ(*,105) TITLEI
    OPEN(3,file=TITLEI)
    WRITE(10,100) (KdPLT)
    WRITE(10,105) TITLER
    WRITE(10,105) TITLEI
100 FORMAT(I2)

    MN=MAX(M,Kd)

105 FORMAT(A)
110 FORMAT(I5)
115 FORMAT(E12.6)

```

```

120  FORMAT(A1)

C    Form data matrix

      DO 125 I=1,Kd+M
      Dy(I)=D((I-1)*DELTA+NSTRTPT)
125  CONTINUE

130  DO 140 I=1,M
      DO 135 J=1,Kd
      A(I,J)=Dy(I+J)
135  CONTINUE
140  CONTINUE

      B(1)=Dy(1)
      DO 145 I=2,M
      B(I)=A(I-1,1)
145  CONTINUE

C    Begin singular value decomposition

      CALL SVD(MACHEP,M,Kd,MN,A,W,MATU,U,MATV,V,IERR,RV1)

C    Errors in SVD?
      IF (IERR .GT. 0.0) THEN
      WRITE (*,*) 'Error in singular value number ',IERR,STOP
      ENDIF
      IF (YN .EQ. 'N') GO TO 190

      DO 150 I=1,Kd
      XP(I)=0.0
150  CONTINUE

C    Discard or compensate eigenvalues
C    Order singular values

      XP(1)=W(1)
      DO 165 I=2,Kd
      DO 160 J=1,I
      IF (W(I) .GT. XP(J)) THEN
      DO 155 K=I+1,J,-1
155  XP(K)=XP(K-1)
      XP(J)=W(I)
      GO TO 165
      ENDIF
160  CONTINUE
      XP(I+1)=W(I)
165  CONTINUE

C    XP( ) now contains ordered singular values-XP(1) is the largest

```

```

C   Discard eigenvalues
   IF (DC .EQ. 'D') THEN
170  DO 170 J=NRT+1,Kd
      W(J)=(0.0)
      ELSE
C   Compensate eigenvalues
      AVG=0.0
      DO 175 J=NRT+1,Kd
      AVG=AVG+XP(J)**2
175  CONTINUE
      IF (Kd .GT. NRT) AVG=AVG/DBLE(FLOAT(Kd-NRT))

      DO 185 J=1,Kd
      DO 180 K=1,Kd
      IF ( W(J) .EQ. XP(K) ) THEN
          IF ( K .GT. NRT ) THEN
              W(J)=0.0
          ELSE
              W(J)=DSQRT(DABS( W(J)*W(J)-AVG))
          ENDIF
          GO TO 185
      ENDIF
180  CONTINUE
185  CONTINUE
      ENDIF

190  DO 200 I=1,M
      DO 195 J=1,M
      UT(I,J)=(U(J,I))
195  CONTINUE
200  CONTINUE

c   Form SIGMA+ (Kd x M)
      DO 210 I=1,Kd
      DO 205 J=1,M
      SIGMA(I,J)=0.0
      IF (I .EQ. J .AND. W(J) .NE. 0.0) THEN
          SIGMA(I,J)=1.0D0/W(J)
      ELSE
          SIGMA(I,J)=0.0d0
      ENDIF
205  CONTINUE
210  CONTINUE

C   Form SIGMA (M x Kd)
      DO 220 I=1,M
      DO 215 J=1,Kd
      SIG(I,J)=0.0
      IF (I .EQ. J) SIG(I,J)=W(J)

```

```

215 CONTINUE
220 CONTINUE

C V=Kd×Kd, SIGMA+=Kd×M, VS=Kd×M
CALL MXMUL(V, SIGMA, Kd, Kd, M, VS)

C VS=Kd×M, UT=M×M, AINV=Kd×M
CALL MXMUL(VS, UT, Kd, M, M, AINV)

C Calculate matrix multiplication of AINV x B, where
C AINV=Kd×M, B=M×1, XP=Kd×1
CALL MXMUL(AINV, B, Kd, M, L, XP)

C Calculate autoregressive coefficients from prediction coefficients
IF (XP(Kd) .EQ. 0.0) THEN
WRITE (*,*) 'ERROR, avoiding division by zero'
STOP
ELSE
B(Kd)=1.0d0/XP(Kd)
ENDIF
DO 225 I=2, Kd
B(I-1)=-B(Kd)*XP(Kd-I+1)
225 CONTINUE

DO 230 I=1, Kd
X(I)=-B(Kd-I+1)
IF (NCAUS .EQ. 1) X(I)=-XP(Kd-I+1)
230 CONTINUE
X(Kd+1)=1.0

C Compute the roots of the polynomial in z
CALL POLRT(X, COF, KD, ROOTR, ROOTI, IER)

IF (IER .NE. 0) WRITE (*,*) 'ERROR with POLRT, IER=', IER, STOP

DO 235 I=1, Kd
WRITE(2,115) ROOTR(I)
WRITE(3,115) ROOTI(I)
S(I)=DCMPLX(ROOTR(I), ROOTI(I))
235 CONTINUE

MAGPOL=0
DO 240 I=1, Kd
IF (CDABS(S(I)) .GE. 1.0d0) MAGPOL=MAGPOL+1
240 CONTINUE

WRITE(*,*) '# of poles with magnitude <= 1', Kd-MAGPOL
WRITE (*,*) 'HIT ANY KEY TO CONTINUE'
READ (*,105) HEADER

```

C Plot poles

```
NOVERLAY=NOVERLAY+1  
CLOSE(2)  
CLOSE(3)  
CALL SUBPLT(NOVERLAY)
```

```
J=0  
K=0
```

```
DO 245 I=1,Kd  
IF (CDABS(S(I)) .LT. 1.0) THEN  
J=J+1  
K=K+1  
WRITE (*,*) S(I),CDABS(S(I))  
ENDIF  
IF (J .EQ. 20) THEN  
WRITE (*,*) 'Enter any key to continue'  
READ (*,105) HEADER  
J=0  
ENDIF
```

```
245 CONTINUE
```

```
WRITE(*,*) 'Poles with magnitude less than one: ',K
```

```
GO TO 85  
13 STOP  
END
```

APPENDIX B: THE CADZOW-SOLOMON POLE EXTRACTION ALGORITHM

The following program implements the Cadzow-Solomon algorithm as described in Chapter 2 of this thesis. The program is written in Fortran 77. The SVD and root-finding subroutines called by this program are found in the EISPACK library [18]. The SVD subroutine is a translation from ALGOL as given in [19]. The matrix multiplication and graphics subroutines, also called by this program, are found in Appendix C and D respectively.

\$LARGE

```

INTEGER IERR,Kd,Kn,M,MN,MAGPOL,NSTRTPT,DELTAY
INTEGER IER,NCAUS,NMENU,INSTRTPT
INTEGER*2 KdPLT
REAL*8 A(70,70),W(70),U(70,70),V(70,70),RV1(70)
REAL*8 VS(70,70),UT(70,70),AINV(70,70),X(70)
REAL*8 XP(70),B(70),SIGMA(70,70),SIG(70,70)
REAL*8 COF(70),ROOTR(70),ROOTI(70)
REAL MAG
REAL*8 D(1024),AVG,MACHEP/1.0E-16/,Dy(140),Dx(1024)
COMPLEX*16 S(70)
LOGICAL MATU/.TRUE./,MATV/.TRUE./,CAUSAL/.TRUE./,LONG/.TRUE./
LOGICAL DSET/.FALSE./,NUFILE/.TRUE./
CHARACTER TTITLE*16,HEADER*64,YN*1,DC*1,TITLER*16,TITLEI*16
CHARACTER TTTL*16,TTITLD*16

```

C Enter parameters for processing

```

14 IF (DSET) CLOSE(10)
NOVERLAY=0
OPEN(10,FILE='PLOT')
IF (DSET) GO TO 215
WRITE (*,*) 'Welcome to signal processing using the'
WRITE (*,*) 'Cadzow-Solomon method'
WRITE (*,*) ' '
WRITE (*,*) 'Do you want '

```

```

WRITE (*,*) ' '
WRITE (*,*) '1. The long version for beginners'
WRITE (*,*) '2. The short version for pros'
WRITE (*,*) ' '
25 WRITE (*,*) 'Please enter 1 or 2 '
   READ (*,*) N
   IF (N .EQ. 1) THEN
   LONG=.TRUE.
   ELSEIF (N .EQ. 2) THEN
   LONG=.FALSE.
   ELSE
   GO TO 25
   ENDIF

   WRITE (*,*) 'Session will begin with entry of parameters needed fo
+r processing'
   WRITE (*,*)
   WRITE (*,*) 'Do you want to enter parameters from'
   WRITE (*,*) ' '
   WRITE (*,*) '1. The keyboard'
   WRITE (*,*) '2. A previously created file of parameters'
   WRITE (*,*) ' '
35 WRITE (*,*) 'Please enter 1 or 2 '
   READ (*,*) N
   IF (N .EQ. 1) THEN
   GO TO 8
   ELSEIF (N .EQ. 2) THEN
13 WRITE (*,*) 'Enter title of file containing parameters'
   READ (*,100) TITL
   OPEN(1,FILE=TITL)
   READ(1,100) TITL
   READ(1,110) NPTS
   READ(1,110) NRT
   READ(1,110) Kd
   READ(1,110) M
   READ(1,110) DELTAY
   READ(1,110) NSTRPT
   READ(1,110) NCAUS
   READ(1,100) TITLD
   READ(1,110) NDPTS
   READ(1,110) Kn
   READ(1,110) INSTRPT
   CLOSE(1)
   GO TO 215
   ELSE
   GO TO 35
   ENDIF
   WRITE (*,*) ' '

8   WRITE (*,*) 'Enter title of file containing excitation waveform'

```



```

READ (*,100) TITLD
OPEN(8,FILE=TITLD)
READ(8,100) HEADER
READ(8,110) N
IF (N .GT. 1024) THEN
WRITE (*,*) 'Number of points in data file exceeds the dimension'
WRITE (*,*) 'of the array used in the program to store the file'
STOP
ENDIF
CLOSE(8)
IF ((N .GE. NDPTS) .AND. DSET) THEN
NDPTS=N
GO TO 215
ENDIF
NDPTS=N

9  WRITE (*,*) 'Enter estimated order of waveform'
   IF (DSET) THEN
   MAXIMUM=NDPTS-M
   IF (MAXIMUM .GT. M-Kd-1) MAXIMUM=M-Kd-1
   IF (MAXIMUM .GT. NDPTS-INSTRPT-Kn-M+1) THEN
   MAXIMUM=NDPTS-INSTRPT-Kn-M+1
   ENDIF
   ELSE
   MAXIMUM=66
   ENDIF
   IF (MAXIMUM .EQ. 1) THEN
   WRITE (*,*) 'The estimated order of the waveform can only be 1'
   IF (DSET) GO TO 215
   GO TO 10
   ELSE
   IF (DSET) THEN
   WRITE (*,*) 'Given the other parameters chosen thus far,'
   ENDIF
45  WRITE (*,*) 'the order may range from           1'
   WRITE (*,*) '                               to',MAXIMUM
   READ (*,*) Kn
   IF (Kn .GE. 1 .AND. Kn .LE. MAXIMUM) THEN
   IF (DSET) GO TO 215
   GO TO 10
   ENDIF
   WRITE (*,*) 'Enter estimated order again'
   WRITE (*,*) ' '
   GO TO 45
   ENDIF
   IF (DSET) GO TO 215

10  INSTRPT=1
55  IF (INSTRPT+Kn+M-1 .GT. NDPTS) THEN
   INSTRPT=INSTRPT-1

```

```

ELSE
INSTRTPT=INSTRTPT+1
GO TO 55
ENDIF
MSTRT=INSTRTPT

IF (INSTRTPT .EQ. 1) THEN
WRITE (*,*) 'The first point can only be 1'
GO TO 215
ELSE
65 WRITE (*,*) 'Enter first point in waveform file to be processed'
WRITE (*,*) 'Given the other parameters chosen thus far,'
WRITE (*,*) 'the starting point may range from          1'
WRITE (*,*) '          to',MSTRT
READ (*,*) INSTRTPT
IF (INSTRTPT .GE. 1 .AND. INSTRTPT .LE. MSTRT) THEN
IF (DSET) GO TO 215
GO TO 1
ENDIF
WRITE (*,*) 'Enter starting point again'
WRITE (*,*) ' '
GO TO 65
ENDIF
IF (DSET) GO TO 215

1 IF (.NOT. DSET) NUFILE=.TRUE.
IF (.NOT. DSET) NSTRTPT=1
WRITE (*,*) 'Enter title of data file to be read'
READ (*,100) TITLE
OPEN(12,FILE=TITLE)
READ(12,100) HEADER
READ(12,110) NPTS
IF (NPTS .GT. 1024) THEN
WRITE (*,*) 'Number of points in data file exceeds the dimension'
WRITE (*,*) 'of the array used in the program to store the file'
STOP
ENDIF
CLOSE(12)

IF (NUFILE) THEN
GO TO 3
ELSEIF (NSTRTPT+(Kd+M-1)*DELTAY .LE. NPTS) THEN
GO TO 215
ELSE
GO TO 6
ENDIF

3 IF (NUFILE) THEN
MAXIMUM=69-Kn-1

```

```

IF (MAXIMUM .GT. NPTS-69) MAXIMUM=NPTS-69
MIN=2
IF (MIN .EQ. MAXIMUM) THEN
Kd=MIN
WRITE (*,*) 'Given the other parameters chosen thus far,'
WRITE (*,*) 'Kd must be ',MIN
GO TO 4
ENDIF

WRITE (*,*) 'Enter Kd, >= the estimated order of the system '

WRITE (*,*) 'Given the other parameters chosen thus far,'
75 WRITE (*,*) 'Kd may range from',MIN
WRITE (*,*) '          to',MAXIMUM
READ (*,*) Kd
IF (Kd .GE. MIN .AND. Kd .LE. MAXIMUM) GO TO 4
GO TO 75

ELSEIF (DSET) THEN
MAXIMUM=M-Kn-1
IF (MAXIMUM .GT. NPTS-M) MAXIMUM=NPTS-M
MIN=2
N=MAXIMUM
85 IF (NSTRTPT+(N+M-1)*DELTAY .LE. NPTS) THEN
MAXIMUM=N
IF (MIN .EQ. MAXIMUM) THEN
Kd=MIN
GO TO 215
ELSEIF (MAXIMUM .LT. MIN) THEN
DELTAY=1
IF (1+(2+M-1)*DELTAY .LE. NPTS) THEN
Kd=2
GO TO 135
ENDIF
WRITE (*,*) 'Error. Kd must be less than 2'
Kd=2
GO TO 215
ENDIF

WRITE (*,*) 'Given the other parameters chosen thus far,'
95 WRITE (*,*) 'Kd may range from          ',MIN
WRITE (*,*) '          to',MAXIMUM
WRITE (*,*) 'Enter Kd'
READ (*,*) Kd
IF (Kd .GE. MIN .AND. Kd .LE. MAXIMUM) GO TO 215
GO TO 95
ELSE
N=N-1
GO TO 85
ENDIF
ENDIF

```

```

C   Determine M
4   IF (NUFILE) THEN
    WRITE (*,*) 'Enter M, the row dimension of the data matrix'
    IF (.NOT. DSET .AND. LONG) THEN
    WRITE (*,*) ' '
    WRITE (*,*) 'Note: Kd+M points in ',title
    WRITE (*,*) '      will be processed '
    WRITE (*,*) ' '
    ENDIF
105  WRITE (*,*) 'M may range from',Kd
    IF (NPTS-Kd .GT. 69) THEN
    WRITE (*,*) '      to      69'
    ELSE
    WRITE (*,*) '      to',NPTS-Kd
    ENDIF
    READ (*,*) M
    IF (M .GT. 69) THEN
    WRITE (*,*) 'M must also be less than 70'
    GO TO 105
    ELSEIF (M .LT. Kd) THEN
    WRITE (*,*) 'M must be greater than or equal to Kd, Kd= ',Kd
    GO TO 105
    ELSEIF (Kd+M .GT. NPTS) THEN
    WRITE (*,*) 'Kd+M must be less than or equal to',NPTS,', '
    WRITE (*,*) 'the number of data points in',TITLE
    WRITE (*,*) ' '
    GO TO 105
    ENDIF
C   Begin part for data already set
    ELSE
    N=Kd
115  IF (NSTRTPT+(Kd+N-1)*DELTAY .LE. NPTS) THEN
    N=N+1
    GO TO 115
    ELSE
    N=N-1
    ENDIF
    IF (N .EQ. Kd) THEN
    WRITE (*,*) 'M must equal',Kd
    M=Kd
    GO TO 215
    ENDIF
    MAXIMUM=N
    IF (MAXIMUM .GT. 69) MAXIMUM=69
    IF (Kd+Kn+1 .EQ. MAXIMUM) THEN
    M=Kd+Kn+1
    GO TO 215
    ELSEIF (Kd+Kn+1 .GT. MAXIMUM) THEN
    WRITE (*,*) 'Kd must be reduced'

```

```

        GO TO 3
        ELSE
        MIN=Kd+Kn+1
        ENDIF
    IF (MIN .LT. Kn+Kd+1) MIN=Kn+Kd+1
125  WRITE (*,*) 'M may range from',MIN
    WRITE (*,*) '          to',MAXIMUM
    WRITE (*,*) 'Enter M'
    READ (*,*) M
    IF (M .GE. MIN .AND. M .LE. MAXIMUM) GO TO 215
    GO TO 125
    ENDIF

c    Determine DELTAY
135  IF (.NOT. NUFILE) GO TO 215
5    N=1
145  IF (NSTRIPT+N*(Kd+M-1) .LE. NPTS) THEN
    N=N+1
    GO TO 145
    ELSE
    N=N-1
    ENDIF
    IF (N .EQ. 1) THEN
    WRITE (*,*) 'Given the other parameters chosen thus far,'
    WRITE (*,*) 'Spacing can only be 1'
    DELTAY=1
    IF (NUFILE) THEN
    GO TO 165
    ELSE
    GO TO 215
    ENDIF
    ENDIF
    IF (.NOT. DSET .AND. LONG) THEN
    WRITE (*,*) 'Enter spacing between the ',Kd+M
    WRITE (*,*) 'data points of ',TITLE
    WRITE (*,*) 'to be processed '
    WRITE (*,*) ' '
    WRITE (*,*) 'If, for example, one is chosen, then ',Kd+M
    WRITE (*,*) 'consecutive points in ',TITLE
    WRITE (*,*) 'will be processed '
    WRITE (*,*) ' '
    ELSE
    WRITE (*,*) 'Enter spacing '
    WRITE (*,*) ' '
    ENDIF
155  WRITE (*,*) 'Spacing may range from          1 '
    WRITE (*,*) '          to',N
    READ (*,*) DELTAY
    IF (DELTAY .GE. 1 .AND. DELTAY .LE. N) THEN
    IF (NUFILE) THEN

```

```

        GO TO 165
        ELSE
        GO TO 215
        ENDIF
    ELSE
    GO TO 155
    ENDIF

165  WRITE (*,*) 'Do you wish to adjust eigenvalues? (y/n)'
      READ (*,150) YN
      IF (YN .EQ. 'N' .OR. YN .EQ. 'n') THEN
      IF (NUFILE) GO TO 6
      GO TO 215
      ENDIF
      IF (YN .NE. 'Y' .AND. YN .NE. 'y') GO TO 165
2    WRITE (*,*) 'Discard or compensate eigenvalues? (d/c)'
      READ (*,150) DC
      IF (DC .EQ. 'D' .OR. DC .EQ. 'd') THEN
      NRT=Kd
      GO TO 175
      ENDIF
      IF (DC .NE. 'C' .AND. DC .NE. 'c') GO TO 2
      WRITE (*,*) 'Enter estimate of the actual order of the system'
      WRITE (*,*) ' '
      IF (LONG) THEN
      WRITE (*,*) 'This estimate will be used to determine the '
      WRITE (*,*) 'number of eigenvalues compensated or discarded '
      ENDIF
175  WRITE (*,*) 'the estimate may range from                2'
      WRITE (*,*) '                                     to',Kd+Kn+1
      READ (*,*) NRT
      IF (NRT .GT. Kd+Kn+1 .OR. NRT .LT. 2) THEN
      GO TO 175
      ELSEIF (.NOT. NUFILE) THEN
      GO TO 215
      ENDIF

6    NSTRIPT=1
185  IF (NSTRIPT+(Kd+M-1)*DELTAY .LE. NPTS) THEN
      NSTRIPT=NSTRIPT+1
      GO TO 185
      ELSE
      NSTRIPT=NSTRIPT-1
      ENDIF
      IF (NSTRIPT .EQ. 1) THEN
      WRITE (*,*) 'Given the other parameters chosen thus far,'
      WRITE (*,*) 'the starting point for processing the data'
      WRITE (*,*) 'must be the first point in the data file'
      GO TO 215
      ENDIF

```



```

WRITE (*,*) 'Enter desired starting point in data file'
IF (.NOT. DSET .AND. LONG) THEN
WRITE (*,*) '1 indicates the first point in the data file '
ENDIF
WRITE (*,*) ' '
WRITE (*,*) 'Given the other parameters chosen thus far,'
195 WRITE (*,*) 'the starting point may range from          1'
WRITE (*,*) '                                to',NSTRTPT
READ (*,*) N
IF (N .GE. 1 .AND. N .LE. NSTRTPT) THEN
NSTRTPT=N
ELSE
WRITE (*,*) 'Enter starting point again'
WRITE (*,*) ' '
GO TO 195
ENDIF
IF (.NOT. NUFILE) GO TO 215

7   IF (DSET) THEN
    IF (NCAUS .EQ. 1) THEN
NCAUS=2
GO TO 215
    ELSE
NCAUS=1
GO TO 215
    ENDIF
ENDIF
WRITE (*,*) 'Do you want the data matrix arrangement to be'
WRITE (*,*) ' '
WRITE (*,*) '1. Causal'
WRITE (*,*) '2. Non-causal'
WRITE (*,*) ' '
205 WRITE (*,*) 'Please enter 1 or 2 '
READ (*,*) NCAUS
IF (NCAUS .EQ. 1) THEN
CAUSAL=.TRUE.
ELSEIF (NCAUS .EQ. 2) THEN
CAUSAL=.FALSE.
ELSE
GO TO 205
ENDIF
GO TO 215

12  WRITE (*,*) 'Enter title of file to contain parameters'
    READ (*,100) TITL
    OPEN(1,FILE=TITL)
    WRITE(1,100) TITL
    WRITE(1,110) NPTS
    WRITE(1,110) NRT

```



```

WRITE(1,110) Kd
WRITE(1,110) M
WRITE(1,110) DELTAY
WRITE(1,110) NSTRIPT
WRITE(1,110) NCAUS
WRITE(1,100) TITLD
WRITE(1,110) NDPTS
WRITE(1,110) Kn
WRITE(1,110) INSTRIPT
CLOSE(1)
IF (DSET) GO TO 215

15  IF (DSET) THEN
    CLOSE(2)
    CLOSE(3)
    CALL SUBPLT(NOVERLAY)
    ENDIF

215  DSET=.TRUE.
    NUFIL=.FALSE.
    WRITE(*,*) ' '
    WRITE(*,*) '1. Data file to be processed          ',T
+ITLE
    WRITE(*,*) ' Number of data points in data file          ',NPTS
    WRITE(*,*) '2. Estimated order of the system          ',NRT
    WRITE(*,*) '3. Kd, the number of columns in the data matrix',Kd
    WRITE(*,*) '4. M, the number of rows in the data matrix',M
    WRITE(*,*) '5. Spacing between data points being processed ',DELTA
+Y
    WRITE(*,*) '6. First point in the data file to be processed',NSTRT
+PT
    WRITE(*,*) ' Last point in the data file to be processed',NSTRT
+PT+Kd+M-1
    IF (NCAUS .EQ. 1) THEN
    WRITE(*,*) '7. Data matrix arrangement for processing          CA
+USAL '
    ELSE
    WRITE(*,*) '7. Data matrix arrangement for processing          NON-CA
+USAL '
    ENDIF
    WRITE(*,*) ' '
    WRITE(*,*) '8. File containing excitation waveform          ',T
+ITLD
    WRITE(*,*) ' Number of data points in above file          ',NDPTS
    WRITE(*,*) '9. Estimated order of the waveform          ',Kn

    WRITE(*,*) '10. First point in the file to be '
    WRITE(*,*) ' input into the data matrix          ',INSTR
+TPT

```

```

WRITE(*,*) ' '

WRITE(*,*) '11. Begin processing using above settings'
WRITE(*,*) '12. Store parameters 1-10 in a file'
WRITE(*,*) '13. Retrieve parameters 1-10 from a previously created
+ file'
WRITE(*,*) '14. Reset overlays'
WRITE(*,*) '15. Re-plot overlays'
WRITE(*,*) '16. End this session of Cadzow-Solomon signal processi
+ng'
WRITE(*,*) ' '
WRITE(*,*) 'Enter an integer from 1 to 16 to make changes as often
+ as you desire'
225 READ (*,*) NMENU
IF (NMENU .LT. 1 .OR. NMENU .GT. 16) THEN
WRITE(*,*) 'Enter an integer from 1 to 16'
GO TO 225
ENDIF

GO TO (1,2,3,4,5,6,7,8,9,10,11,12,13,14,15,16),NMENU

11 OPEN(12,FILE=TITLE)
READ(12,100) HEADER
READ(12,110) NPTS
READ(12,120) XQ
READ(12,120) XQ
DO 235 I=1,NPTS
READ(12,120) D(I)
235 CONTINUE
CLOSE(12)

OPEN(8,FILE=TITLD)
READ(8,100) HEADER
READ(8,110) NDPTS
READ(8,120) XQ
READ(8,120) XQ
DO 245 I=1,NDPTS
READ(8,120) Dx(I)
245 CONTINUE
CLOSE(8)

KdPLT=Kd
WRITE(*,*) 'enter title of file to contain real part of poles'
READ(*,100) TITLER
OPEN(2,FILE=TITLER)

WRITE(*,*) 'enter title of file to contain imaginary part of poles'
READ(*,100) TITLEI
OPEN(3,FILE=TITLEI)

```

```

WRITE(10,130) (KdPLT)
WRITE(10,100) TITLER
WRITE(10,100) TITLLEI
130  FORMAT(I2)

MN=MAX(M,Kd+Kn+1)

100  FORMAT(A)
110  FORMAT(I5)
120  FORMAT(E12.6)
150  FORMAT(A)

DO 255 I=1,Kd+M
Dy(I)=D((I-1)*DELTAY+NSTRTPT)
255  CONTINUE

265  DO 285 I=1,M
DO 275 J=1,Kd+Kn+1
A(I,J)=Dy(I+J)
IF (J .GE. Kd+1) A(I,J)=Dx(I+J+INSTRTPT-2-Kd)
275  CONTINUE
285  CONTINUE

B(1)=Dy(1)
DO 295 I=2,M
B(I)=A(I-1,1)
295  CONTINUE

N=Kd+Kn+1

C    Begin singular value decomposition

CALL SVD(MACHEP,M,N,MN,A,W,MATU,U,MATV,V,IERR,RV1)

C    Errors in SVD?
IF (IERR .GT. 0.0) THEN
WRITE (*,*) 'Error in singular value number ',IERR,STOP
ENDIF
IF (YN .EQ. 'N') GO TO 385

DO 305 I=1,Kd+Kn+1
XP(I)=0.0
305  CONTINUE

C    Discard or compensate eigenvalues
c    Order singular values

XP(1)=W(1)

```

```

DO 335 I=2,Kd+Kn+1
DO 325 J=1,I
if (W(I) .GT. XP(J)) THEN
DO 315 K=I+1,J,-1
315 XP(K)=XP(K-1)
XP(j)=W(i)
GO TO 335
ENDIF
325 CONTINUE
XP(I+1)=W(I)
335 CONTINUE

C XP( ) now contains ordered singular values: XP(1) is the largest

C Discard eigenvalues
IF (DC .EQ. 'D') THEN
DO 345 J=NRT+1,Kd+Kn+1
345 W(J)=(0.0)
ELSE
C Compensate eigenvalues
AVG=0.0
DO 355 J=NRT+1,Kd+Kn+1
AVG=AVG+XP(J)**2
355 CONTINUE
IF (Kd+Kn+1 .GT. NRT) AVG=AVG/DBLE(FLOAT(Kd+Kn+1-NRT))

DO 375 J=1,Kd+Kn+1
DO 365 K=1,Kd+Kn+1
IF ( W(J) .EQ. XP(K) ) THEN
IF ( K .GT. NRT ) THEN
W(J)=0.0
ELSE
W(J)=DSQRT(DABS( W(J)*W(J)-AVG))
ENDIF
GO TO 375
ENDIF
365 CONTINUE
375 CONTINUE
ENDIF

385 DO 405 I=1,M
DO 395 J=1,M
UT(I,J)=(U(J,I))
395 CONTINUE
405 CONTINUE

C Form SIGMA+ (Kd+Kn+1 x M)
DO 425 I=1,Kd+Kn+1
DO 415 J=1,M

```

```

        SIGMA(I,J)=0.0
        IF (I .EQ. J .AND. W(J) .NE. 0.0) THEN
            SIGMA(I,J)=1.0d0/W(J)
        ELSE
            SIGMA(I,J)=0.0D0
        ENDIF
415     CONTINUE
425     CONTINUE

C     Form SIGMA (M x Kd+Kn+1)
        DO 445 I=1,M
        DO 435 J=1,Kd+Kn+1
            SIG(I,J)=0.0
            IF (I .EQ. J) SIG(I,J)=W(J)
435     CONTINUE
445     CONTINUE

C     V=Kd+Kn+1xKd+Kn+1, SIGMA+=Kd+Kn+1xM, VS=Kd+Kn+1xM
        CALL MXMUL(V,SIGMA,Kd+Kn+1,Kd+Kn+1,M,VS)

C     VS=Kd+Kn+1xM, UT=MxM, AINV=Kd+Kn+1xM
        CALL MXMUL(VS,UT,Kd+Kn+1,M,M,AINV)

C     Calculate matrix multiplication of AINV x B, where
C     AINV=Kd+Kn+1xM, B=Mx1, XP=Kd+Kn+1x1
        CALL MXMUL(AINV,B,Kd+Kn+1,M,L,XP)

C     Compute autoregressive coefficients from prediction coefficients

        IF (XP(Kd) .EQ. 0.0) THEN
            WRITE (*,*) 'ERROR, avoiding division by zero'
            STOP
        ELSE
            B(Kd)=1.0d0/XP(Kd)
        ENDIF
        DO 455 I=2,Kd
            B(I-1)=-B(Kd)*XP(Kd-i+1)
455     CONTINUE

        DO 465 i=1,Kd
            X(I)=-B(Kd-I+1)
            IF (NCAUS .EQ. 1) X(I)=-XP(Kd-I+1)
465     CONTINUE
            X(Kd+1)=1.0

C     Compute the roots of the polynomial in z

        CALL POLRT(X,COF,KD,ROOTR,ROOTI,IER)

        IF (IER .NE. 0) WRITE (*,*) 'ERROR with POLRT, IER=',IER,STOP

```

```

DO 475 I=1,Kd
WRITE(2,120) ROOTR(I)
WRITE(3,120) ROOTI(I)
S(I)=DCMPLX(ROOTR(I),ROOTI(I))
475 CONTINUE

MAGPOL=0
DO 485 I=1,Kd
IF (CDABS(S(I)) .GE. 1.0D0) MAGPOL=MAGPOL+1
485 CONTINUE

WRITE(*,*) '# of poles with magnitude <= 1',Kd-MAGPOL
WRITE (*,*) 'HIT ANY KEY TO CONTINUE'
READ (*,100) HEADER

C Plot poles
NOVERLAY=NOVERLAY+1
CLOSE(2)
CLOSE(3)
CALL SUBPLT(NOVERLAY)

J=0
K=0

DO 495 I=1,Kd
IF (CDABS(S(I)) .LT. 1.0) THEN
WRITE (*,*) S(I),CDABS(S(I))
J=J+1
K=K+1
ENDIF
IF (J .EQ. 20) THEN
WRITE (*,*) 'HIT ANY KEY TO CONTINUE'
READ (*,100) HEADER
J=0
ENDIF
495 CONTINUE

WRITE (*,*) 'Poles with magnitude less than one ',K
WRITE (*,*) 'HIT ANY KEY TO CONTINUE'
READ (*,100) HEADER

GO TO 215

16 STOP
END
^Z

```

APPENDIX C. MATRIX MULTIPLICATION

```
SUBROUTINE MXMUL(A,B,RA,CA,CB,AB)
INTEGER RA,CA,CB
REAL*8 A(70,70),B(70,70),AB(70,70)
```

```
C   Calculates matrix multiplication of  $A \times B = AB$ , where
C    $A = RA \times CA$ ,  $B = CA \times CB$ ,  $AB = RA \times CB$ 
```

```
DO 30 I=1,RA
DO 20 J=1,CB
AB(I,J)=0.0
DO 10 K=1,CA
AB(I,J)=AB(I,J)+A(I,K)*B(K,J)
10 CONTINUE
20 CONTINUE
30 CONTINUE
RETURN

END
```


APPENDIX D. GRAPHICS ROUTINE

SUBROUTINE SUBPLT(NOVERLAY)

```

C
C MS-FORTRAN Program using "Grafmatic" Library Subroutines.
C Plots a Solid Line and Optional Overlay Plot for Comparison.
C Written by M.A. Morgan with Latest Update August 1989.
C
C Default Printer is "IBM Graphics" (e.g. Epson, Okidata, IBM)
C With Plot Rotated 90 degrees From the Vertical. "GrafPlus.Com"
C May be Run to Rotate Plot Upright on Paper and to Use a Variety
C of Impact Printers. "GrafLaser.Com" May be Run to Use a Laser
C Printer. See GrafPlus/Laser Manual From Jewell Technology.
C
C
CHARACTER*1 YN,YN1,DUM,YN2,SYMBOL,BELL,FEED,FFYN
CHARACTER*4 LINE
CHARACTER*7 SYMB
CHARACTER*16 LTTT,CTTT,FNAME,TITLER,TITLEI
CHARACTER*64 TITLE,HCOPY
REAL CRTR(70),CRTI(70),NRTR(70),NRTI(70)
INTEGER*2 N,JROW,JCOL,ISYM1,ISYM2,ITYPE1,ITYPE2,NSCRN
INTEGER*2 CYAN,GREEN,WHITE,YELLOW,RED,BLACK,BLUE,NTWO
INTEGER*2 JROW1,JROW2,JCOL1,JCOL2,CROSS,KdPLT,I
INTEGER*2 PURPLE,RUST
EXTERNAL XFUN,YFUNF,YFUNN
LINE='— '
WHITE=7
GREEN=10
CYAN=11
YELLOW=14
RED=12
BLACK=0
BLUE=1
NTWO=2
PURPLE=5
RUST=6
BELL=CHAR(7)
FEED=CHAR(12)

C Clear Screen and Put Up Introduction - on Blue Background for EGA
C Only; Another Background Color is Possible by Changing "BLUE"
C in the Calls to QPREG and QOVSCN.
CALL QSMODE(NTWO)
CALL QPREG(0,BLUE)

```

```
CALL QOVSCN(BLUE)
WRITE(*,*) BELL
  NS=1
  NSCRN =16
  ITYPE2=0
```

C Calling GRAFMATIC Routines and Plotting F1 Solid Line Graph

```
ITYPE1=0
ISYM1=-1
NDOTS1=0
  JROW1=1
  JROW2=350
  JCOL1= 75
  JCOL2= 565
  XMIN=-1.2
  XMAX=1.2
  YMIN=-1.2
  YMAX=1.20
  YOVERX=1.115
  XORG=0.0
  YORG=0.0
XST=-1.1
XFIN=1.1
YST=-1.1
YFIN=1.1
```

25 CALL QSMODE(NSCRN)
CALL QPLOT(JCOL1,JCOL2,JROW1,JROW2,XMIN,XMAX,YMIN,YMAX,XORG,YORG,
+1,YOVERX,1.5)

```
CALL QSETUP(NDOTS1,CYAN,ISYM1,RED)
IF(XFIN-XST .LE. 9.0) XMAJOR=0.6
IF(XFIN-XST .LE. 6.0) XMAJOR=0.4
IF(XFIN-XST .LE. 3.3) XMAJOR=0.2
IF(XFIN-XST .GE. 9.0) XMAJOR=(XFIN-XST)/10.0
```

```
MINOR=0
LABEL=1
NDEC=2
  CALL QXAXIS(XST,XFIN,XMAJOR,MINOR,LABEL,NDEC)
  YMAJOR=XMAJOR
  CALL QYAXIS(YST,YFIN,YMAJOR,MINOR,LABEL,NDEC)
```

c Plot unit circle

```
A=-1.0
B=1.0
```

```
CALL QCURV(XFUN,YFUNP,A,B)
CALL QCURV(XFUN,YFUNN,A,B)
```

```
IF (NOVERLAY-1 .LT. 1) THEN
  IF (NOVERLAY-1 .EQ. 0) THEN
```

```

WRITE (*,3) NOVERLAY-1
ELSE
NZERO=0
WRITE (*,3) NZERO
ENDIF
ELSEIF (NOVERLAY-1 .GT. 1) THEN
WRITE (*,3) NOVERLAY-1
ELSE
WRITE (*,4) NOVERLAY-1
ENDIF
3  FORMAT (I3,' OVERLAYS')
4  FORMAT (I3,' OVERLAY ')
REWIND(10)

DO 20 I=1,NOVERLAY
READ (10,110) KdPLT
READ (10,100) TITLER
READ (10,100) TITLLEI
OPEN(2,FILE=TITLER)
OPEN(3,FILE=TITLLEI)
NKd=KdPLT
DO 27 J=1,KdPLT
READ (2,120) NRTR(J)
READ (3,120) NRTI(J)
IF (DSORT(NRTR(J)**2+NRTI(J)**2) .GT. 1.1) THEN
NKd=NKd-1
NRTR(J)=0.0
NRTI(J)=0.0
ENDIF
27 CONTINUE
PURPLE=5
RUST=6
WHITE=7
GREEN=10
CYAN=11
YELLOW=14
RED=12
BLUE=1
IF (I .EQ. 1) THEN
CALL QSETUP (NDOTS1,CYAN,ISYM1,RED)
ELSEIF (I .EQ. 2) THEN
CALL QSETUP (NDOTS1,CYAN,ISYM1,GREEN)
ELSEIF (I .EQ. 3) THEN
CALL QSETUP (NDOTS1,CYAN,ISYM1,YELLOW)
ELSEIF (I .EQ. 4) THEN
CALL QSETUP (NDOTS1,CYAN,ISYM1,BLUE)
ELSEIF (I .EQ. 5) THEN
CALL QSETUP (NDOTS1,CYAN,ISYM1,WHITE)
ELSEIF (I .EQ. 6) THEN
CALL QSETUP (NDOTS1,CYAN,ISYM1,PURPLE)

```

```

ELSEIF (I .EQ. 7) THEN
  CALL QSETUP(NDOTS1,CYAN,ISYML,RUST)
ELSE
  CALL QSETUP(NDOTS1,CYAN,ISYML,RED)
ENDIF
CALL QTABL(ITYPE1,KdPLT,NRTR,NRTI)
20  CONTINUE

READ (*,100) DUM
GO TO 40
HCOFY='HARDCOPY—> ENTER P OR p'
CALL QPTXT(30,HCOFY,RED,25,1)
CALL QCMOV(55,1)
HCOFY='
CALL QPTXT(40,HCOFY,BLACK,25,1)
IF (DUM .NE. 'P' .AND. DUM .NE. 'p') GO TO 40
CALL QPSCRN
OPEN (1,FILE='PRN')
WRITE (1,160) FEED
100  FORMAT(A)
110  FORMAT(I2)
120  FORMAT(E12.6)
160  FORMAT(' ',A,\)
40   CONTINUE
CALL QSMODE(NTWO)
CALL QPREG(0,BLUE)
CALL QOVSCN(BLUE)
WRITE(*,*) NKd,'points were plotted'
RETURN
END

REAL FUNCTION XFUN(T)
XFUN=T
RETURN
END

REAL FUNCTION YFUNP(T)
YFUNP=SQRT(1.0-T*T)
RETURN
END

REAL FUNCTION YFUNN(T)
YFUNN=-SQRT(1.0-T*T)
RETURN
END

```

LIST OF REFERENCES

1. C. E. Baum, On the Singularity Expansion Method for the Solution of Electromagnetic Interaction Problems, Air Force Weapons Laboratory Interaction Note 88, December 1971.
2. D. L. Moffatt and R. K. Mains, "Detection and discrimination of radar targets," IEEE Trans. on Antennas and Propagation, AP-23, May 1975, pp 358-367.
3. Michael A. Morgan, "Singularity expansion representations of fields and currents in transient scattering," IEEE Trans. on Antennas and Propagation, AP-23, May 1984, pp 466-473.
4. Ramdas Kumaresan, and D.W. Tufts, "Estimating the parameters of exponentially damped sinusoids, and pole-zero modeling in noise," IEEE Trans. Acoustics, Speech, and Sig. Proc., December 1982, pp 833-840.
5. James A. Cadzow and Otis M. Solomon Jr., "Algebraic approach to system identification," IEEE Trans. Acoustics, Speech and Sig. Proc., ASSP-34, 3, June 1986, pp 462-469.
6. E.M. Kennaugh, "The K-pulse concept," IEEE Trans. on Antennas and Propagation, AP-29, March 1981.
7. James B. Dunavin, Identification of Scatterers Based Upon Annihilation of Complex Natural Resonances, Master's Thesis, Naval Postgraduate School, Monterey, CA, September 1985.
8. Michael A. Morgan and James B. Dunavin, "Discrimination of scatterers using natural resonance annihilation," Abstracts of 1986 National Radio Science Meeting, Philadelphia, PA, June 1986.
9. K. M. Chen, D. P. Nyquist, E.J. Rothwell, L.L. Webb, and B. Drachman, "Radar target discrimination by convolution of radar returns with extinction-pulses and single-mode extraction signals." IEEE Trans. on Antennas and Propagation, AP-34, July 1986, pp 896-904.
10. Michael A. Morgan, "Scatterer discrimination based upon natural resonance annihilation," Journal of Electromagnetic Waves and Applications, 2,2, 1987, pp 155-176.

11. Michael A. Morgan, Signal Generator Program, Naval Postgraduate School, Monterey, CA, 1989.
12. Michael A. Morgan, Time-Domain Thin-Wire Integral Equation Program, Naval Postgraduate School, Monterey, CA, 1989.
13. Choong Y. Chong, Investigation of Non-linear Estimation of Natural Resonances in Target Identification, Master's Thesis, Naval Postgraduate School, Monterey, CA, December 1983.
14. S. Lawrence Marple, Jr., Digital Spectral Analysis with Applications, (Englewood Cliffs, NJ: Prentice-Hall, Inc.) 1987.
15. Ramdas Kumaresan, Estimation the Parameters of Exponentially Damped or Undamped Sinusoidal Signals in Noise, Ph.D. Thesis, University of Rhode Island, Kingston, RI, October 1982.
16. S. A. Norton, "Radar target classification by natural resonances: signal processing algorithms," Engineer's Thesis, Naval Postgraduate School, Monterey, CA, Mar 1988.
17. Norman J. Walsh, "Bandwidth and Signal to Noise Ratio Enhancement of the NPS Transient Scattering Laboratory," Master's Thesis, Naval Postgraduate School, Monterey, CA, Dec 1989.
18. J.M. Boyle, EISPACK Subroutine Library, Argonne National Laboratory, 1973.
19. G. H. Golub and C. Reinsch, "Singular value decomposition and least squares solutions," Numer. Math., 14, 1970, pp 403-420.

INITIAL DISTRIBUTION LIST

	No. Copies
1. Defense Technical Information Center Cameron Station Alexandria, Virginia 22304-6145	2
2. Library, Code 0412 Naval Postgraduate School Monterey, California 93943-5002	2
3. Defense Logistic Studies Information Exchange U.S. Army Logistics Management College Fort Lee, Virginia 23801-6043	1
4. Department Chairman, Code 62 Department of Electrical and Computer Engineering Naval Postgraduate School Monterey, California 93943-5002	1
5. Professor Michael A. Morgan, Code 62Mw Department of Electrical and Computer Engineering Naval Postgraduate School Monterey, California 93943-5002	10
6. Professor Ralph Hippenstiel, Code 62Hi Department of Electrical and Computer Engineering Naval Postgraduate School Monterey, California 93943-5002	1
7. Commandant of the Marine Corps Code TE 06 Headquarters, U.S. Marine Corps Washington, D.C. 20380-0001	1
8. Electronic Material Officer USS Blue Ridge (LCC-19) FPO San Francisco, California 96628-3300	2
9. Dr. John N. Entzminger Director, Tactical Technology Office Defense Advanced Research Projects Agency 1400 Wilson Blvd. Arlington, Virginia 22209	2

10. Mr. D. Jiglio 1
Tactical Technology Office
Defense Advanced Research Projects Agency
1400 Wilson Blvd.
Arlington, Virginia 22209
11. Dr. Arthur Jordan 1
Code 1114SE
Office of Naval Research
800 N. Quincy St.
Arlington, Virginia 22209
12. Dr. Rabiner Madan 1
Code 1114SE
Office of Naval Research
800 N. Quincy St.
Arlington, Virginia 22209
13. Professor K. M. Chen 1
Department of Electrical Engineering and
Systems Science
Michigan State University
East Lansing, Michigan 48824
14. Dr. M. L. VanBlaricum 1
Toyon Research Corporation
75 Aero Camino, Suite A
Goleta, California 93160
15. Capt. Peter D. Larison 1
1145 Lenox Court
Cape Coral, Florida 33904
16. Dr. Carl Baum 1
Air Force Weapons Laboratory
Kirtland Air Force Base, New Mexico 87117
17. Mr. Daniel Carpenter 1
TRW Military Electronics Division
One Rancho Carmel
San Diego, California 92128
18. Dr. C. Ray Smith 1
AMSMI-RD-AS-RA
Redstone Arsenal, Alabama 35898
19. Professor Herbert Uberall 1
Physics Department
Catholic University of America
Washington, D.C. 20064

Thesis

L2676 Larison

c.1 Evaluation of system
identification algorithms
for aspect-independent
radar target classifica-
tion.



thesL2676

Evaluation of system identification algo



3 2768 000 89047 9

DUDLEY KNOX LIBRARY